

Spring 2012

Trace metal applications in atmospheric and watershed dynamics: Case studies of mercury deposition in New England and bedrock groundwater-surface water mixing

Melissa A. Lombard

University of New Hampshire, Durham

Follow this and additional works at: <https://scholars.unh.edu/dissertation>

Recommended Citation

Lombard, Melissa A., "Trace metal applications in atmospheric and watershed dynamics: Case studies of mercury deposition in New England and bedrock groundwater-surface water mixing" (2012). *Doctoral Dissertations*. 658.
<https://scholars.unh.edu/dissertation/658>

This Dissertation is brought to you for free and open access by the Student Scholarship at University of New Hampshire Scholars' Repository. It has been accepted for inclusion in Doctoral Dissertations by an authorized administrator of University of New Hampshire Scholars' Repository. For more information, please contact nicole.hentz@unh.edu.

**Trace metal applications in atmospheric and watershed dynamics:
Case studies of mercury deposition in New England
and bedrock groundwater – surface water mixing**

BY

MELISSA A. LOMBARD

B.A., William Smith College, 1995

M.S., Rensselaer Polytechnic Institute, 2002

DISSERTATION

Submitted to the University of New Hampshire

In Partial Fulfillment of

The Requirements for the Degree of

Doctor of Philosophy

In

Earth and Environmental Science

May 2012

UMI Number: 3525066

All rights reserved

INFORMATION TO ALL USERS

The quality of this reproduction is dependent upon the quality of the copy submitted.

In the unlikely event that the author did not send a complete manuscript and there are missing pages, these will be noted. Also, if material had to be removed, a note will indicate the deletion.

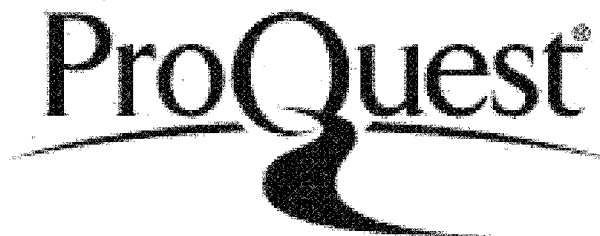


UMI 3525066

Published by ProQuest LLC 2012. Copyright in the Dissertation held by the Author.

Microform Edition © ProQuest LLC.

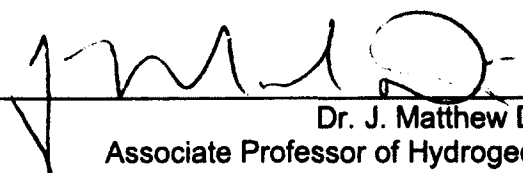
All rights reserved. This work is protected against unauthorized copying under Title 17, United States Code.

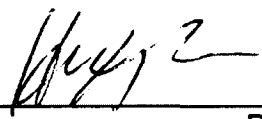


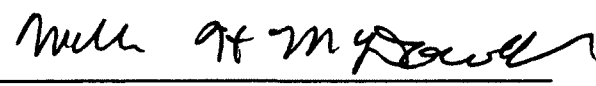
ProQuest LLC
789 East Eisenhower Parkway
P.O. Box 1346
Ann Arbor, MI 48106-1346

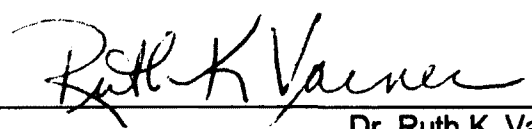
This dissertation has been examined and approved.


Dissertation Director, Dr. Julia G. Bryce
Associate Professor of Geochemistry


Dr. J. Matthew Davis
Associate Professor of Hydrogeology


Dr. Huiting Mao
Associate Professor of Chemistry
SUNY Environmental Science and Forestry


Dr. William McDowell
Professor of Environmental Science


Dr. Ruth K. Varner
Research Associate Professor of Earth Sciences
and Environmental Sciences

4-30-12
Date

ACKNOWLEDGEMENTS

I would like to acknowledge the various funding sources that allowed me to return to graduate school and pursue this degree. The Leitzel Center at the University of New Hampshire through the Partnerships for Research Opportunities to Benefit Education (PROBE) project funded by the National Science Foundation GK-12 program (NSF award DGE-0338277) and the Transforming Earth Systems Science Education (TESSE) project funded by the NSF directorate for geosciences (NSF award GEO-0631377) provided me with funding as well as valuable teaching and learning experiences in science education. Support was also provided by the Office of Oceanic and Atmospheric Research of the National Oceanic and Atmospheric Administration under AIRMAP grant #NA06OAR4600189 to UNH. The NSF award ATM-0837833 provided additional support. Thank you also to the UNH Department of Earth Sciences for awarding me the Karen VonDamm memorial scholarship. I'm grateful I had the opportunity to work with Karen, if only briefly. I'm highly appreciative for the UNH Natural Resources and Earth System Science (NRESS) program for providing me with tuition waivers during my final semesters. Also thanks to the various people I've worked with while finishing up my dissertation, especially Nora Traviss at Keene State College, as well as the staff at the NH State Geological Survey and Franklin Pierce University.

I would like to thank my advisor, Julie Bryce, and dissertation committee members, Ruth Varner, Bill McDowell, Huiting Mao, and Matt Davis for contributing to my educational experience. I would also like to acknowledge committee contributions from Rob Griffin and Alex Pszenny during my early days at UNH. Additional UNH faculty who have provided strong moral support are Karen Graham and Wally Bothner for which

I am very appreciative. Several UNH students and staff assisted with lab work and field sampling. These include Kevan Carpenter, Michelle Daly, Jennie Garcia, Ian Honsberger, Sara Keach, Laura Nichols, Cheryl Parker, Florencia Prado, Laura Preston, Kerri Schorzman, Rosie Simpson, and Jennifer St. Louis.

And lastly, a huge thank you to my family, friends, and “long-suffering” boyfriend, fiancé and now husband for their support, friendship, and patience as I traveled down this long and seemingly unending road. The Four Morseketeers and Thundering Aces kept things fun and grounded with skateboards, volcano cake, kumquats, motorcycles, and bamboo torches in that bizarre world of Morse Hall. Thank you ladies (and one boy)! Most importantly I thank my parents for providing me with the freedom to explore my childhood curiosity with rocks and instilling in me the values of honesty and hard work.

TABLE OF CONTENTS

ACKNOWLEDGEMENTS	iii
LIST OF TABLES.....	vii
LIST OF FIGURES.....	viii
ABSTRACT.....	ix
INTRODUCTION.....	1
References.....	5
MERCURY DEPOSITION IN SOUTHERN NEW HAMPSHIRE, 2006-2009.....	7
Introduction	7
Sample collection and analysis.....	10
Hg wet deposition seasonal patterns and inter-annual variability.....	13
Comparison with MDN sites	20
Influence of meteorological conditions and other trace gases on Hg wet deposition..	21
Linkage between RGM and Hg wet deposition	23
Scavenging of RGM during precipitation events	24
Estimation of RGM dry deposition	26
Comparison between RGM dry deposition and Hg wet deposition	28
Summary and conclusions	31
References.....	33
MERCURY WET DEPOSITION IN THE MARINE ENVIRONMENT: COMPARISON TO A COASTAL SITE AND RELATIONSHIPS WITH DISSOLVED ORGANIC CARBON AND MAJOR ION CONCENTRATIONS.....	37
Introduction	37
Methods	39
Site Descriptions	39
Precipitation collection.....	40
Analytical methods	41
Backward trajectories	41
Results and Discussion	42
Precipitation and sample collection variability between TF2 and AI	42
A comparison of total aqueous Hg at TF2 and AI	43
Major ions and DOC in precipitation at AI	47
Major ion and Hg concentrations in rainwater at Appledore Island.....	47
DOC and Hg concentrations in rainwater at Appledore Island	56
Conclusions.....	59
References.....	60
QUANTIFICATION OF ENVIRONMENTALLY MOBILE Hg ^P : METHOD DEVELOPMENT AND APPLICATION TO AN INTENSIVE SAMPLING CAMPAIGN ON APPLIEDORE ISLAND, SUMMER 2009	64
Introduction	64
Methods	66
Sampling Methods.....	67
Laboratory Methods.....	67
Data Analysis	69
Results	69
Blanks and external standards.....	69
Summer 2009 Appledore Island field samples.....	70
Sequential extractions	71
Discussion and conclusions	72

References.....	73
STRONTIUM ISOTOPES IN WATERS FROM THE MT. PAWTUCKAWAY REGION OF THE LAMPREY RIVER WATERSHED	75
Introduction and background	75
Methods	80
Results and Discussion	84
Spatial Variability in ⁸⁷ Sr/ ⁸⁶ Sr	84
Connections with Stable Isotope Studies in the Lamprey River Watershed	88
Conclusions.....	89
References.....	90
APPENDIX.....	93

LIST OF TABLES

Table II.1. Seasonal and annual total precipitation, Hg wet deposition, and concentration summary statistics for Thompson Farm	19
Table II.2. Kendall's τ correlation co-efficients for Hg wet deposition and Hg concentration with meteorological conditions and gas phase measurements at Thompson Farm	22
Table II.3. Seasonal and annual Hg wet deposition and estimated RGM dry deposition, and the sum of Hg wet deposition and estimated RGM dry deposition at TF. The asterisks indicate seasons missing more than 3 days of RGM measurements	30
Table II.4. A comparison between annual Hg wet deposition and RGM dry deposition values reported in the literature and calculated in this study	31
Table III.1. Analytical methods and detection limits for chemical species examined in this study.	41
Table III.2. Summary statistics for total aqueous Hg in rainwater collected at Appledore Island (AI) and Thompson Farm 2 during summer 2009.	44
Table III.3. Summary statistics for DOC and major ions in rainwater at AI.	47
Table IV.1. A summary of various filter materials and acid extraction methods used previously by other researchers to measure Hg ^P	66
Table IV.2. A summary of results from blanks and certified reference material. Detection limit for blanks is 0.01 ppqv	70
Table IV.3. Results from sequential filter extractions.	72
Table V.1. Whole rock ⁸⁷ Sr/ ⁸⁶ Sr values in the study area.....	80
Table V.2. Sample information and ⁸⁷ Sr/ ⁸⁶ Sr results for all samples included in this study	85

LIST OF FIGURES

Figure II.1. Thompson Farm location and Mercury Deposition Network Locations in Maine and New Hampshire.	11
Figure II.2. Time series of wet deposition samples from Thompson Farm; (a) Hg concentration, (b) Hg wet deposition, (c) precipitation amount.....	14
Figure II.3 Seasonal Hg volume weighted mean concentration (a), Hg wet deposition (b), and precipitation amount (c), at Thompson Farm and Mercury Deposition Network sites located in Maine.	18
Figure II.4. Seasonal variations in RGM at TF.....	24
Figure II.5. Seasonal and annual Hg wet deposition and estimated RGM dry deposition at TF.....	28
Figure II.6. Seasonal Hg wet deposition and estimated RGM dry deposition at TF.....	29
Figure III.1 Thompson Farm and Appledore Island sampling locations.....	40
Figure III.2. Hg sample volumes collected at AI (circles) and TF2 (squares) and precipitation amounts with associated linear regressions and r^2 values.	43
Figure III.3a-c. Total aqueous Hg concentration, Hg deposition, and precipitation for samples collected at AI and TF2 during summer 2009	46
Figure III.4a-h. Hg and major ion concentrations in rainwater from AI.	49
Figure III.5a-f Hg concentration and percent of major ion attributed to sea salt for samples collected at AI.....	51
Figure III.6. HYPSPPLIT model back trajectory ending at AI at 1200 UTC on 14 June 2009	53
Figure III.7. HYPSPPLIT model back trajectory ending at AI at 1400 UTC on 29 August 2009	54
Figure III.8. HYPSPPLIT model back trajectory ending at AI at 0800 UTC on 18 July 2009.	54
Figure III.9. HYSPLIT model back trajectory ending at AI at 2200 UTC on 21 July 2009..	55
Figure III.10. Precipitation amount and Hg concentration for rain events at AI.....	56
Figure III.11 Mercury deposition compared to the percent of sea salt in precipitation samples at AI.....	56
Figure III.12 Hg and DOC concentrations in rain at AI.	58
Figure IV.1. Hg ^P bulk aerosol filter results from Appledore Island sampling campaign..	71
Figure V.1. Location of the Lamprey River Watershed, New Hampshire.	77
Figure V.2. Bedrock lithology of the Lamprey River watershed.....	78
Figure V.3. Mineral modes for the Massabesic Gneiss and Pawtuckaway diorite and monzonite.....	80
Figure V.4. Lamprey River hydrograph for water year 2006 from USGS gauge site 01073500 located downstream of the study area	82
Figure V.5. ⁸⁷ Sr/ ⁸⁶ Sr results for surface water samples.....	86
Figure V.6 ⁸⁷ Sr/ ⁸⁶ Sr ratios for whole rock, surface water and groundwater samples from the various bedrock units underlying the study area	88

ABSTRACT

TRACE METALS IN THE ENVIRONMENT: ATMOSPHERIC DEPOSITION OF MERCURY, AND STRONTIUM ISOTOPES IN WATERS FROM THE LAMPREY RIVER WATERSHED

By

Melissa A. Lombard

University of New Hampshire, May, 2012

The studies presented in this dissertation focus on the environmental chemistry of two trace metals, mercury (Hg) and strontium (Sr). Both are naturally occurring and exist in the environment at trace levels.

Chapters II-IV of this dissertation focus on understanding the atmospheric chemistry of Hg and the wet and dry deposition of this toxic element. Chapter II presents results from Hg wet deposition measurements and ambient reactive gaseous Hg (RGM) measurements collected at Thompson Farm located in Durham, NH over a 3 year time period. The duration of this study allowed for seasonal and inter-annual comparisons. Seasonally, Hg wet deposition was greatest in the summer and spring and lowest in the winter and fall. Evidence of ineffective scavenging of RGM is provided due to the less frequent depletion of RGM during winter precipitation events in comparison with other seasons. RGM dry deposition estimates based on real time concentration measurements are greatest during the winter and spring. Ratios of the seasonal Hg wet deposition to RGM dry deposition vary greatly from 1.6 to 80.

A comparison between Hg wet deposition at Thompson Farm and a marine site, Appledore Island, is included in Chapter III. There were no significant differences in event concentration or deposition between the two sites, however, the sample collection efficiency varied greatly between the sites and may effect the results. Additionally, major

ion concentrations were measured at the Appledore Island site and compared to the Hg concentrations. The analytical results coupled with air mass back trajectories suggest that the greatest amount of Hg wet deposition occurs when polluted continental air mixes with marine air.

A new filter extraction method for determining the environmentally mobile Hg concentration in bulk aerosol filters is presented in Chapter IV. This method is applied during a 2 week intensive sampling campaign at Appledore Island during summer 2009.

Chapter V explores the use of Sr isotope ratios to determine groundwater inputs to the Lamprey River. The groundwater and surface waters in the watershed exhibit large differences in $^{87}\text{Sr}/^{86}\text{Sr}$ indicating this geochemical indicator could be a useful tool in hydrogeologic studies of the watershed.

CHAPTER I

INTRODUCTION

The studies presented in this dissertation focus on the environmental chemistry of two trace metals, mercury (Hg) and strontium (Sr). Three of the chapters (II-IV) focus on the trace element Hg with a fourth chapter (V) about Sr isotope ratios. Both of these elements are naturally occurring and exist in the environment at trace level amounts. The primary objectives of the Hg work are to measure and investigate factors contributing to its atmospheric deposition in a rural coastal site in Southern New Hampshire and an offshore location in Maine. The Sr project explores the possible use of Sr isotope ratios to determine groundwater inputs to the Lamprey River located in Southern New Hampshire.

Mercury is a global contaminant of concern primarily due to its known toxicity in methylated forms, monomethyl Hg (MMHg) and dimethyl Hg (DMHg). Methyl mercury (MHg) is bio-magnified within aquatic food webs and the consumption of fish is the primary exposure route of mercury to humans. Atmospheric deposition via wet and dry mechanisms is the primary source of Hg to terrestrial and aquatic ecosystems. Sources of Hg to the atmosphere include both natural and anthropogenic primary emissions and natural secondary emissions of Hg originally mobilized by anthropogenic activities. The current atmospheric Hg burden is estimated to be between 2.5 and 1.7x greater than the preindustrial burden (Selin, 2009) and Hg deposition is estimated to be 2-4x greater. The major anthropogenic sources of Hg to the atmosphere are coal combustion, oil product combustion, cement production, nonferrous metal production, pig iron and steel

production, caustic soda production, mercury and gold production and waste disposal (Pacyna et al., 2006). Natural emissions of Hg are non-negligible and include volcanic emissions and emissions from Hg enriched soils and rocks (Gustin et al., 2008, Selin, 2009). The oceans are also a major emission source of mercury (Mason and Sheu, 2002, Selin 2009). While government policy efforts have reduced anthropogenic emissions in North America and Europe, global emissions are expected to increase with the industrial and economic growth of China and India (Feng et al., 2008; Mukherjee et al., 2008; Streets et al., 2008).

The complexity of understanding the fate and transport of Hg in the environment is due to its unique chemical and physical properties. Under environmental conditions Hg exists in the gaseous elemental form (Hg^0) and gaseous oxidized form Hg^{2+} commonly referred to as reactive gaseous mercury (RGM). In the atmosphere Hg exists largely in the gaseous phase and elemental Hg (Hg^0) is the predominant species (~95%) with an atmospheric lifetime of approximately one year (Lin and Pehkonen, 1999; Selin 2009). Reactive gaseous mercury (RGM) typically constitutes 5% or less of the total gaseous mercury (TGM) and has a much shorter atmospheric lifetime of several days to a few weeks (Lin and Pehkonen, 1999). Atmospheric Hg also exists in particulate form (Hg^P) and is considered to be minor (0.3%-0.9%) in background air but can be much more abundant in industrial regions constituting up to 40% of TGM (Lin and Pehkonen, 1999). Natural emission sources consist largely of Hg^0 while anthropogenic sources can emit Hg^0 , RGM, and Hg^P . Dry deposition of all Hg species, Hg^0 , RGM, and Hg^P can occur.

Hg in precipitation is thought to consist primarily of scavenged RGM and Hg^P . Reactive mercury species (Hg^{2+}) have been reported to compose from 14 to 95 % of the total mercury measured in precipitation samples (Hammerschmidt et al., 2007 and

sources therein). The scavenging of Hg^{P} is important near anthropogenic sources and urban areas and composed up to 96% of total Hg in precipitation in polluted areas of China (Guo et al., 2008). MMHg species have been measured in precipitation samples at very low levels in the range of 0.08 to 0.82 ng L⁻¹ (Hammerschmidt et al., 2007; Guo et al., 2008). The production of MMHg in aquatic ecosystems is primarily a biologically mediated transformation of Hg (Ullrich et al., 2001).

The Mercury Deposition Network (MDN), part of the National Atmospheric Deposition Program, began in 1996 and currently has over 100 sampling sites located throughout the United States and southern Canada. Weekly precipitation samples are collected and analyzed at a central laboratory for consistency. The purpose of this network is to monitor spatial and temporal trends in Hg wet deposition. Few of the MDN sites collect concurrent gas phase Hg measurements. Chapter II presents a multi-year dataset of Hg wet deposition collected at the Thompson Farm site in Durham, NH. This site had several co-located atmospheric gas phase measurements allowing for comparisons between Hg wet deposition and RGM, CO, and NO_y. Two purposes of this study were to quantify the Hg wet deposition and examine relationships with other atmospheric constituents. A third objective was to quantify RGM dry deposition based on real time measurements and compare to Hg wet deposition. The calculated RGM dry deposition is compared to the wet deposition and seasonal differences are noted. Understanding and quantifying Hg dry deposition is the largest gap in understanding total fluxes of Hg (Lindberg et al., 2007).

Hg wet deposition in the marine environment is examined in Chapter III. During the summer of 2009 precipitation samples were collected at Appledore Island, ME, located approximately 10 km from the New Hampshire coast, and at Thompson Farm. The Hg wet deposition at these two sites is compared. Relationships between sea salt

ion concentrations and Hg concentrations in precipitation from Appledore Island are also examined. These relationships provide some evidence for the interaction between sea salt aerosols and gas phase Hg.

While wet deposition of Hg is a straightforward measurement the determination of Hg dry deposition is more complex. There are limited data available for the dry deposition of Hg^P (Zhang et al., 2009) and a review of field studies measuring Hg^P indicates the lack of consistent sample collection and extraction techniques. A recent study with using co-located samplers, an automated instrument and bulk filter collection with subsequent filter extraction and laboratory analysis indicates that the two methods did not have comparable results (Talbot et al., 2011). Chapter IV presents a laboratory method developed to determine the environmentally mobile fraction of Hg^P collected from bulk aerosol filters. This method was applied to a field sampling campaign on Appledore Island, Maine during summer 2009.

Unlike Hg, Sr is a non-toxic element in its natural form. Strontium (Sr) has four naturally occurring stable isotopes; ⁸⁴Sr, ⁸⁶Sr, ⁸⁷Sr, and ⁸⁸Sr. ⁸⁷Sr is the radioactive decay product of ⁸⁷Rb. The present day ratio of ⁸⁷Sr/⁸⁶Sr in a rock or mineral reservoir is dependent on the initial ratio present plus the accumulation over time of ⁸⁷Sr from the decay of ⁸⁷Rb. The measurements of different ⁸⁷Sr/⁸⁶Sr ratios within rocks have historically been used to estimate ages and sources of rocks. More recently and primarily due to increases in analytical instrument precision, ⁸⁷Sr/⁸⁶Sr has been used as a tracer in hydrologic studies. In bedrock groundwater systems the isotopic ratio of groundwater will evolve toward the ratio of the host rock as the rock and water interact. Strontium does not typically occur in aggregate quantities in rock. It is a trace metal and typically substitutes for calcium in mineral structures due to their common ionic charge

(+2) and similar ionic radii (1.13Å and 1.00Å). Sr commonly substitutes for calcium in plagioclase feldspar, apatite, and limestone.

When two rock types with different $^{87}\text{Sr}/^{86}\text{Sr}$ occur adjacent to each other the ratio has the potential to be useful as a groundwater tracer. This bedrock situation exists in the Lamprey river watershed where two bedrock units of varying age and chemical composition exist next to each other. Chapter V examines $^{87}\text{Sr}/^{86}\text{Sr}$ values measured in groundwater and surface water from the Lamprey River watershed.

Improving the scientific understanding of trace metal behavior and mobility in our environment is important. For naturally occurring toxic metals such as Hg it is necessary to understand the factors affecting mobility, accumulation, and toxic exposure routes in order to enact relevant environmental policy. As population increases so will demands for natural resources such as water. Using a relatively inexpensive, and non-invasive technique such as the geochemical tracer $^{87}\text{Sr}/^{86}\text{Sr}$, to understand the mobility of groundwater is a valuable tool. Having a better understanding of groundwater – surface water interactions should lead to better protection strategies for water resources.

References

- Feng, X., et al., 2008. Mercury emissions from industrial sources in China. In *Mercury Fate and Transport in the Global Atmosphere: Measurements, Models, and Policy Implications, Interim Report of the United Nations Environmental Programme Global Mercury Partnership, Mercury Air Transport and Fate Research Partnership Area*, ed. N. Pirrone and R. Mason, p 47-56.
- Guo, Y., Feng, X., Li, Z., Tianrong, H, Yan, H., Meng, B., Zhang, J., Qiu, G., 2008. Distribution and wet deposition fluxes of total and methyl mercury in Wujiang River Basin, Guizhou, China, *Atmos. Environ.*, 42:30, 7096-7103.
- Gustin, M.S., Lindberg, S.E., Weisberg, P.J., 2008. An update on the natural sources and sinks of atmospheric mercury, *Applied Geochemistry*, 23, 482-493.
- Hammerschmidt, C.R., Lamborg, C.H., Fitzgerald, W.F., 2007. Aqueous phase methylation as a potential source of methylmercury in wet deposition, *Atmos. Environ.*, 41, 1663-1668.
- Lin, C.J., Pehkonen, S.O., 1999. The chemistry of atmospheric mercury: a review,

- Atmos. Environ., 33, 2067-2079.
- Lindberg, S., Bullock, R., Ebinghaus, R., Engstrom, D., Feng., Fitzgerald, W., Pirrone, N., Prestbo., E., Seigneur, C., 2007. A synthesis of progress and uncertainties in attributing the source of mercury in deposition, *Ambio*, 8, 19-32.
- Mason, R.P., Sheu, G.R., 2002. Role of the ocean in the global mercury cycle, *Global Biogeochem. Cycles*, 10.1029/2001GB001440.
- Mukherjee, A.B. et al., 2008, Mercury emissions from industrial sources in India and its effect on the environment. In *Mercury Fate and Transport in the Global Atmosphere: Measurements, Models, and Policy Implications, Interim Report of the United Nations Environmental Programme Global Mercury Partnership, Mercury Air Transport and Fate Research Partnership Area*, ed. N. Pirrone and R. Mason, p. 57-82.
- Pacyna, E.G., Pacyna, J.M., Steenhuisen, F., Wilson, S., 2006. Global anthropogenic mercury emission inventory for 2000, *Atmos. Environ.*, 40, 4048-4063.
- Selin, N.E., 2009. Global biogeochemical cycling of mercury: a review, *Annu. Rev. Environ. Resourc.* 34, 43-63.
- Streets, D.G., et al., 2008, Mercury emissions from coal combustion in China. In *Mercury Fate and Transport in the Global Atmosphere: Measurements, Models, and Policy Implications, Interim Report of the United Nations Environmental Programme Global Mercury Partnership, Mercury Air Transport and Fate Research Partnership Area*, ed. N. Pirrone and R. Mason, p.37- 46.
- Talbot, R., Mao, H., Feddersen, D., Smith, M., Kim, S., Sive, B., Haase, K., Ambrose, J., Zhou, Y., Russo, R., 2011. Comparison of particulate mercury measured with manual and automated methods, *Atmosphere*, 2, 1-20; doi:10.3390/atmos2010001.
- Ullrich, S.M., Tanton, T.W., Abdrashitova, S.A., 2001. Mercury in the aquatic environment: A review of factors affecting methylation, *Critical Reviews in Environmental Science and Technology*, 31:3, 241-293.
- Zhang L., Wright, L.R., Blanchard, P., 2009. A review of current knowledge concerning dry deposition of atmospheric mercury, *Atmos. Environ.*, 43, 5853-5864.

CHAPTER II

MERCURY DEPOSITION IN SOUTHERN NEW HAMPSHIRE, 2006-2009

Introduction

Mercury (Hg) is a naturally occurring contaminant of global concern due to its toxicity and ubiquitous presence in the atmosphere. It exists in diverse chemical forms comprised of gaseous elemental mercury (Hg^0), reactive gaseous mercury (RGM = $\text{HgCl}_2 + \text{HgBr}_2 + \text{HgOBr} + \dots$), and particulate mercury (Hg^P). Deposition of atmospheric Hg, mainly the more soluble forms of RGM and Hg^P , is an important source of Hg to terrestrial (Rea et al., 2002; Bushey et al., 2008; Choi et al., 2008, Selvendiran et al., 2008) and aquatic ecosystems (Landis and Keeler, 2002; Ariya et al., 2004). Methylated forms of Hg bioaccumulate in fish, and their consumption is the major exposure route of Hg to humans (Downs et al., 2007).

Previous studies suggest that the magnitude of Hg wet deposition varies geographically and seasonally due to climatic conditions, atmospheric chemistry, and human influences (VanArsdale et al., 2005; Selin and Jacob, 2008; Prestbo and Gay, 2009). In North America seasonal patterns in wet deposition are observed in both depositional flux and concentration with the highest values in the summer and lowest values in the winter (Sorensen et al., 1994; Mason et al., 2000; Guentzel et al., 2001; Keeler et al., 2005; VanArsdale et al., 2005; Choi et al., 2008; Prestbo and Gay, 2009). Explanations for this observation include more effective Hg scavenging by rain compared to snow (Sorensen et al., 1994; Mason et al., 2000; Keeler et al., 2005; Selin and Jacob, 2008), a greater availability of soluble Hg due to convective transport in

summer events (Guentzel et al., 2001; Keeler et al., 2005), and a summer increase in Hg-containing soil derived particles in the atmosphere (Sorensen et al., 1994).

Geographic differences in Hg wet deposition may be explained in part by the proximity to atmospheric sources. Results from the National Atmospheric Deposition Program's (NADP) Mercury Deposition Network (MDN) sites in the Northeastern United States exhibit a geographic trend with southern and coastal sites receiving higher Hg concentrations and depositional fluxes (VanArsdale et al., 2005; Prestbo and Gay, 2009). The sites with elevated Hg deposition are nearer to the East coast megalopolis and downwind of anthropogenic emission sources such as coal burning power plants and waste incinerators. Inconsistent results are reported in studies comparing Hg wet deposition fluxes and/or concentrations between rural and urban sites. Some report elevated annual fluxes (Mason et al., 2000) and concentrations (Steding and Flegal, 2002; Engle et al., 2009) at urban locations while others report no significant differences in mean concentrations (Sorensen et al., 1994; Guentzel et al., 2001; Hall et al., 2005). Gaseous evasion of Hg⁰ from marine waters is a significant global source of atmospheric Hg and may also contribute to elevated depositional fluxes in coastal regions (Mason and Sheu, 2002). Holmes et al. (2009) suggest that elevated levels of Br in the marine boundary layer are important in transforming Hg⁰ to RGM, the more readily deposited gaseous form of Hg.

Like many areas in New England, New Hampshire (NH) air quality is adversely affected by large power plants in the Midwest as well as urban areas located to the south along the East coast of the United States (NHDES, 2004). Two coal combustion power plants are also located in the southern portion of NH and are likely contributors to the local atmospheric load of Hg. Within the waterways of the Northeastern United States, including NH, biological species have been identified as containing elevated Hg

levels (Chen et al., 2005; Evers, 2007) with atmospheric deposition considered the dominant source in undisturbed watersheds (Chen et al., 2005). Three MDN sites were previously located in NH with sample collection lasting from 7 to 16 months and the most recent sampling terminated in 2005. This lack of Hg wet deposition information was filled using measurements conducted by the AIRMAP program (<http://airmap.unh.edu>) at the University of New Hampshire (UNH). Event -based wet deposition samples were collected over a 36-month time period from July 2006 – August 2009. In this study, seasonal and annual variations of Hg wet deposition and concentration from a site in Southern NH are compiled and compared to contemporaneous results from MDN sites in the adjacent state of Maine (ME) and data from three MDN sites previously located in New Hampshire. The purpose of this study is to provide an overview of the seasonal Hg wet deposition patterns at TF, briefly examine meteorological conditions and gas phase indicators of anthropogenic air mass sources in relation to Hg wet deposition, and compare RGM measurements and estimated RGM dry deposition to Hg wet deposition.

Event-based precipitation sampling is necessary to elucidate relationships with meteorological and atmospheric chemical conditions. MDN sites predominantly collect weekly samples, not individual event samples. Results indicate single weekly samples contribute significantly to the annual Hg load (VanArsdale et al., 2005). Collecting samples over pre-determined time intervals can obscure the contribution of single events and relationships with other factors. An event-based sampling site in Underhill, VT (MDN site VT99) reports discrete precipitation events can contribute between 5-17% of the total annual wet deposition (Keeler et al., 2005). The event-based sampling at TF provides the opportunity to evaluate relationships between Hg wet deposition, meteorological conditions and gas phase species.

The more soluble gaseous species, RGM, is thought to be the predominant source of Hg in wet deposition with minor contributions from washout of Hg^P (Schroeder and Munthe, 1998; Guentzel et al., 2001; Sakata and Asakura, 2007; Kieber et al., 2008). Simultaneous measurements of gas phase Hg species and wet deposition offer the opportunity for a more thorough understanding of processes affecting Hg deposition and more accurate estimates of wet + dry deposition. Long-term Hg wet deposition measurements exist at many locations within the United States and Canada as part of the MDN; however, long-term contemporaneous Hg gas phase and Hg wet deposition measurements are lacking (Lindberg et al., 2007; Selin, 2009; Zhang et al., 2009). A recent study (Engle et al., 2010) reports Hg gas phase speciation data, Hg^P, and Hg wet deposition fluxes at nine sites located in the central and eastern United States and Puerto Rico, none of which had data for more than one year. Zhang et al. (2009) provide an overview of the current knowledge regarding the dry deposition of Hg including Hg⁰, RGM, and Hg^P. The limited measurement data that are available for RGM deposition have large uncertainties due to the very low ambient concentration and instrument detection limits, the frequent use of surrogate surfaces in measurement techniques, the small vertical gradients in RGM concentration, and the effects of fast chemical reactions and advections from local sources (Zhang et al., 2009). In this study we use automated continuous RGM measurements over a 35 month time period to generate a simple estimate of the RGM deposition velocity (V_d) and RGM dry deposition. This is the first multi-year comparison of Hg wet deposition and RGM and provides insights into seasonal variations in Hg deposition pathways.

Sample collection and analysis

Precipitation samples were collected at Thompson Farm (TF) (43.11°N, -70.95°W, 24 m elevation) located in Durham, New Hampshire, USA (Figure II.1). The

sample site is situated in a rural, residential and agricultural setting immediately surrounded by agricultural fields and mixed hardwood and pine forests. It is approximately 25 km from the Gulf of Maine and 110 km north of the city of Boston. The UNH AIRMAP program maintains and collects numerous atmospheric chemistry measurements at TF (Mao and Talbot, 2004; Chen et al., 2007; Darby et al., 2007; Mao et al., 2008; Sigler et al., 2009a). Meteorological data used in this study (temperature, solar radiation, precipitation amount) are from the NOAA Climate Reference Network (CRN) site co-located at TF. Information about CRN data measurement and collection techniques is available at www.ncdc.noaa.gov/crn/instrdoc.html.

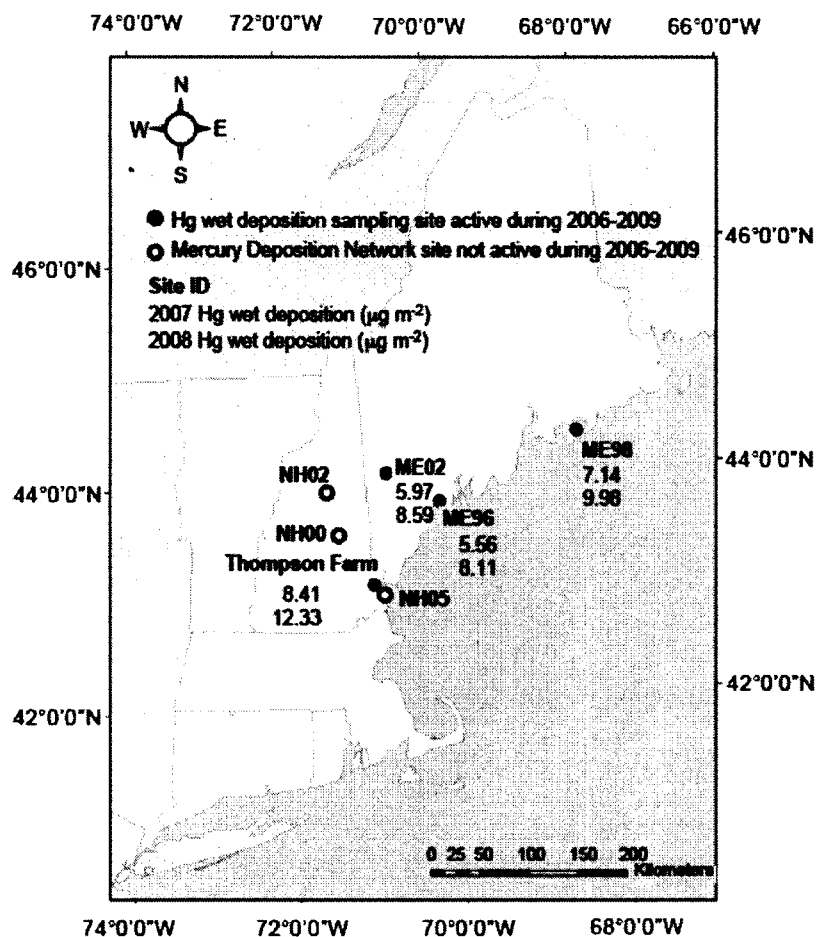


Figure II.1. Thompson Farm location and Mercury Deposition Network Locations in Maine and New Hampshire.

Wet deposition samples were collected using a modified Aerochem automated precipitation sampler, identical to samplers used in the MDN. Sample collection bottles were manually changed on a primarily event-based schedule. Trace metal sampling techniques were followed in accordance with EPA method 1669. The sampling train consisted of acid washed polyethylene funnels placed directly into pre-acidified and acid washed fluorinated ethylene propylene (FEP) bottles. Prior to sample deployment, bottle blanks were collected and sample bottles were treated with 1.25 mL of 6N HCl for sample preservation.

Upon collection, samples were preserved in the original collection bottle with the addition of trace metal grade hydrochloric acid and bromine monochloride to a final concentration of 0.5%. Samples were analyzed with a Tekran model 2600 dual amalgamation cold vapor atomic fluorescence spectrometer following a modified version of EPA method 1631 recommended in the Tekran user's guide. The average system blank value over all sample analyses was 0.45 ng L⁻¹ and the average method detection limit was 0.08 ng L⁻¹ as determined by three times the standard deviation of the system blank. The average bottle blank abundance was 0.09 ng. ORMS-3 and ORMS-4 (National Research Council, Canada) were used as external standards and results are within range of the accepted values. Final concentration values were corrected for system and bottle blanks. Precipitation samples with a collected volume of less than 20 ml are excluded from this data set (n=21). The Hg wet deposition data discussed in this study consist of 162 wet-only samples collected from 21 July 2006 to 30 August 2009.

RGM has been measured at TF since November 2006 using a KCl-coated denuder module attached to a cold vapor atomic fluorescence spectrometer (Tekran model 2537A; for details see Sigler et al., 2009a). The RGM sampling interval was 2 hours followed by a 30 minute flush with zero air and heating cycle to desorb the RGM

and allow for quantification as Hg^0 by the Tekran 2537A unit. Due to the addition of in-line Hg^{P} measurements in February 2009, the desorption interval increased to 60 minutes. Following this change the zero flushes showed no evidence of contamination, and there were no significant differences in Hg^0 and RGM levels. The limit of detection for RGM determined from three times the standard deviation of the average blank was approximately 0.1 ppqv.

Hg wet deposition seasonal patterns and inter-annual variability

Wet-only samples were collected at TF from July 21, 2006 to August 30, 2009 and represent 260 precipitation events. In this study, we define a precipitation event as a period of precipitation bordered by a twelve-hour time interval of no precipitation. An in-depth analysis of the meteorological conditions resulting in precipitation was not conducted as part of this study, therefore the potential exists that our definition of an event could include the passage of two different storm fronts within 12 hours of each other. Ninety-seven samples (60%) represent single events and 45 samples (28%) represent two precipitation events. Figures II.2a-c show the measured concentration, calculated deposition, and total precipitation for each sample in the study period. The maximum Hg concentration was 65.09 ng L^{-1} occurring on July 12, 2007. The maximum single event deposition was 1.74 $\mu\text{g m}^{-2}$ and occurred from July 23 to July 24, 2008. This single precipitation event constituted almost 6% of the total wet deposition at TF during this three-year study and 14% of the annual load for 2008. As shown in Figure II.2b, single precipitation events with elevated Hg deposition levels can account for a substantial portion of the total deposition. Similarly, Keeler et al. (2005) also report a single event contributing approximately 17% to the annual Hg wet deposition load from event-based sampling in Underhill, VT.

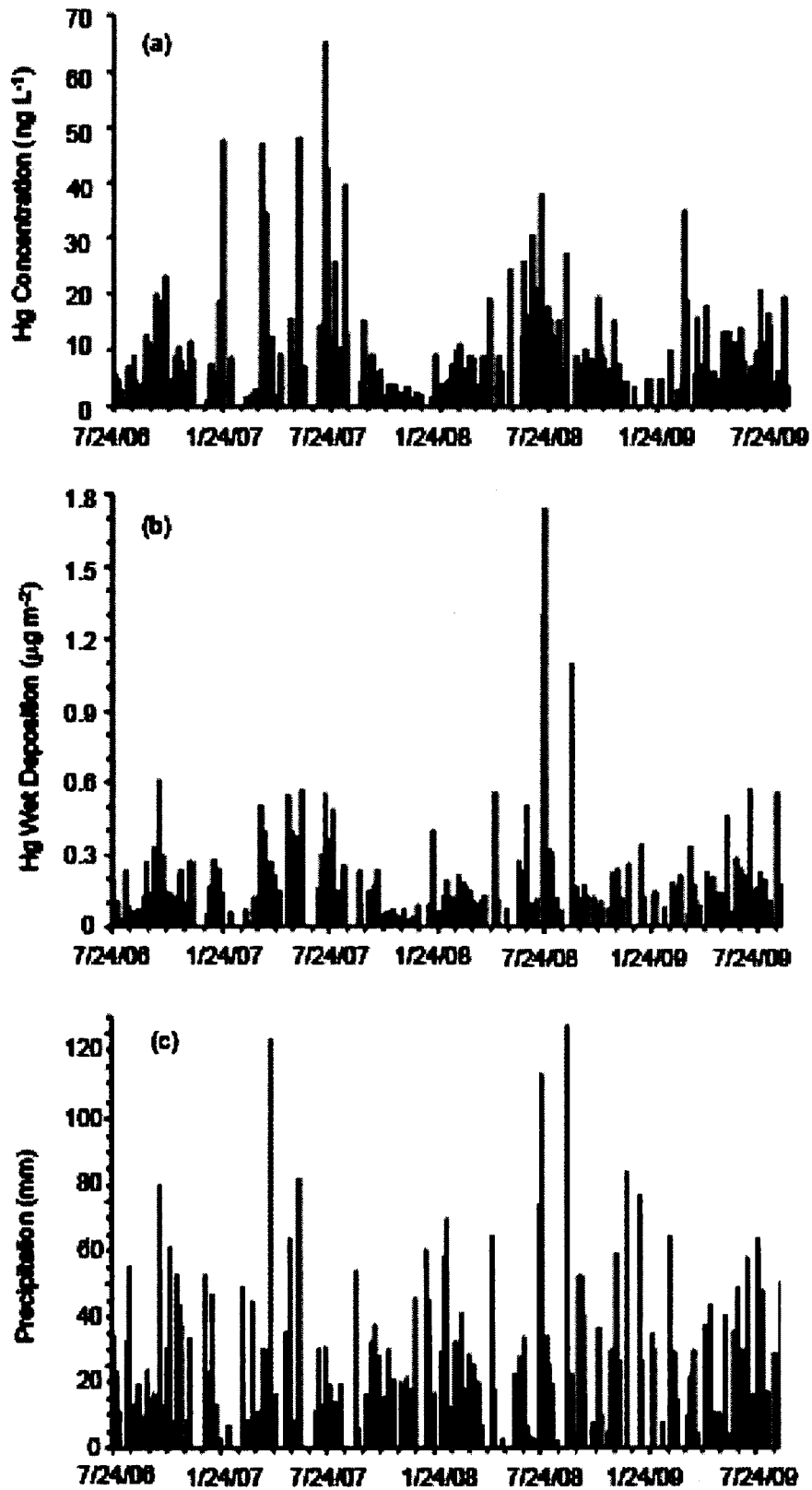


Figure II.2. Time series of wet deposition samples from Thompson Farm; (a) Hg concentration, (b) Hg wet deposition, (c) precipitation amount.

During the 37-month sampling period at TF, the cumulative Hg wet deposition was $30.78 \mu\text{g m}^{-2}$ and the total precipitation depth was 4.28 meters. The seasonal and annual variations in Hg concentration and wet deposition are summarized in Table II.1. In this study, seasons are delineated according to the calendar definition. In general, the summer and spring exhibited elevated Hg concentrations and wet deposition with an unusually large wet deposition value in summer 2008.

The seasonal volume weighted mean (VWM) concentrations of Hg in precipitation at TF are shown in Figure II.3a and listed in Table II.1. The VWM concentrations are elevated during the spring and summer seasons in comparison to the fall and winter seasons. These seasonal variations in VWM Hg concentrations are annually repeatable. The greatest seasonal VWM Hg concentrations at TF occurred in both summer seasons (summer 2007 = 14.85 ng L^{-1} ; summer 2008 = 12.48 ng L^{-1}), with the second highest seasonal concentrations occurring in the spring seasons of each year. The summer VWM Hg concentrations are 2.2 - 3.4 times greater than the fall and winter values. There is little variability in the VWM concentrations at TF for the same season from year-to-year. These seasonal variations are similar to previously reported patterns at MDN sites within northeastern North America (Keeler et al., 2005; VanArsdale et al., 2005; Prestbo and Gay, 2009).

Total seasonal Hg wet deposition at TF is shown in Figure II.3b and listed in Table II.1. The Hg wet deposition is calculated as the product of the event concentration and amount of precipitation (Figure II.3c). Patterns in seasonal Hg wet deposition are less consistent than the VWM concentrations and are linked more closely to precipitation totals. In 2007 the highest seasonal deposition, $3.39 \mu\text{g m}^{-2}$, occurred in the spring, while in 2008 it was observed in the summer with a value of $6.39 \mu\text{g m}^{-2}$. The

large deposition in summer 2008 reflects the combination of typically greater summer Hg concentrations and the above normal precipitation for that season (Figure II.3c). The total amount of precipitation received in summer 2008 was 180% above the 30 year summer average in New Hampshire (<http://www.nrcc.cornell.edu>). Similarly, the elevated deposition at TF during the 2007-2008 winter, compared to other winters, is most likely due to the elevated amount of precipitation, which was 154% above the 30 year winter average (<http://www.nrcc.cornell.edu>).

Annual Hg wet deposition varied over the duration of this study and was strongly linked to annual precipitation totals. During the calendar years 2007 and 2008 the Hg wet deposition at TF was $8.41 \mu\text{g m}^{-2} \text{yr}^{-1}$ and $12.33 \mu\text{g m}^{-2} \text{yr}^{-1}$, respectively with corresponding precipitation totals of 114.1 cm and 160.3 cm. Between these two years the amount of precipitation increased by 40% and the annual Hg wet deposition increased by 47%. These increases are similar in magnitude, indicating that the large annual Hg wet deposition for 2008 is primarily a consequence of enhanced precipitation. The amount of precipitation in New Hampshire during 2008 was 43% above the 30 year normal and the highest annual amount of precipitation based on a 114 year record (<http://www.nrcc.cornell.edu>). In contrast, the amount of precipitation at TF during 2007 was only 11% above the normal. To put the annual Hg wet deposition in context, the typical annual fluxes reported for MDN sites in the northeastern United States (NY, NJ, and New England) and eastern Canada from 1996-2005 were $4\text{-}8 \mu\text{g m}^{-2} \text{yr}^{-1}$ (Prestbo and Gay, 2009). The Hg annual wet deposition at TF for 2007 is slightly above this range, whereas the annual deposition for 2008 is >50% higher. This comparison in annual Hg wet deposition is made to emphasize the elevated deposition measured at TF during 2008. Comparisons between different time periods and locations should be made

with caution due to the varying conditions such as the proximity and output of emission sources that may affect deposition and change with time and location.

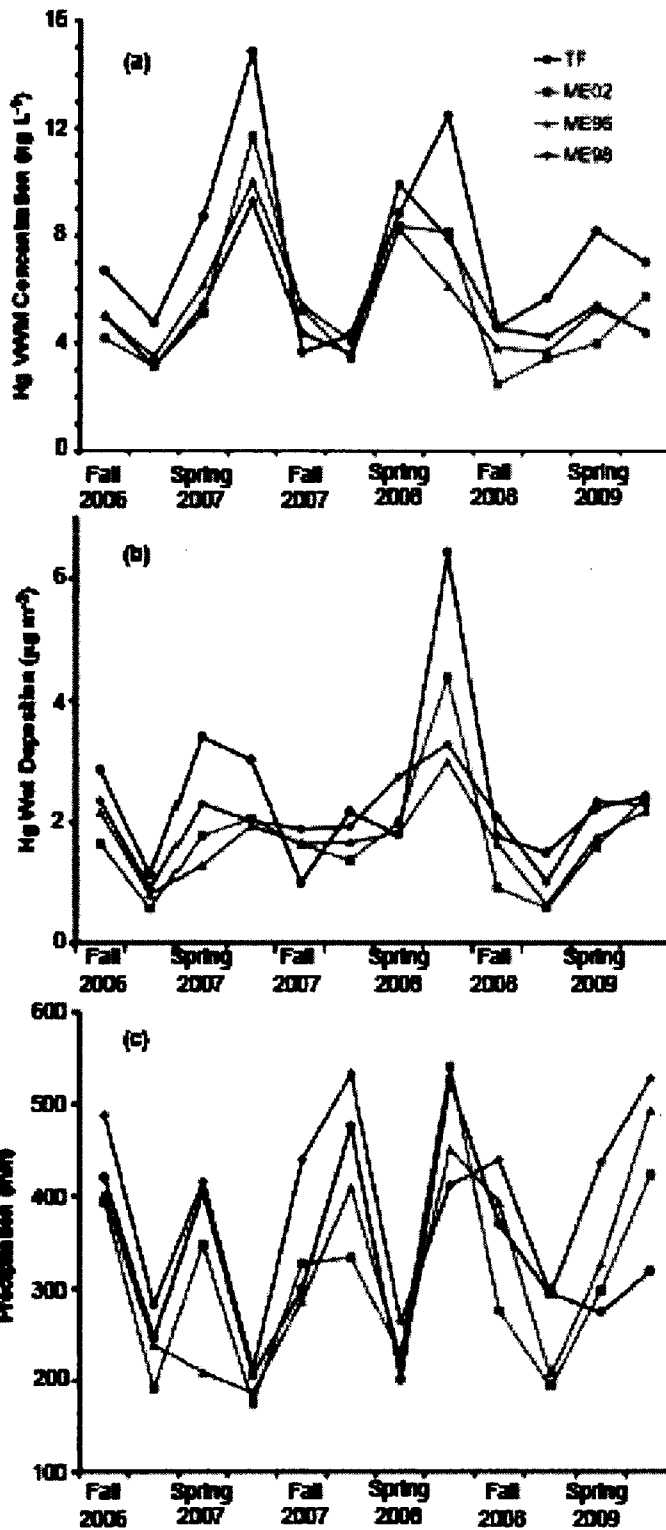


Figure II.3. Seasonal Hg volume weighted mean concentration (a), Hg wet deposition (b), and precipitation amount (c), at Thompson Farm and Mercury Deposition Network sites located in Maine.

Season	Precipitation Total (cm)	Total	Deposition ($\mu\text{g m}^{-2}$)			Concentration (ng L^{-1})			VWM concentration (ng L^{-1})
			Mean	Median	Range	Mean	Median	Range	
7/21/06 to 9/20/06	22.46	1.16	0.116	0.089	0.027 – 0.263	6.16	5.05	1.39-12.51	5.23
Fall 2006	42.02	2.85	0.190	0.139	0.058 – 0.600	9.63	8.10	2.28 – 23.06	6.71
Winter 2006- 2007	24.58	1.12	0.125	0.121	0.016 – 0.274	10.50	5.90	0.96 – 47.50	4.76
Spring 2007	40.13	3.39	0.339	0.379	0.030 – 0.561	18.14	10.57	0.99 – 47.89	8.69
Summer 2007	20.59	3.02	0.275	0.234	0.090 – 0.548	22.84	14.24	4.24 – 65.09	14.85
Fall 2007	30.26	0.99	0.083	0.061	0.023 – 0.231	3.39	2.71	0.75 – 8.94	3.67
Winter 2007- 2008	47.53	2.17	0.135	0.117	0.055 – 0.399	5.79	5.36	1.41 – 10.88	4.33
Spring 2008	19.97	1.79	0.162	0.107	0.066 – 0.553	12.49	8.64	3.48 – 25.81	8.84
Summer 2008	52.52	6.37	0.354	0.112	0.015 – 1.737	15.29	14.74	4.21 – 37.72	12.48
Fall 2008	37.00	1.76	0.125	0.114	0.039 – 0.256	7.55	6.77	2.24 – 19.21	4.60
Winter 2008- 2009	29.86	1.49	0.149	0.133	0.050 – 0.339	9.04	4.50	2.72 – 34.83	5.67
Spring 2009	27.37	2.23	0.172	0.137	0.020 – 0.452	9.52	7.86	3.57 – 17.76	8.18
6/21/09 to 8/30/09	37.36	2.62	0.202	0.168	0.042 – 0.565	9.94	9.70	3.34 – 20.62	7.02
Year 2007	114.1	8.41	0.205	0.155	0.016-0.561	13.68	6.88	0.75-65.09	7.97
Year 2008	160.3	12.33	0.209	0.115	0.015-1.74	10.41	8.41	1.66-37.72	8.09

Table II.1. Seasonal and annual total precipitation, Hg wet deposition, and concentration summary statistics for Thompson Farm. Spring and summer are shaded for easier visual comparison by season.

Comparison with MDN sites

The wet only results from TF are compared to samples collected during the same time period at MDN sites located in Maine (Figure II.3a-c). These MDN sites were chosen for comparative purposes due to their proximity to TF, the coastal locations of ME96 and ME98 and locations downwind of the city of Boston. Patterns in seasonal VWM concentrations and Hg wet deposition are generally consistent between TF and the Maine MDN sites (Figures II.3a and II.3b) with elevated levels during spring and summer seasons. The greatest seasonal VWM concentration during this sampling period occurred at all locations for summer 2007. The 2006-2007 winter had the lowest seasonal VWM Hg concentration at TF and all Maine MDN sites with the exception of ME02. Similarly, all sites had the highest total seasonal Hg wet deposition in summer 2008 and low wet deposition totals during the winter seasons.

The seasonal VWM Hg concentrations and seasonal wet deposition at TF are typically greater than the Maine MDN sites (Figures II.3a and II.3b), possibly due to a combination of elevated Hg concentrations and precipitation. TF is the most southerly of the sites resulting in slightly warmer temperatures compared to the MDN sites and is also located nearer large urban pollution sources such as Boston and New York. Mao and Talbot (2004) indicate TF can be influenced by transport of polluted air masses from the Boston and Mid-Atlantic States region. Thus it is reasonable to hypothesize that TF receives more Hg due to the proximity of anthropogenic emissions. Also the amount of precipitation recorded at TF is consistently second highest amongst these sites with MDN site ME98 regularly receiving the most precipitation. In-depth studies are warranted to understand the causes for such geographic differences in Hg wet deposition.

For an historical perspective, results from this study are briefly compared to the three MDN sites previously located in New Hampshire (Figure II.1). The only historical

site with results for four complete seasons is NH05 with data available from March 2001 to June 2002. At NH05, summer 2001 had the highest VWM concentration (11.51 ng L^{-1}) and spring 2002 had the greatest seasonal Hg deposition and precipitation totaling $2.59 \mu\text{g m}^{-2}$ and 37.3 cm, respectively. Hg wet deposition data is available for NH02 from February 2004 to February 2005. For the seasons with complete data available, spring 2004 had the highest VWM Hg concentration (9.02 ng L^{-1}). Summer 2004 had the greatest wet deposition and precipitation totaling $3.47 \mu\text{g m}^{-2}$ and 46.3 cm, respectively. At NH00 data are only available for seven months from May 2001 through December 2001. The summer had greater Hg wet deposition and VWM concentration than the fall. The seasonal variations in the data collected from the MDN sites previously located in NH are consistent with our findings at TF. The spring and summer have elevated VWM concentrations and Hg wet deposition in comparison to the fall and winter.

Influence of meteorological conditions and other trace gases on Hg wet deposition

Relationships were examined between Hg wet deposition, Hg concentration, and meteorological parameters including temperature and solar radiation at the TF site. Non-parametric Kendall's τ was calculated to determine correlations between these parameters. Only precipitation samples representative of single events are included in this analysis. Table II.2 summarizes these statistical results.

	Hg wet deposition τ	Hg concentration τ
Daily average temperature	0.07	0.23*
Daily total solar radiation	-0.02	0.29*
Daily average CO	-0.01	0.00
Daily average NO _y	-0.09	-0.11
Daily maximum RGM	0.07	0.09
RGM depletion during precipitation event	0.10	-0.02

Table II.2. Kendall's τ correlation co-efficients for Hg wet deposition and Hg concentration with meteorological conditions and gas phase measurements at Thompson Farm. Asterisks indicate $p < 0.05$.

Previous studies attribute regional and seasonal differences in Hg wet deposition to temperature differences (Keeler et al., 2005). On an event basis there is weak correlation between the average daily temperature and Hg concentration ($\tau = 0.23$, $p < 0.05$). The correlation between average daily temperature and Hg wet deposition is very minor and not statistically significant. Additionally, studies suggest photochemistry is important in the production of RGM (Lin and Pehkonen, 1999; Sigler et al., 2009a) implying a relationship with Hg wet deposition (Selin and Jacob, 2008). In this study we looked into relationships between solar radiation and Hg wet deposition. At TF, Hg concentration is correlated with total daily solar radiation ($t=0.29$, $p < 0.05$). The lack of strong correlations on an event basis between temperature, solar radiation and Hg wet deposition and concentrations indicates that effects from these parameters are not directly related to Hg wet deposition.

To investigate anthropogenic contributions to Hg wet deposition, we examined links with Hg wet deposition and gas phase concentrations of carbon monoxide (CO), and total reactive nitrogen (NO_y), commonly used indicators for anthropogenic influence (Mao et al., 2008). CO is emitted mainly from mobile combustion sources while NO_y includes compounds emitted directly from fossil-fuel combustion and oxidation products of such compounds. This initial investigation of relationships between CO, NO_y, and Hg

concentration in precipitation and wet deposition does not suggest strong or statistically significant correlations ($p < 0.05$). An in-depth analysis of individual events with identified air mass source regions may provide more information on the lack of influence of these trace gases on Hg wet deposition.

Linkage between RGM and Hg wet deposition

RGM is more soluble than Hg^0 and therefore important in contributing to both the wet and dry deposition of Hg (Schroeder and Munthe, 1998; Selin, 2009). However, few studies report long-term concurrent measurements of RGM and Hg wet deposition (Engle et al., 2010). RGM has been measured at TF since October 2006 (Sigler et al., 2009a; Mao et al., 2011) and we compare these measurements with Hg wet deposition measurements during the nearly three-year period from October 2006 through August 2009.

Elevated RGM mixing ratios typically occur in winter and spring seasons at TF (Figure II.4), and the typical diurnal cycle for RGM is a minimum at night with a rapid increase during the morning to peak levels at midday (Sigler et al., 2009a; Mao et al., 2011). Based on relationships of RGM with trace gases such as CO, CO₂, and SO₂, and meteorological conditions at TF, Sigler et al. (2009) suggest the elevated RGM mixing ratios during winter months may be due to local emissions from heating sources and slower RGM removal processes. The elevated spring RGM mixing ratios are attributed to photochemical production and high biogenic emissions of Hg^0 .

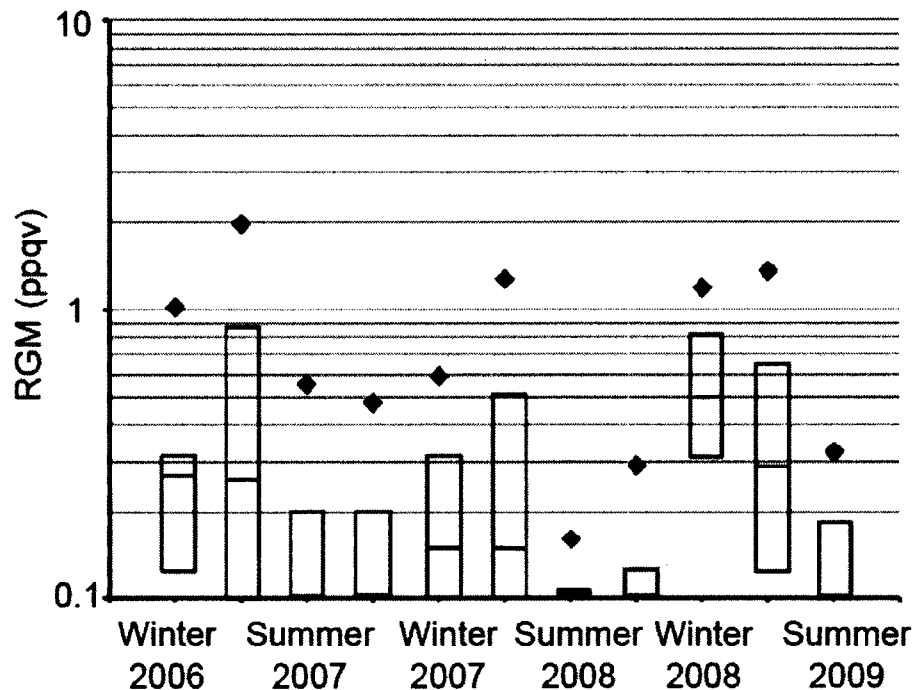


Figure II.4. Seasonal variations in RGM at TF. Each box encompasses the 25th to 75th percentiles and the solid horizontal line within each box represents the median value. The black diamonds indicate the 90th percentile.

Scavenging of RGM during precipitation events

RGM mixing ratios typically decline during precipitation events at TF. Sigler et al. (2009a,b) and Mao et al. (2011) observed RGM depletion during precipitation events at this site and others have made similar observations at diverse locations (Lindberg and Stratton, 1998; Laurier and Mason, 2007; Yatavelli et al., 2006). Despite this indication of RGM scavenging during precipitation events at TF, correlations between Hg wet deposition and Hg concentration in precipitation versus daily maximum RGM and RGM depletion during precipitation events were not statistically significant (Table II.2). Our results indicate a disconnect between seasonal surface level RGM mixing ratios and total aqueous Hg in wet deposition. RGM mixing ratios are greatest during the winter however Hg concentrations in precipitation and wet deposition are lowest during the winter. Possible explanations for the low Hg wet deposition in winter are the

underestimation of wet deposition due to inefficient snow collection and/or less effective scavenging of RGM by snow.

A comparison between the collected sample volume and precipitation amount reveals that lower sampling efficiencies occur most frequently during winter precipitation events. Based on the surface area of the funnel used in our sampling train, 1 mm of precipitation should result in 12 ml of collected sample. A linear regression between the actual amount of sample collected and amount of precipitation during the non-winter seasons at TF reveals the same result (i.e. 1 ml of precipitation ~ 12 ml of sample, $r^2 = 0.99$). Not all winter precipitation events are under sampled, however 13 of a total 16 precipitation events with a sampling efficiency of less than 80% occur during the winter. It is not known how the inefficient collection of snow affects the measured Hg concentration at TF, however based on a limited study at a nearby MDN site, the lower sampling efficiency may result in low Hg concentrations. Nelson et al. (2008) compare event based snow sampling techniques at MDN site ME98. Their results show higher snow water equivalents (i.e. collection efficiency) and Hg snowfall concentrations in samples collected using a collection method different than the MDN.

In this study, ineffective scavenging of RGM by snow is evidenced by the less frequent depletion of RGM below the limit of detection (LOD, 0.1 ppqv) during winter precipitation events at TF. Seven of 19 winter precipitation events (37%) result in RGM mixing ratios below the LOD. RGM mixing ratios during summer precipitation events dip below the LOD at a much higher frequency; 17 of 20 events (85%). These seasonal variations in RGM removal efficiencies substantiate the hypothesis that seasonal variations in Hg wet deposition are due in part to less effective scavenging of gas phase Hg by snow (Keeler et al., 2005; Selin and Jacob, 2008).

Estimation of RGM dry deposition

It is important to gauge the relative contribution of Hg wet deposition in comparison with other atmospheric Hg sinks such as RGM dry deposition. To accomplish this we performed an order-of-magnitude estimate for RGM dry deposition using long-term continuous measurements of RGM mixing ratios. Estimates of RGM dry deposition velocity and deposition at TF were calculated based on nighttime depletion events, which are most common during warm season (May to September) nocturnal inversions in the planetary boundary layer. The method has been employed in Talbot et al. (2005), Mao et al. (2008), and Sigler et al. (2009a), and the step-by-step estimate is elucidated in Russo et al. (2010). A brief explanation of this method is given here. Nocturnal inversions at TF are evidenced by the depletion (<5ppbv) of atmospheric ozone and Hg⁰ (Mao et al., 2008). Concurrent depletions were also observed in RGM. To obtain a robust estimate we used the diurnal cycle average over all days from the warm season with the occurrence of nocturnal inversions. The average rates of RGM depletion and RGM concentration during these inversions were calculated to solve for the deposition velocity in the following equation:

$$V_d = \frac{dC}{dt} \cdot \frac{H}{\bar{C}} \quad (1)$$

where V_d is the deposition velocity, dC/dt is the rate of change in RGM concentration from the average diurnal cycle in RGM over all inversion events, \bar{C} is the average RGM concentration over the depletion period, and H is the boundary layer height. In these calculations a constant boundary layer height of 125 m is applied (Talbot et al., 2005; Mao et al., 2008; Russo et al., 2010). This calculation also assumes that during the nocturnal inversions dry deposition is the only loss mechanism of RGM and there is no RGM production, therefore the calculated V_d should be considered a maximum due to the potential for RGM loss due to aerosol uptake.

Nocturnal inversion events were identified by the nighttime depletion of ozone to less than 5 ppbv with a corresponding decrease in RGM to less than 0.1 ppqv. The number of inversion events per warm season varied from 17 to 21 during 2007 to 2009. The average RGM concentration over the depletion period varied annually from 0.13 to 0.20 ppqv however, the RGM depletion based on the average diurnal cycle was always complete in the time window of 00:00 to 03:00 UTC. Using Eq. (1) the average RGM dry deposition velocity at TF is estimated to be 2.31 cm s^{-1} . This estimate is within the range of RGM dry deposition velocities reported in the literature (0.5 to 7.6 cm s^{-1}) from a variety of measurement methods, surface compositions, locations, and seasons (Zhang et al., 2009 and references therein).

RGM dry deposition at TF was estimated using measured RGM mixing ratios and a dry deposition velocity of 2.31 cm s^{-1} . The seasonal and annual estimated RGM dry deposition and comparison to Hg wet deposition is shown in Figure II.5 and Table II.3. There is distinct variation in seasonal dry deposition of RGM. The greatest seasonal RGM dry deposition ($>0.6 \mu\text{g m}^{-2}$) occurs in the winter and spring (excluding winter 2007), following the seasonal pattern in RGM mixing ratios. Summer and fall exhibit low RGM dry deposition values, all below $0.4 \mu\text{g m}^{-2}$ (Figure II.5).

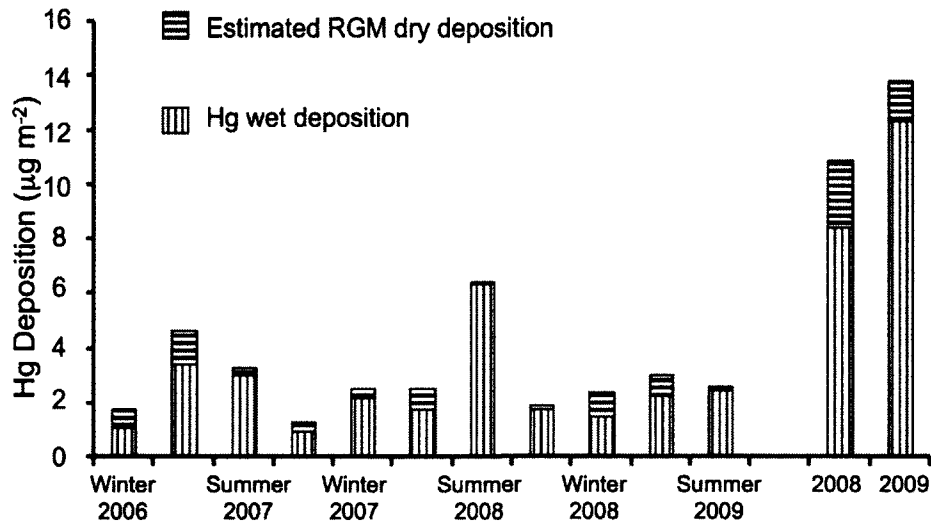


Figure II.5. Seasonal and annual Hg wet deposition and estimated RGM dry deposition at TF.

Comparison between RGM dry deposition and Hg wet deposition

Estimated RGM dry deposition is less than the measured Hg wet deposition for all seasons and on an annual basis (Figure II.5). Our results suggest that the relative contribution of Hg wet deposition and RGM dry deposition to the total Hg deposition flux at TF varies greatly by season and is opposite in phase with ratios of Hg wet deposition to RGM dry deposition ranging from 1.6 in the winter to 80 during summer 2008 (Figure II.6). Large Hg wet deposition and low RGM dry deposition typically occurs in summer. The greatest ratio occurred in summer 2008 reflecting the exceptionally large amount of precipitation and Hg wet deposition and the lowest RGM dry deposition estimate of all summers. On an annual basis the ratios of Hg wet deposition to RGM dry deposition are moderate in comparison to the large seasonal variations at TF. The ratio for annual year 2008 is more than double the ratio for 2007 (8.5 and 3.5, respectively) and the large ratio likely reflects the record amount of precipitation in 2008.

We can compare our calculations to only a few studies from the literature reporting both Hg wet deposition and RGM dry deposition (Table II.4). Published

comparisons of Hg wet deposition to total Hg dry deposition ($\text{Hg}^0 + \text{RGM} + \text{Hg}^{\text{P}}$) in New Hampshire are based on modeled results (Miller et al., 2005; Han et al., 2008). Miller et al. (2005) estimate a total Hg flux of $21.1 \mu\text{g m}^{-2} \text{y}^{-1}$ in New Hampshire with approximately equal contributions of 7.4 and $7.5 \mu\text{g m}^{-2} \text{y}^{-1}$, respectively, from Hg^0 and RGM dry deposition followed by a wet deposition contribution of $5.8 \mu\text{g m}^{-2} \text{y}^{-1}$. Minor contributions are attributed to Hg^{P} and cloud water at 0.38 and $0.058 \mu\text{g m}^{-2} \text{y}^{-1}$, respectively. Miller et al. (2005) state that their RGM estimates should be considered within the correct order magnitude but they have low confidence in the exact value due to the lack of measurement data for comparison. Han et al. (2008), simulated the total atmospheric deposition of RGM and Hg^{P} in New Hampshire for the years 1996, 1999, and 2002 based on Hg emission inventories for the state and adjacent areas. Their ratios of annual wet to dry Hg deposition range from 1.01 to 0.57. RGM deposition ranges from a factor of 6 to 21 times greater than Hg^{P} deposition. The model used by Han et al. (2008) does not account for regional and global sources of Hg or atmospheric reactions.

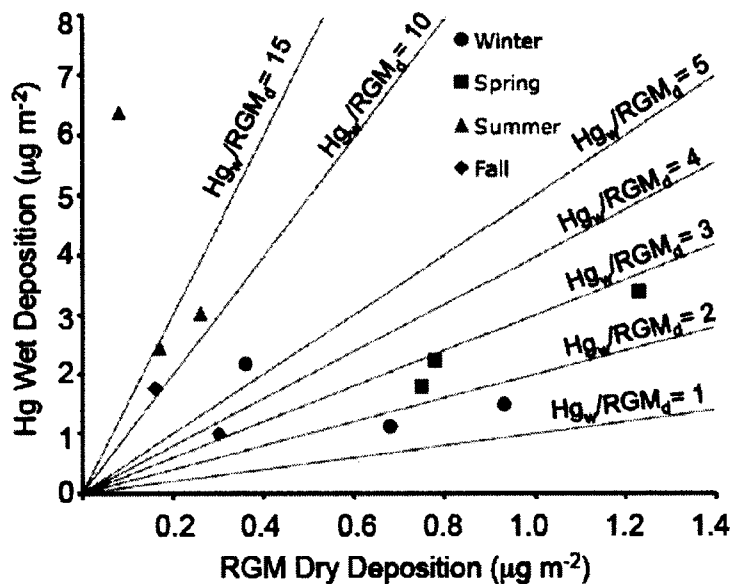


Figure II.6. Seasonal Hg wet deposition and estimated RGM dry deposition at TF. Contour lines represent wet to dry deposition (Hg_w/RGM_d) ratios.

Annual ratios of Hg wet deposition to RGM dry deposition for eight sites located in the eastern United States and Puerto Rico were calculated from data in Engle et al. (2010). Engle et al. (2010) determine RGM dry deposition using continuous RGM concentration measurements and a numerical resistance-based deposition model base. Miller et al. (2005) estimate higher annual fluxes of RGM dry deposition than Hg wet deposition for New Hampshire. In comparison the TF ratio for 2007 is within the range of values from Engle et al. (2010) for rural and coastal sites and the TF ratio for 2008 is slightly greater (excluding Puerto Rico). In contrast to the findings of Miller et al. (2005), results from our study, as well as those of Engle et al. (2010), demonstrate that annual Hg wet deposition fluxes are typically greater than RGM dry deposition fluxes. The observations hold across many different sites, with the exception of one urban site of Engle et al. (2010), in spite of differences in geographic location and sampling years.

Season	Hg wet deposition ($\mu\text{g m}^{-2}$)	RGM dry deposition ($\mu\text{g m}^{-2}$)	Wet plus RGM dry deposition ($\mu\text{g m}^{-2}$)
Winter 2006-2007	1.12	0.68	1.80
Spring 2007	3.39	1.23	4.62
Summer 2007	3.02	0.26	3.28
Fall 2007	0.99	0.30	1.29
Winter 2007-2008	2.17	0.36	2.53
Spring 2008	1.79	0.75	2.54
Summer 2008	6.37	0.08*	6.45
Fall 2008	1.76	0.16*	1.92
Winter 2008-2009	1.49	0.93*	2.42
Spring 2009	2.23	0.78	3.01
6/21/09 to 8/30/09	2.44	0.17	2.61
Year 2007	8.41	2.43	10.84
Year 2008	12.33	1.45	13.78

Table II.3. Seasonal and annual Hg wet deposition and estimated RGM dry deposition, and the sum of Hg wet deposition and estimated RGM dry deposition at TF. The asterisks indicate seasons missing more than 3 days of RGM measurements. The seasonal daily average RGM was used to fill gaps in the data and calculate a total RGM flux. Spring and summer are shaded for easier visual comparison by season.

Location	Dates	Hg wet deposition ($\mu\text{g m}^{-2} \text{yr}^{-1}$)	RGM dry deposition ($\mu\text{g m}^{-2} \text{yr}^{-1}$)	Hg wet dep./RGM dry dep.	Reference
Alabama	12 April 2005 - 11 April 2006	10.9	2.2	4.95	Engle et al. (2010)
Illinois	01 Jan 2004 - 31 Dec 2004	11.0	51.8	0.21	Engle et al. (2010)
Massachusetts	5 Feb 2008 – 3 Feb 2009	2.9	1.0	2.9	Engle et al. (2010)
New Hampshire	None given	5.8	7.5	0.77	Miller et al. (2005)
New Hampshire	01 Jan 2007 - 31 Dec 2007	8.41	2.43	3.46	This study
New Hampshire	01 Jan 2008 - 31 Dec 2008	12.33	1.45	8.50	This study
North Dakota	01 Jan 2004 - 12 Dec 2004	3.3	1.7	1.94	Engle et al. (2010)
Puerto Rico	01 Jan 2006 - 31 Dec 2006	29.5	0.5	59	Engle et al. (2010)
South Carolina	23 May 2006 - 22 May 2007	6.5	1.8	3.61	Engle et al. (2010)
Virginia	01 Jan 2006 - 12 Dec 2006	9.0	1.4	6.43	Engle et al. (2010)
Wisconsin	28 June 2004 – 6 June 2005	6.7	5.3	1.26	Engle et al. (2010)

Table II.4. A comparison between annual Hg wet deposition and RGM dry deposition values reported in the literature and calculated in this study. Hg wet deposition to RGM dry deposition ratios are calculated from data provided in Engle et al. (2010) and Miller et al. (2005).

Summary and conclusions

Total aqueous Hg in precipitation samples collected at TF in Durham, NH from July 2006 to September 2009 demonstrate seasonal Hg wet deposition and VWM concentration patterns consistent with previous observations for the northeastern United

States with elevated values during the summer and spring seasons. Wet deposition samples from regional MDN sites collected during the same sampling interval exhibit similar seasonal patterns. Comparisons of the relative Hg precipitation concentrations and wet deposition fluxes between the TF and MDN sites suggest that the proximity to anthropogenic Hg sources may partially explain observed differences.

The quantity of precipitation also contributes to the seasonal and annual variations in Hg wet deposition. As observed at TF, the winter 2007-2008 and summer 2008 had above normal precipitation amounts and high Hg wet deposition fluxes. This relationship is also exhibited on an annual basis with the anomalously high amount of precipitation that fell during 2008 contributing to the very high annual Hg wet deposition flux for the year. While this observation may seem rudimentary (i.e., more precipitation equates to more wet deposition), it warrants noting as observed and predicted increases in precipitation amount and intensity in the mid-latitudes due to climate change (Easterling et al., 2000) imply Hg wet deposition fluxes will also increase.

Our multi-year dataset and event based sampling of Hg wet deposition and RGM measurements allows for seasonal comparisons. The inefficient scavenging of RGM by snowfall is evidenced by the less frequent depletion of RGM below the LOD during winter months. Although the winter wet deposition values are low, the RGM dry deposition estimates at TF indicate enhanced dry deposition in the winter. These seasonal changes in Hg deposition pathways are reflected in the seasonal ratios of Hg wet deposition to RGM dry deposition. These ratios differ greatly by season and range from a summer value of 79.6 to a winter value of 1.60. In general, the winter and spring ratios are lowest while the summer ratios are greatest. The elevated amounts of precipitation during 2008 likely influence our ratios of Hg wet to RGM dry deposition. The seasonality in the atmospheric Hg depositional mechanisms (wet vs. dry) may subsequently affect the fate and transport of Hg in aquatic and terrestrial ecosystems.

Improved quantification of Hg wet and dry deposition, via long term simultaneous measurements and advances in measurement technology, will lead to a better understanding of the biogeochemical cycle of Hg.

References

- Ariya, P.A., Dastoor, A.P., Amyot, M., Schroeder, W.H., Barrie, L., Anlauf, K., Raofie, F., Ryzhkov, A., Davignon, D., Lalonde, J., Stefen, A., 2004. The artic: a sink for mercury, *Tellus*, 56B, 397-403.
- Bushey, J.T., Nallana, A.G., Montesdeoca, M.R., Driscoll, C.T., 2008. Mercury dynamics of a northern hardwood canopy, *Atmos. Environ.*, 42, 6905-6914.
- Chen, C.Y., Stemberger, R.S., Kamman, N.C., Mayes, B. M., Folt, C.L., 2005. Patterns of Hg bioaccumulation and transfer in aquatic food webs across multi-lake studies in the Northeast US, *Ecotoxicology*, 14, 135-147.
- Chen, M., Talbot, R., Mao, H., Sive, B., Chen J., Griffin, R.J., 2007. Air mass classification in coastal New England and its relationship to meteorological conditions, *J. Geophys. Res.*, 112, D10S05.
- Choi, H.D., Sharac, T.J., Holsen, T.M., 2008. Mercury deposition in the Adirondacks: A comparison between precipitation and throughfall, *Atmos Environ.* 42: 1818-1827.
- Darby, L.S., McKeen, S.A., Senff, C.J., White, A.B., Banta, R., Post, M.J., Brewer, W.A., Marchbanks, R., Alvarez II, R.J., Peckham, S.E., Mao, H., Talbot, R., 2007. Ozone differences between near-coastal and offshore sites in New England: Role of meteorology, *J. Geophys. Res.*, 112, D16S91.
- Downs S.G., MacLeod, C.L., Lester, J.N., 2007. Mercury in Precipitation and its relation to bioaccumulation in fish: a literature review, *Water, Air and Soil Pollution* 108, 149-187.
- Easterling, D.R., Meehl, G.A., Parmesan, C., Changnon, S.A., Karl, T.R., Mearns, L.O., 2000. Climate Extremes: Observations, Modeling, and Impacts, *Science*, 289:5487, 2068-2074.
- Engle, M.A., Tate, M.T., Krabbenhoft, D.P., Schauer, J.J., Kolker, A., Shanley, J.B., Bothner, M.H., 2010. Comparison of atmospheric mercury speciation and deposition at nine sites across central and eastern North America, *J. Geophys. Res.*, 115, D18306, doi:10.1029/2010JD014064.
- Evers, D.C., Han, Y.J., Driscoll, C.T., Kamman, N.C, Goodale, M.W., Lambert, K.F., Holsen, T.M., Chen, C.Y., Clair, T.A., Butler, T., 2007. Biological mercury hotspots in the northeastern United States and southeastern Canada, *Bioscience*, 5, 29-43.
- Guentzel, J.L., Landing, W.M., Gill, G.A., Pollman, C.D., 2001. Processes influencing

- rainfall deposition of mercury in Florida, *Environ. Sci. Tech.*, 35, 863-873.
- Hall, B.D., Manolopoulos, H., Hurley, J.P., Schauer, J.J., St.Louis, V.L., Kenski, D., Graydon, J., Babiarz, C.L., Cleckner, L.B., Keeler, G.J., 2005. Methyl and total mercury in precipitation in the Great Lakes region, *Atmos. Environ.*, 39, 7557-7569.
- Holmes, C.D., Jacob, D.J., Mason, R.P., Jaffe, D.A., 2009. Sources and deposition of reactive gaseous mercury in the marine atmosphere, *Atmos. Environ.*, 43, 2278-2285, doi:10.1016/j.atmosenv.2009.01.051.
- Keeler, G.J., Gratz, L.E., Al-Wali, K., 2005. Long-term Atmospheric Mercury Wet Deposition at Underhill, Vermont. *Ecotoxicology*, 14, 71-83.
- Landis, M.S., and Keeler, G.J., 2002. Atmospheric mercury deposition to Lake Michigan during the Lake Michigan mass balance study, *Environ. Sci. Technol.*, 36, 4518-4524.
- Laurier, F., and Mason, R., 2007. Mercury concentration and speciation in the coastal and open ocean boundary layer, *J. Geophys. Res.*, 112, D06302, doi:10.1029/2006JD007320.
- Lin, C.J., Pehkonen, S.O., 1999. The chemistry of atmospheric mercury: a review, *Atmos. Environ.*, 33, 2067-2079.
- Lindberg, S.E., Stratton, W.J., 1998. Atmospheric mercury speciation: concentrations and behavior of reactive gaseous mercury in ambient air, *Environ. Sci. Technol.*, 32, 49-57.
- Lindberg, S., Bullock, R., Ebinghaus, R., Engstrom, D., Feng, F., Fitzgerald, W., Pirrone, N., Prestbo, E., Seigneur, C., 2007. A synthesis of progress and uncertainties in attributing the source of mercury in deposition, *Ambio*, 16, 19-32.
- Mao, H., Talbot, R., 2004. O₃ and CO in New England: Temporal variations and relationships, *J. Geophys. Res.*, 109, D21304, doi:10.1029/2004JD004913.
- Mao, H., Talbot, R.W., Sigler, J.M., Sive, B.C., Hegarty, J.D., 2008. Seasonal and diurnal variations of Hg⁰ over New England, *Atmos. Chem. Phys.*, 8, 1403-1421, www.atmos-chem-phys.net/9/1403/2008/.
- Mao, H., Talbot, R.W., in prep. Speciated mercury at a marine, coastal and inland sites in New England: Part 1. Temporal Variabilities, *Atmos.Chem, Phys. Discuss.*
- Mason, R.P., Lawson, N.M., Sheu, G.R., 2000. Annual and seasonal trends in mercury deposition in Maryland, *Atmos. Environ.*, 34, 1691-1701.
- Mason, R.P., Sheu, G.R., 2002. Role of the ocean in the global mercury cycle, *Global Biogeochem. Cycles*, 16, 1029-1040, doi:10.1029/2001GB001440.
- Miller E.K., Vanarsdale, A., Keeler, G.J., Chalmers, A., Poissant, L., Kamman, N.C., Brulotte, R., 2005. Estimation and mapping of wet and dry mercury deposition across northeastern North America, *Ecotoxicology*, 14, 53-70, 2005.

- NADP/MDN: National Atmospheric Deposition Program (NRSP-3)/Mercury Deposition Network, 2001, NADP Program Office, Illinois State Water Survey, 2204 Griffith Drive, Champaign, IL 61820, 2006-2009.
- Nelson, S.J., Johnson, K.B., Weathers, K.C., Loftin, C.S., Fernandez, I.J., Kahl, J.S., Krabbenhoft, D.P., 2008. A comparison of winter mercury accumulation at forested and no-canopy sites measured with different snow sampling techniques, *Applied Geochemistry*, 23, 384-398, doi:10.1016/j.apgeochem.2007.12.009.
- NHDES (New Hampshire Department of Environmental Services), 2004. *Air Pollution Transport and How it Affects New Hampshire*. NHDES, Concord, New Hampshire.
- Pacyna, E.G., Pacyna, J.M., 2002. Global emission of mercury from anthropogenic sources in 1995, *Water, Air and Soil Pollution*, 137, 149-165.
- Prestbo, E.M., and Gay D.A., 2009. Wet deposition of mercury in the U.S. and Canada, 1996-2005: Results and analysis of the NADP mercury deposition network (MDN), *Atmos. Environ.*, 25, 4223-4233.
- Rea, A.W., Lindberg, S.E., Scherbatskoy, T., Keeler, G.J., 2002. Mercury accumulation in foliage over time in two northern mixed hardwood forests, *Water, Air, and Soil Pollution*, 133, 49-67.
- Russo, R.S., Zhou, Y., Haase, K.B., Wingenter, O.W., Frinak, E.K., Mao, H., Talbot, R.W., Sive, B.C., 2010. Temporal variability, sources, and sinks of C₁-C₅ alkyl nitrates in coastal New England, *Atmos. Chem. Phys.*, 10, 1865-1883.
- Schroeder, W.H., Munthe, J., 1998. Atmospheric mercury- an overview, *Atmos. Environ.*, 32(5), 809-822.
- Seinfeld, J.H., Pandis, S.N, 1998. *Atmospheric chemistry and physics: From air pollution to climate change*, John Wiley and Sons, New York.
- Selin, N.E., and Jacob, D.J., 2008. Seasonal and spatial patterns of mercury wet deposition in the United States: Constraints on the contribution from North American anthropogenic sources, *Atmos. Environ.*, 42, 5193-5204.
- Selin, N.E., 2009. Global biogeochemical cycling of mercury: a review, *Annu. Rev. Environ. Resourc.* 34, 43-63.
- Selvendiran, P., Driscoll, C.T., Montesdeoca, M.R., Bushey, J.T., 2008. Inputs, storage, and transport of total methyl mercury in two temperate forest wetlands, *J. Geophys. Res.*, 113, G00C01, doi: 10.1029/2008JG000739.
- Sigler, J. M., Mao, H., and Talbot, R., 2009a. Gaseous elemental and reactive mercury in southern New Hampshire, *Atmos. Chem. Phys.*, 9, 1929-1942.
- Sigler, J.M., Mao, H., Sive, B.C., Talbot, R., 2009b. Oceanic influence on atmospheric mercury at coastal and inland sites: a springtime nor'easter in New England, *Atmos. Chem. Phys.*, 9, 4023-4030, www.atmos-chem-phys.net/9/4023/2009/.

- Sorensen J.A., Glass, G.E., Schmidt, K.W., 1994. Regional patterns of wet mercury deposition, *Environ. Sci. Tech.* 28(12), 2025-2032.
- Steding, D.J., and Flegal, A.R., 2002. Mercury concentration in coastal California precipitation: Evidence of local and trans-Pacific fluxes of mercury to North America, *J. Geophys. Res.*, 107(D24), 4764, doi:10.1029/2002JD002081.
- Talbot, R., Mao, H., Sive, B., 2005. Diurnal characteristic of surface level O₃ and other important trace gases in New England, *J. Geophys. Res.*, 110, D09307, doi:10.1029/2004JD005449.
- Vanarsdale, A., Weiss, J., Keeler, G., Miller, E., Boulet, G., Brulotte, R., Poissant, L., 2005. Patterns of mercury deposition and concentration in northeastern North America (1996-2002), *Ecotoxicology*, 14, 37-52.
- Yatavelli, R.L.N., Fahrni, J.K., Kim, M., Crist, K.C., Vickers, C.D., Winter, S.E., and Connell, D.P., 2006. Mercury, PM_{2.5} and gaseous co-pollutants in the Ohio River Valley region: Preliminary results from the Athens supersite, *Atmos. Environ.*, 40, 6650-6665.
- Zhang L., Wright, L.R., Blanchard, P., 2009. A review of current knowledge concerning dry deposition of atmospheric mercury, *Atmos. Environ.*, 43, 5853-5864.

CHAPTER III

MERCURY WET DEPOSITION IN THE MARINE ENVIRONMENT: COMPARISON TO A COASTAL SITE AND RELATIONSHIPS WITH DISSOLVED ORGANIC CARBON AND MAJOR ION CONCENTRATIONS

Introduction

The ocean-atmosphere interface is important in the global Hg cycle. Gaseous evasion of Hg from the oceans is the largest worldwide natural source accounting for approximately 35% of the total Hg global emissions (Pirrone et al., 2008). Atmospheric Hg exists in the gaseous phase primarily as elemental Hg (Hg^0) with an atmospheric lifetime of approximately one to two years (Lin and Pehkonen, 1999). Reactive gaseous mercury (RGM = HgCl_2 , HgBr_2 , HgOBr , and HgOCl) typically constitutes 5% or less of the total gaseous mercury (TGM) and has a much shorter atmospheric lifetime of several days to a few weeks (Lin and Pehkonen, 1999). Atmospheric Hg also exists in particulate form (Hg^{P}) at minor amounts (0.3%-0.9%) in background air (Lin and Pehkonen, 1999). Hg in precipitation consists primarily of scavenged RGM and Hg^{P} due to the higher solubility of these forms of Hg. Reactive mercury species (Hg^{2+}) are reported to compose from 14 to 95 % of the total mercury measured in precipitation samples (Hammerschmidt et al., 2007 and sources therein).

Recent studies indicate that brominated compounds, which are typically found in the marine environment, may facilitate oxidation of Hg^0 and contribute to the rapid cycling of Hg in the coastal and marine atmosphere (Holmes, et al., 2010; Hedgecock and Pirrone, 2001). Malcolm et al. (2003) suggest that sea salt aerosol may be an important sink for RGM in the marine boundary layer. Feddersen et al. (in prep) measured the size distribution of Hg^{P} at Appledore Island, the marine location discussed

in this manuscript, and found that 50-60% of the Hg^{P} was in aerosols of aerodynamic diameters $>2\mu\text{m}$. The association of Hg^{P} with these large size aerosols collected in the marine environment indicates a connection with sea salt.

Few studies compare Hg wet deposition in the marine environment to the coastal or continental environment. Mason et al. (1992) compare total mercury, reactive mercury and methyl mercury concentrations in precipitation samples collected in the equatorial Pacific Ocean and rural Wisconsin. The average Hg concentration in the Pacific Ocean precipitation was lower than the average continental concentration and was attributed to lower concentrations of Hg^{P} in the marine atmosphere compared to the Wisconsin site. In this study results are presented from a precipitation sampling campaign at marine and coastal locations. During summer 2009 precipitation samples were collected in the marine boundary layer from Appledore Island, (AI) and a coastal site, Thompson Farm (TF2). Samples at both locations were analyzed for total aqueous Hg to compare rainfall concentration and deposition between a marine and coastal site.

Co-located samples from AI were also analyzed for dissolved organic carbon (DOC) and a suite of major ions including Cl^- , SO_4^{2-} , NO_3^- , Na^+ , K^+ , Ca^{2+} , Mg^{2+} , and NH_4^+ . Studies of lake and stream waters show correlations between DOC and Hg concentrations (Driscoll et al., 1995; Dittman et al., 2009) however only Kieber et al. (2008) briefly compare these constituents in rainwater. Similarly, no recent studies compare major ion concentrations and Hg concentrations in rainwater. The major ions are useful in determining the relative contribution of sea salt to the ionic composition of the rainwater and provide insights on the potential relationship between Hg associated with sea salt and Hg concentrations in rainwater.

The objectives of this study are to quantify Hg wet deposition in the marine environment, compare its characteristics to the coastal environment and understand Hg

cycling through relationships between Hg, DOC, and major ions in rainwater from the marine environment.

Methods

Site Descriptions

Precipitation samples were collected at the Shoals Marine Laboratory on Appledore Island (AI), ME and at Thompson Farm (TF2) in Durham, NH (Figure III.1). Both locations are part of the AIRMAP network and previous atmospheric chemistry studies (Ambrose et al., 2007; White et al., 2008; Mao et al., 2008; Lombard et al., 2011; Mao et al., 2011;).

Appledore Island. AI is a small island located approximately 10 km east of the New Hampshire and Maine coasts in the Gulf of Maine (42.97°N, -70.62°W). Precipitation samplers were placed on the roof of a WWII lookout tower at an elevation of 30 m above sea level. Precipitation amounts were obtained from a manual rain gauge that was monitored and recorded daily by staff members at AI. This location is in the marine boundary layer and is influenced by continental outflow (Chen et al., 2007).

Thompson Farm 2. Precipitation samples were collected at the location known as Thompson Farm 2 (TF2) (43.1078N, 70.9517W) atop a ~24m walk-up measurement tower. AIRMAP previously conducted atmospheric measurements at the Thompson Farm location approximately 500 m from TF2. A National Oceanic and Atmospheric Administration (NOAA) climate reference network site (<http://ncdc.noaa.gov/crn>) is located at TF and is the source of meteorological information (wind speed, precipitation amount) for TF2. The TF2 site is in a rural location and surrounded by mixed hardwood forest. TF can be influenced by polluted air masses from the Boston and Mid-Atlantic States region (Mao and Talbot, 2004) as well as marine air masses (Chen et al., 2007).

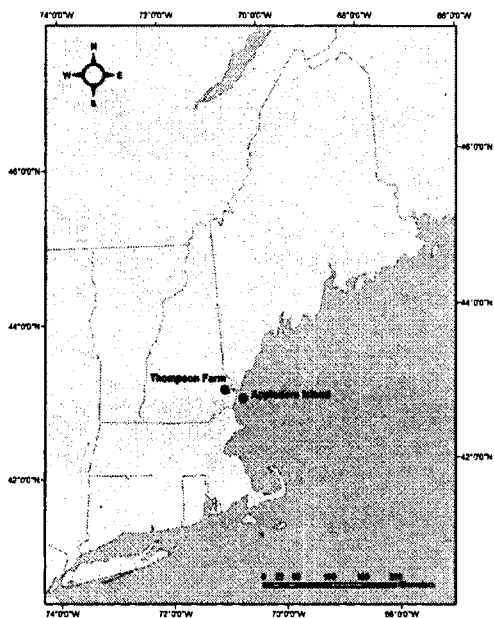


Figure III.1. Thompson Farm and Appledore Island sampling locations.

Precipitation collection

Rain samples were collected for Hg analyses at AI and TF2 using N-CON Systems Company, Inc., MDN 00-125-4 automatic precipitation samplers. This sampler is approved for use in the National Atmospheric Deposition Program Mercury Deposition Network (NADP, MDN). Samples obtained from AI for DOC and major ion analyses were collected in a co-located N-CON Systems Company, Inc., atmospheric deposition sampler. The Hg, DOC, and major ion samples were collected over the same time intervals at AI allowing comparisons between these analytes. On a weekly basis samples collected at AI were transported via boat to the UNH campus.

Hg samples were collected using trace metal sampling techniques in accordance with EPA method 1669. The sampling train consisted of acid washed polyethylene funnels placed directly into preacidified and acid washed fluorinated ethylene propylene (FEP) bottles. Prior to sample deployment, bottle blanks were collected and sample bottles were treated with 1.25mL of 6N HCl for sample preservation.

Analytical methods

The DOC and major ion analyses were conducted by the NH Water Resources Research Center Water Quality Analysis Laboratory at UNH. These samples were passed through GF/F 0.7 mm filters prior to analysis. The Hg samples were analyzed in the trace metal lab at UNH and were not filtered prior to analysis. A summary of the analytes, analytical methods, and method detection limits is given in Table III.1. Triplicate analyses of all Hg samples were performed and the average is reported. The relative percent difference of the standard deviations to the sample concentrations was between 0.43-2.25%.

Analyte	Analytical Method	Method detection limit
Hg	EPA 1631	0.20 mg L ⁻¹
DOC	EPA 415.1	0.05 mg L ⁻¹
Cl ⁻	EPA 300.1	0.02 mg L ⁻¹
NO ₃ ⁻	EPA 300.1	0.009 mg L ⁻¹
SO ₄ ²⁻	EPA 300.1	0.12 mg L ⁻¹
Na ⁺	Proposed EPA method – ion chromatography with suppressed conductivity	0.1 mg L ⁻¹
K ⁺	Proposed EPA method – ion chromatography with suppressed conductivity	0.05 mg L ⁻¹
Mg ²⁺	Proposed EPA method – ion chromatography with suppressed conductivity	0.1 mg L ⁻¹
Ca ²⁺	Proposed EPA method – ion chromatography with suppressed conductivity	0.1 mg L ⁻¹
NH ₄ ⁺	EPA 350.1	0.005 mg L ⁻¹

Table III.1. Analytical methods and detection limits for chemical species examined in this study.

Backward trajectories

Air mass back trajectories were run for each precipitation event at Appledore Island using the NOAA Hybrid Single Particle Lagrangian Integrated Trajectory (HYPSPLIT) model (Draxler and Rolph, 2012). Trajectory start date and times were

based on hourly rainfall data from the NOAA climate reference network site at TF. Trajectories were started during the mid-point of a rainfall event and run for 72 hours preceding the start time. The EDAS 40km dataset was used and trajectories were run at elevations of 500, 1000, and 2000m above ground level.

Results and Discussion

Precipitation samples were collected at AI from 14 June 2009 to 30 August 2009 and at TF2 from 15 June 2009 – 30 August 2009 and analyzed for total aqueous Hg. Co-located samples at AI were collected for DOC, and major ions including Cl^- , SO_4^{2-} , Na^+ , K^+ , Ca^{2+} , Mg^{2+} , NH_4^+ , NO_3^- . Large amounts of insects (on the order of hundreds) were present in Hg samples collected at AI from 1-27 August 2009. These samples were discarded and represent five days with recorded precipitation with three of those receiving minimal amounts (< 6mm). In essence, precipitation samples representing events from 18 June 2009 to 31 July 2009 and one sample from an event occurring 28-29 August 2009 are discussed in the comparison between AI and TF2. In the comparison of DOC, major ions and mercury concentrations at AI, an additional precipitation event that occurred on 14 June 2009 is included.

Precipitation and sample collection variability between TF2 and AI

During this study a total of 10 precipitation samples were collected at TF2 and 13 samples were collected at AI. There was one day (4 July 2009) with rain recorded and collected at TF2 but no rain occurred at AI. This precipitation event is included in the dataset for TF2 but contained a minimal amount of rain with less than 1.9 mm. There was also one rain event (11 July 2009) containing low amounts of precipitation at both TF2 (2.2 mm) and AI (5.8 mm). The sample volume collected at TF2 during this event was too small for reliable Hg analysis, and is excluded from the TF2 data however this event is included in the AI dataset. During this sampling campaign there were four rain events with discrete samples collected each at AI and TF. The remaining samples

contain more than one event at either AI or TF and are useful in comparing the overall deposition between the sites but cannot be directly compared on an event basis.

Despite using automated precipitation samplers of the same make and model at AI and TF2, sample collection efficiency between the sites varied. The total sample volume collected for Hg analysis at TF was 3.42 L for 328 mm of precipitation while at AI, 1.94 L was collected from 352 mm of precipitation. Linear regressions of the collected sample volume and corresponding precipitation depth show a consistent relationship at TF, with greater variability and under sampling at AI (Figure III.2). This discrepancy is attributed to the higher wind speeds experienced at AI. Wind speed data from both locations for concurrent time periods are available from 15 June 2009 to 1 July 2009 with an average hourly wind speed of 6.64 ms⁻¹ at AI compared to 1.21 ms⁻¹ at TF2.

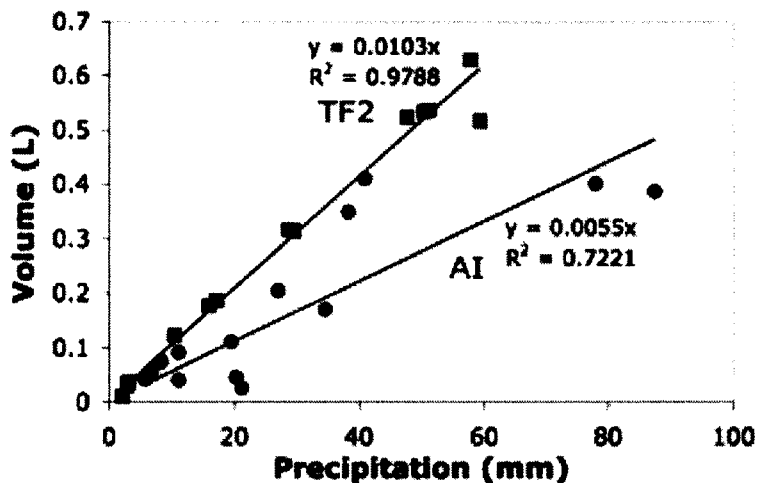


Figure III.2. Hg sample volumes collected at AI (circles) and TF2 (squares) and precipitation amounts with associated linear regressions and R2 values.

A comparison of total aqueous Hg at TF2 and AI

The average, median, and volume weighted mean (VWM) Hg concentrations measured during this sampling campaign at AI and TF2 are listed in Table III.2. The average Hg concentrations for the duration of the campaign show less than 5%

variability between AI and TF2 and the VWM concentration between the sites differ by less than 1%. A statistical comparison (Wilcoxon rank sum test) between the Hg concentrations at the two sites indicates they are not significantly different. Similarly, the Hg deposition per sample is not statistically different between the sites. The total Hg wet deposition was greater at AI and is most likely due to the greater amount of precipitation.

Site	Total Precipitation (mm)	Total Collected Volume (L)	Average Hg concentration (ng L ⁻¹)	Hg concentration range (ng L ⁻¹)	Volume weighted mean Hg concentration (ng L ⁻¹)	Total Hg deposition (µg m ⁻²)
AI	363	1.94	6.85	2.53-13.61	5.62	2.05
TF2	330	3.42	7.18	2.69-13.81	5.57	1.91

Table III.2. Summary statistics for total aqueous Hg in rainwater collected at Appledore Island (AI) and Thompson Farm 2 during summer 2009.

Event based comparison. Variations exist in Hg concentrations at TF2 and AI when the results are compared on an event-based time scale. Figures III.3a-c show Hg concentrations, Hg wet deposition, and amount of precipitation at TF2 and AI for samples representing the same time periods. During this sampling campaign there were four single precipitation events sampled concurrently at AI and TF2 and these are designated as events A – D. The remaining sampling periods are VWM concentrations for samples representing more than one precipitation event.

The Hg concentration values measured at TF2 and AI for the same precipitation events are not consistently higher at one site versus the other. During the seven concurrent sampling periods represented in Figures III.3a-c, four of the Hg concentrations are greater at AI than TF2. When the samples from the individual events A-D are compared, two event Hg concentrations are greater at AI and the remaining 2 are greater at TF2. Most of the Hg concentration measurements differ by less than 1.5 ng/L between the sites. There are only 2 time periods/events where this is not the case. The samples collected during 30 June to 9 July at TF2 have a VWM Hg concentration

that is 2.94 ng/L greater than AI. Despite containing one less rain event at AI than TF2 during this time period, the amount of precipitation received at both sites is essentially equal (57.8 mm at TF2; 57.9 mm at AI), however the sample volumes collected at the sites differ by 173 ml (630 ml at TF2; 457 ml at AI). The rainwater samples collected during the single event from the 21-22 July have a Hg concentration at AI that is 5.14 ng L⁻¹ greater than TF. The amount of precipitation measured at AI during this event (20.3 mm) was approximately double the amount measured at TF2 (10.4 mm) (Figure III.3c) however the sample volume collected at TF2 was more than double the volume collected at AI (122 ml at TF2; 45 ml at AI). The different sampling efficiencies may explain these large differences in Hg concentration between the sites.

There is limited information about the effect of precipitation sampling efficiency on Hg concentration measurements. A multi-year study in the eastern North Atlantic collected 96 matched pair precipitation samples and found that differences between sample pairs could be as high as $\pm 50\%$ but when comparing one year average values the difference reduced to $\pm 5\%$ (Wangberg et al., 2007). Nelson et al. (2008) compared snow samplers and found that the more efficient sampler yielded higher Hg concentrations. A recent study (Kelly et al., 2012) comparing the sampling efficiency and rainwater ion concentrations from two different commercially available co-located samplers found that major ion concentrations are greater in the samples from the more efficient collector. Other studies have shown that a large percentage of the total ion deposition occurs during the early stages of a rain event (Seymour and Stout, 1983; Pryor et al., 2007) and emphasize the importance of capturing the initial rainfall from a precipitation event to accurately determine rainfall concentrations and wet deposition. There do not appear to be any published studies that examine the sampling efficiency of rainwater and consequences on Hg concentration measurements. Additionally, during this study, it is unknown if sample collection was deficient during initial rainfall or

throughout the duration of an event, however if wind is considered the major cause of inefficiency then the missed sample collection most likely occurred over the duration of rain events.

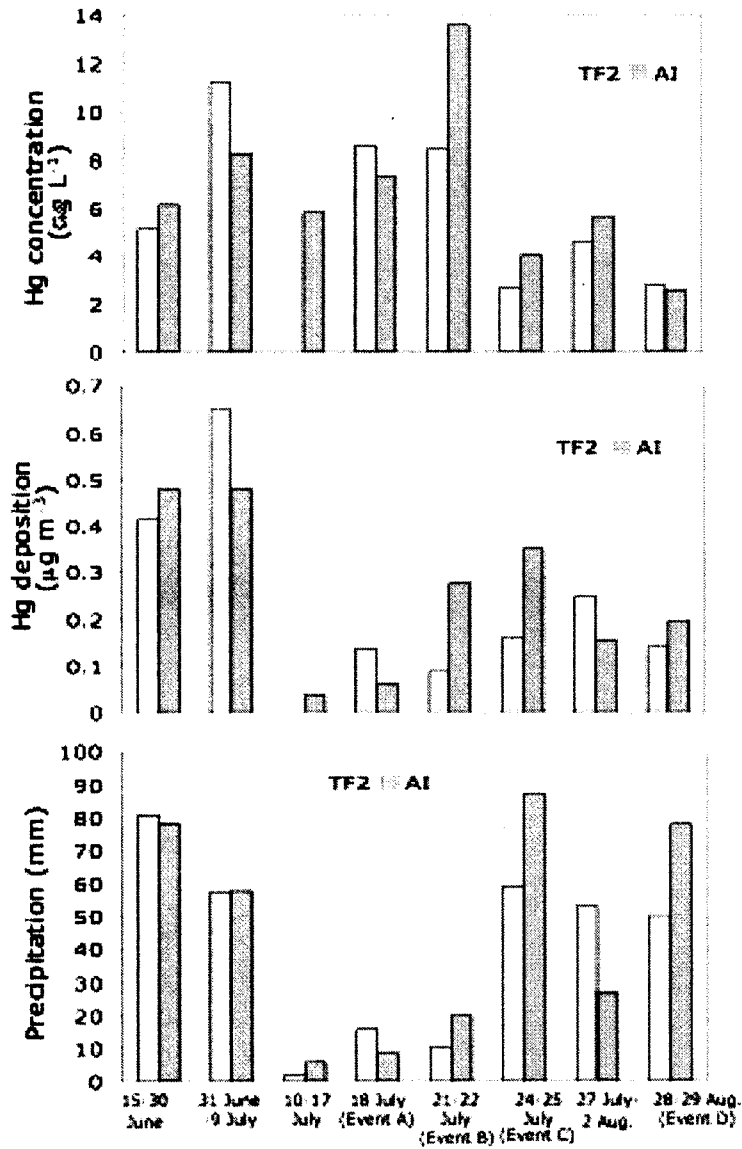


Figure III.3a-c. Total aqueous Hg concentration, Hg deposition, and precipitation for samples collected at AI and TF2 during summer 2009. Individual events with discrete samples collected at both locations are designated as Event A, B, C, D.

Major ions and DOC in precipitation at AI

Precipitation samplers for the analysis of DOC and major ions were co-located with the Hg precipitation sampler at AI. 13 rainwater samples were collected from 14 June 2009 to 30 August 2009. Summary statistics for the concentrations of these analytes during this sampling campaign are in Table III.3. With the exception of Ca²⁺ and Mg²⁺ all reported concentrations are above the method detection limits (See Table III.1). Values reported below the detection limit for Ca²⁺ and Mg²⁺ were used to calculate sea salt ratios.

Analyte	Concentration range (mg L ⁻¹)	Average concentration (mg L ⁻¹)	Median concentration (mg L ⁻¹)	Volume weighted mean concentration (mg L ⁻¹)
DOC	0.31-2.15	1.18	1.04	0.93
NO ₃ ⁻	0.18-1.73	0.85	0.75	0.60
Cl ⁻	1.42-12.78	4.51	3.60	6.66
SO ₄ ²⁻	0.57-2.43	1.41	1.47	1.52
Na ⁺	0.30-7.65	2.60	2.03	4.00
K ⁺	0.08-0.40	0.22	0.20	0.27
Mg ²⁺	0.07-0.89	0.30	0.20	0.40
Ca ²⁺	0.03 – 1.28	0.64	0.63	0.66
NH ₄ ⁺	0.031-0.794	0.304	0.295	0.222

Table III.3. Summary statistics for DOC and major ions in rainwater at AI.

Major ion and Hg concentrations in rainwater at Appledore Island

Comparisons between the concentrations of Hg and the major ions NO₃⁻, SO₄²⁻, NH₄⁺, Ca²⁺, Na⁺, Cl⁻, K⁺, and Mg²⁺ in rainwater at AI are shown in Figures III.4a-h. Nitrate and sulfate ions are indicative of anthropogenic pollution sources, however sulfate is also a component of sea salt. Ammonia (NH₃) is the most significant gas phase base in the atmosphere and can neutralize atmospheric acids to form ammonium nitrate, ammonium sulfate and bisulfate (Finlayson-Pitts and Pitts, 2000). The major emission sources of NH₃ are livestock wastes and fertilizers (Finlayson-Pitts and Pitts, 2000). The Ca²⁺, Na⁺, Cl⁻, K⁺, and Mg²⁺ ions have a wide variety of emission sources including

industrial and natural sources such as dust and sea salt. Ratios of these ions are used to quantify natural source inputs such as sea salt.

Linear regressions were run for the data shown in each of Figures III4a-h. The major ion concentrations exhibiting the greatest linear relationships with Hg concentration are NH_4^+ and NO_3^- ($r^2=0.2935$ and 0.1840 , respectively). All other linear regressions have R^2 values < 0.0966 . Linear correlation co-efficients (Pearson's r) were calculated to further examine the relationships between Hg and NH_4^+ and NO_3^- . The results indicate positive correlations that approach statistical significance (Hg and NH_4^+ , $r=0.54$, $p=0.06$; Hg and NO_3^- , $r=0.43$, $p=0.14$). These data also suggest that ammonium nitrate is the predominate NH_4^+ compound in the precipitation at AI with a statistically significant linear correlation between NH_4^+ and NO_3^- ($r=0.74$, $p=0.004$). The relationship between Hg concentrations and NH_4^+ and NO_3^- is interesting because of their different atmospheric sources. Ammonium sources to the environment are typically agricultural which are not considered large atmospheric sources of NO_3^- or Hg. The relationship between Hg and NH_4^+ might be due to their similar positive charges resulting in similar atmospheric behavior.

In contrast, the linear relationship between Hg and NO_3^- observed at AI is most likely a result of common atmospheric sources. VanArsdale et al. (2005) also report linear relationships between Hg, and NO_3^- concentrations in precipitation collected from Mercury Deposition Network (MDN) sites located throughout northeastern North America. Additionally, VanArsdale et al. (2005) report linear relationships between SO_4^{2-} and Hg, and NO_3^- and SO_4^{2-} concentrations. The data from AI do not exhibit a strong linear relationship between Hg and SO_4^{2-} , which suggests that sea salt contributions from clean marine to the sulfate concentrations. The NO_3^- and SO_4^{2-} concentrations at AI are linearly related however the r^2 values from the linear regression are much lower than those reported by VanArdale et al., 2005.

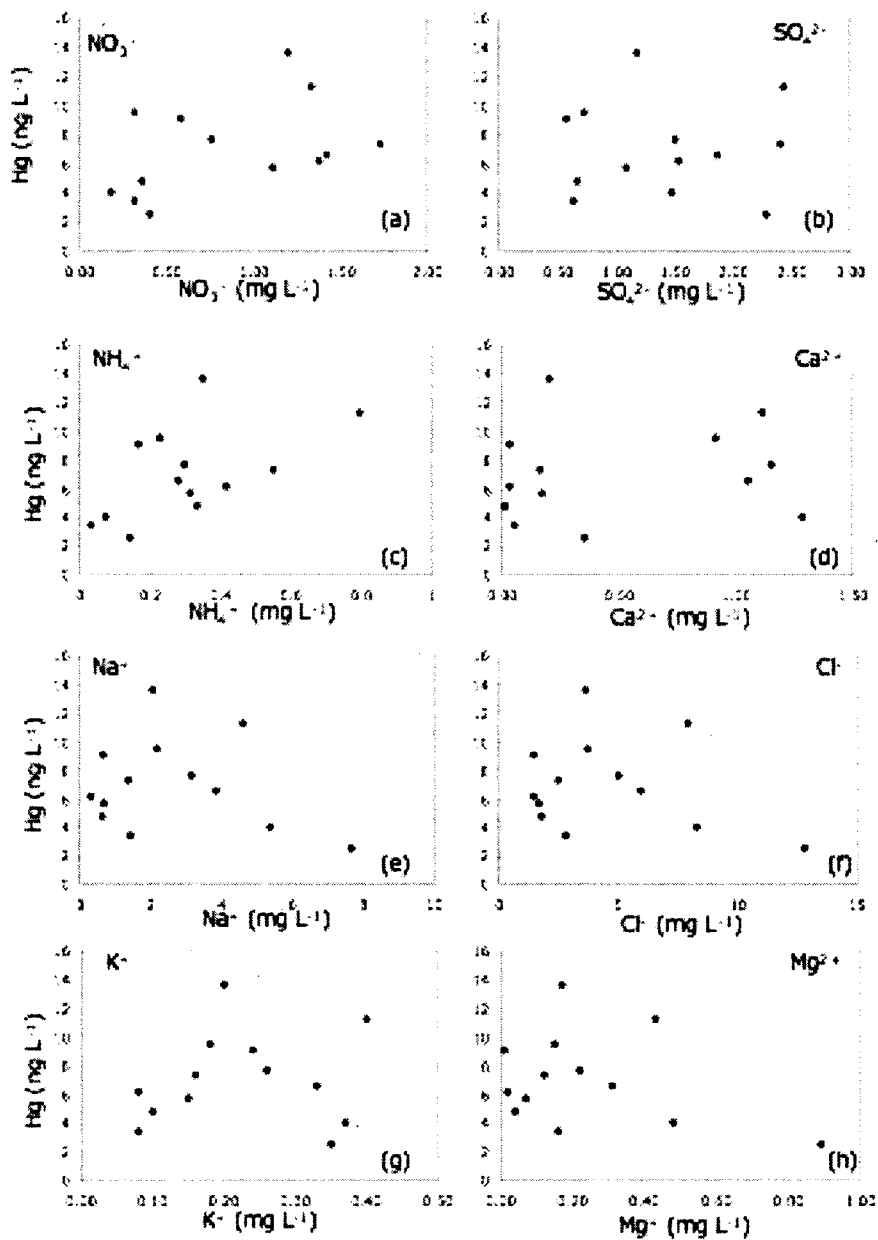


Figure III.4a-h. Hg and major ion concentrations in rainwater from AI.

The sea salt contribution of Cl⁻, SO₄²⁻, Na⁺, K⁺, and Ca²⁺ in precipitation samples from AI was calculated using the method outlined by Keene et al., 1986. Mg²⁺ was selected as the conservative sea salt reference ion based on the observed Mg/Na ratios in our samples, which suggest either an enhancement of Na or a depletion of Mg with respect to sea salt.

To investigate the contribution of Hg associated with sea salt aerosols to the Hg wet deposition at AI, comparisons were made between the percent of an ion concentration attributed to sea salt and the corresponding Hg concentration (Figures III.5a-f). Precipitation events containing Cl^- and Ca^{2+} concentrations depleted with respect to their sea salt ratio with Mg, result in values greater than 100% for the percent of the ion attributed to sea salt. The percent of sea salt attributed to each ion varies within the same precipitation sample as illustrated by comparing Na^+ (Figure III.5c) to K^+ (Figure III.5e). The percent of Na^+ attributed to sea salt is greater than 50% in all except one precipitation event; alternatively the percent of K^+ attributed to sea salt is <50% for 11 of the 13 samples. Despite these differences there is general consistency among sampling events when they are ranked according to percent sea salt based on the various ions. For example, the precipitation sample collected from 28-29 August 2009 had the highest percent of sea salt based on all of the ions examined in this study, excluding Ca^{2+} . Likewise the sample collected from 14-15 June 2009 had the lowest percentage of sea salt based on the concentrations of Cl^- , K^+ , and Na^+ , and the second lowest percentage based on SO_4^{2-} . There was greater variability among the events with mid-range percentage of sea salt concentrations and these differences likely reflect the variety of emission sources for these elements in the atmosphere.

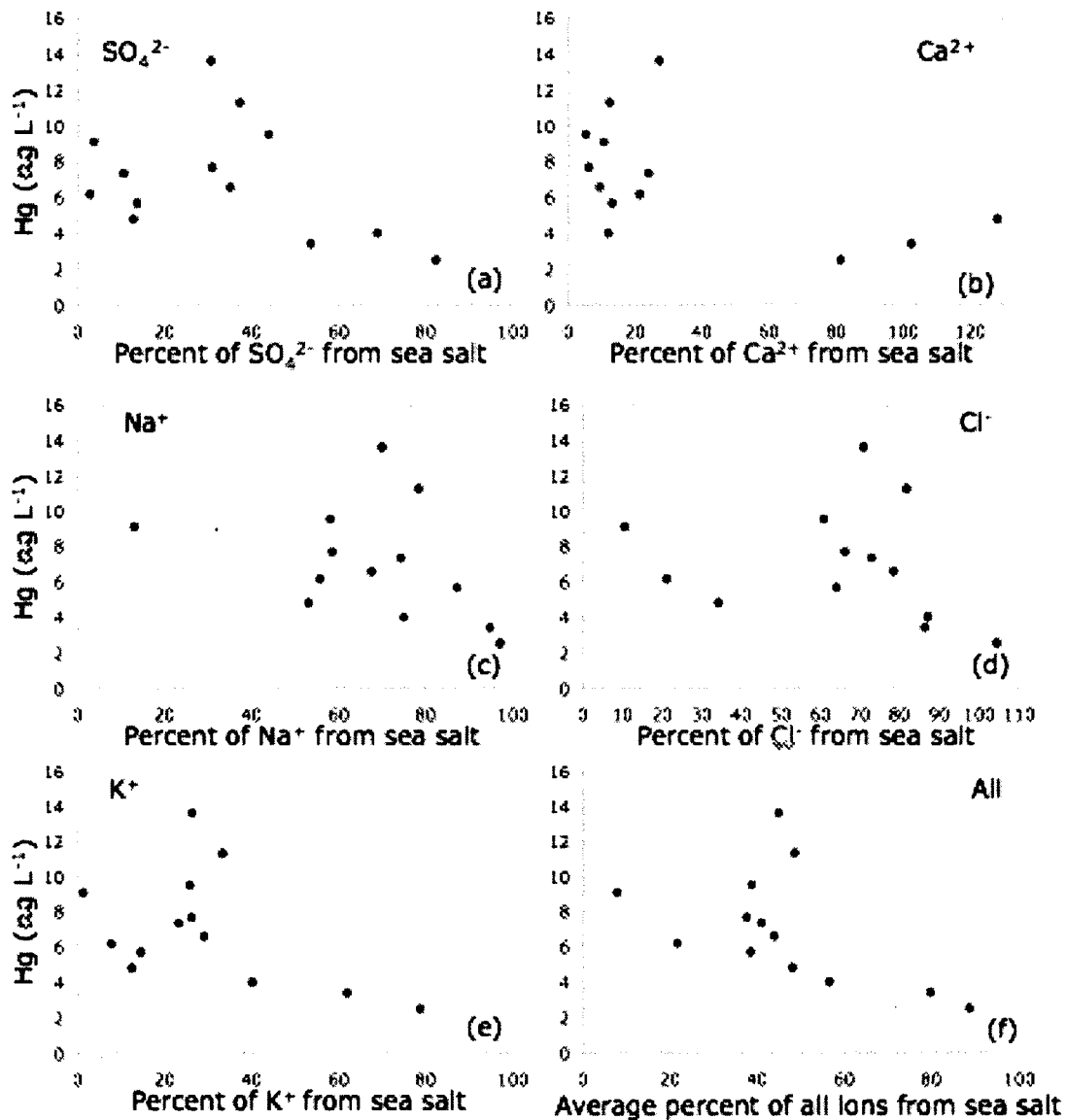


Figure III.5a-f. Hg concentration and percent of major ion attributed to sea salt for samples collected at AI.

In order to smooth these differences the average percent of sea salt present in each precipitation event was calculated by taking the average of the sea salt percentages for all of the ions. This average percentage of sea salt is plotted with the Hg concentrations in Figure 5f and has a pattern similar to the K⁺ and Cl⁻ plots (Figures III.5d and III.5e). Figures III.5a-f show similar patterns between the percent of an ion from sea salt and Hg concentrations in rainwater. This is in contrast to Figures III.4a-h, which compare the ion concentrations and show few similarities among the ions.

Figures III.5a-f show that the precipitation events with the lowest Hg concentrations have the greatest percentage of sea salt. The precipitation event with the highest Hg concentration has a mid-range percentage of sea salt and the events with higher Hg concentrations tend to be in the mid-range of percent sea salt. The precipitation event with the lowest percentage of sea salt has a moderately high Hg concentration. These patterns indicate that rainwater dominated by a marine sea salt signature has a relatively low Hg concentration and rainwater with a continental signature contains a moderate concentration of Hg. The Hg concentration seems to be enhanced when there is a mixture of marine and continental air masses resulting in mid-range percentage of sea salt.

Air mass back trajectories were compared to the sea salt percentage results and provide further information about the air mass source regions, and in general the two substantiate each other. The rain event from 14-15 June 2009 had the lowest percentage of sea salt (8%) in the samples collected and the back trajectory indicates this air mass arrived at AI from the west after traveling across continental southern Canada and New England (See Figure III.6). The Hg concentration in the rainwater from this event was moderately high (9.09 ng L^{-1}). In contrast, the precipitation event from 28-29 August 2009 contained the highest percentage of sea salt ions (89%). This event was the remnant of a tropical storm and the back trajectory indicates that for three days previous to arriving at AI, the air mass was over the Atlantic Ocean (See Figure III.7). This marine event had the lowest Hg concentration (2.53 ng L^{-1}) measured during the sampling campaign.

The majority of events (9 of 13) sampled during this campaign contain between 38% and 57% sea salt calculated from the average of all ions examined. The back trajectories for these typically show air masses arriving at AI from the south that have traveled across the Midwestern US and then north along the coast. Figure III.8 is a

typical back trajectory for these mid-range sea salt events and is from the 18 July 2009 rain event containing an average of 41% sea salt and a Hg concentration of 7.34 ng L^{-1} . The rainfall event with the greatest Hg concentration (13.61 ng L^{-1}) at AI during this sampling campaign contained an average of 45% sea salt. The back trajectory for this rain event indicates a marine air mass from south traveling parallel to the East Coast of the United States (Figure III.9). The mid-range percentage of sea salt and the elevated Hg concentration from this event suggest that polluted continental air was entrained in the air mass as it traveled along the coast. The results from the Hg and ion concentrations in rainwater and back trajectories complement each other and indicate that the highest Hg concentrations occur when continental air mixes with marine air, which is common in the coastal environment.

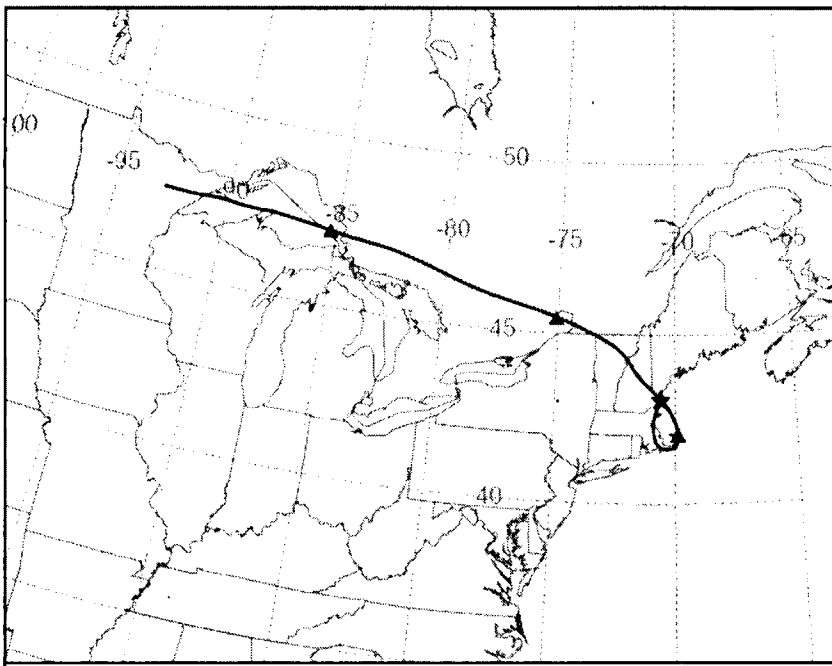


Figure III.6. HYPSPPLIT model back trajectory ending at AI at 1200 UTC on 14 June 2009. The model was run at an elevation of 2000 m above ground level for 72 hours preceding the start time using the EDAS dataset. The red triangles indicate 24 hour intervals at 0000UTC.

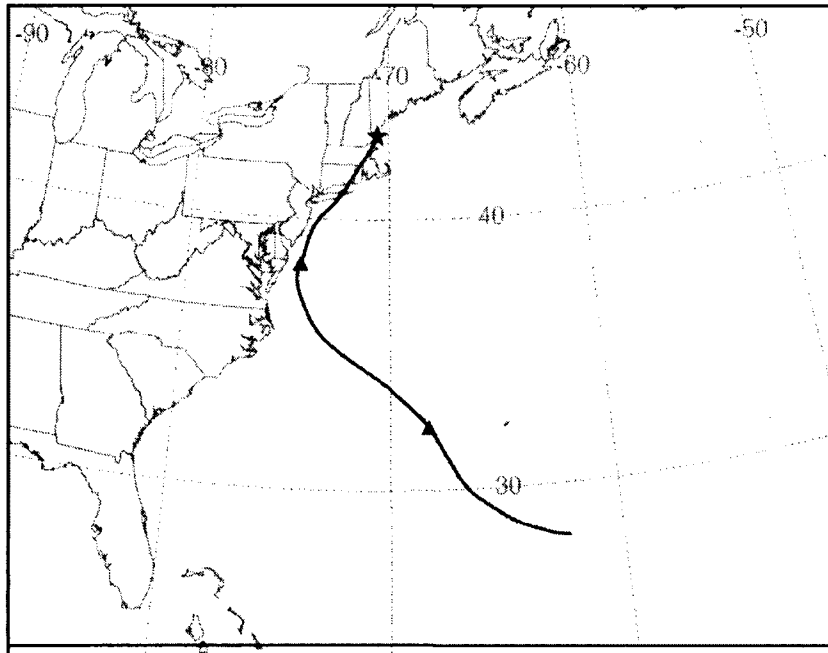


Figure III.7. HYPSPPLIT model back trajectory ending at AI at 1400 UTC on 29 August 2009. The model was run at an elevation of 2000 m above ground level for 72 hours preceding the start time using the EDAS dataset. The red triangles indicate 24 hour intervals at 0000UTC.

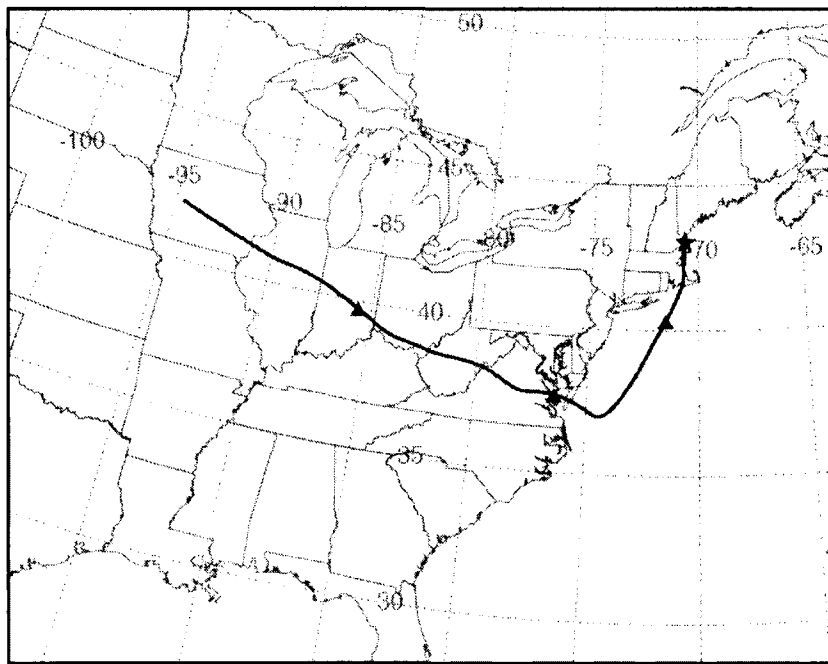


Figure III.8. HYPSPPLIT model back trajectory ending at AI at 0800 UTC on 18 July 2009. The model was run at an elevation of 2000 m above ground level for 72 hours preceding the start time using the EDAS dataset. The red triangles indicate 24 hour intervals at 0000UTC.

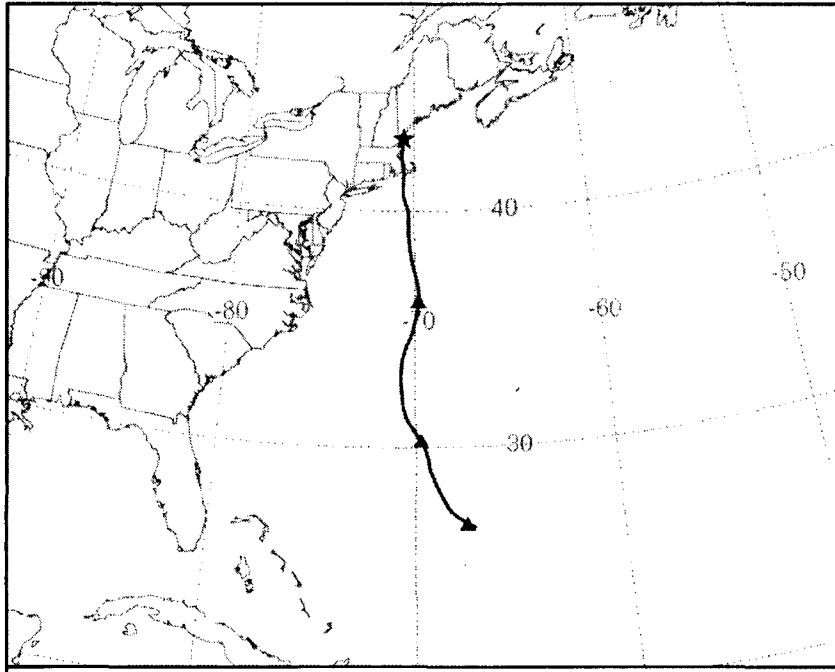


Figure III.9. HYSPLIT model back trajectory ending at AI at 2200 UTC on 21 July 2009. The model was run at an elevation of 2000 m above ground level for 72 hours preceding the start time using the EDAS dataset. The red triangles indicate 24 hour intervals at 0000UTC.

A possible confounding factor when comparing the sea salt percentages and Hg concentrations is the amount of rainfall during each event. The Hg concentration may be diluted during large rainfall events. A plot of the Hg concentration versus the amount of precipitation for each event (Figure III.10) reveals a non-linear relationship between these parameters. The two events with >70mm of rain do have lowest Hg concentrations (<4 ng L⁻¹) observed in this study, however an event containing 35mm of precipitation also has a Hg concentration <4 ng L⁻¹. Furthermore, the rain events with the least amount of rainfall do not have the highest Hg concentrations. Figure III.10 indicates that the amount of precipitation does not directly determine the Hg concentration in the rainwater. To examine this further the mass of Hg in each rain event was determined as the product of the Hg concentration and the amount of rainfall and

was compared to the average percent of sea salt in each rain event (Figure III.11). The pattern of elevated Hg deposition in the mid-range percentage of sea salt persists.

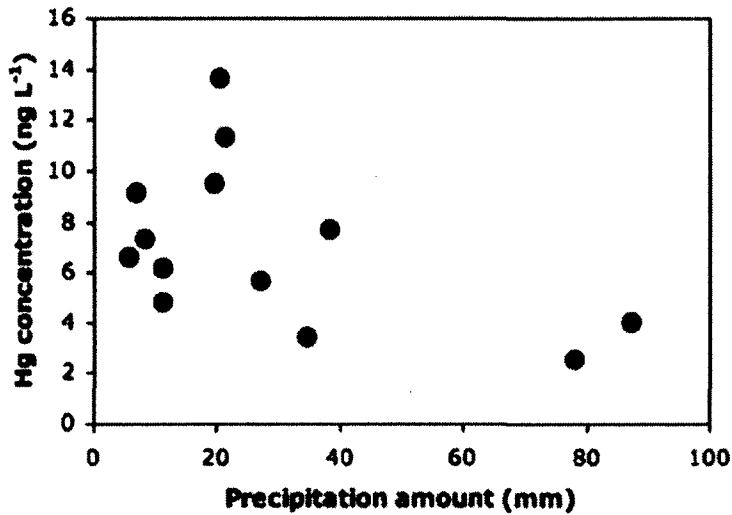


Figure III.10. Precipitation amount and Hg concentration for rain events at AI.

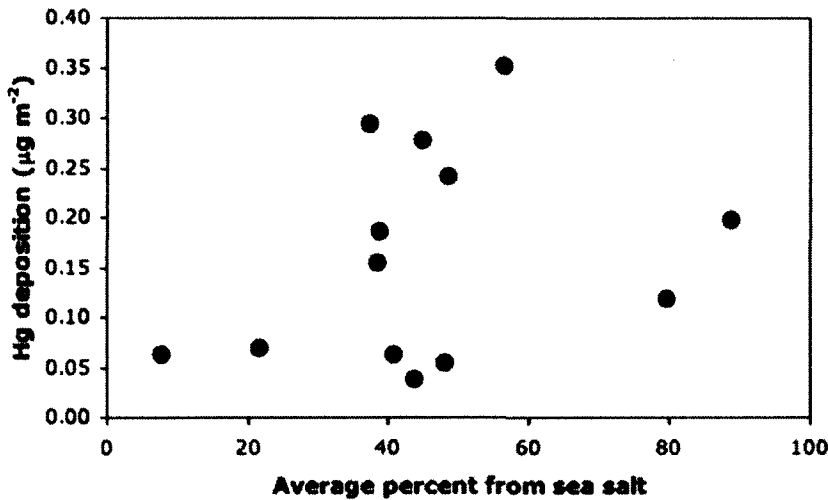


Figure III.11 Mercury deposition compared to the percent of sea salt in precipitation samples at AI.

DOC and Hg concentrations in rainwater at Appledore Island

Dissolved organic matter (and by extension DOC) is important in the aquatic cycling of Hg. The presence of dissolved organic matter generally enhances the dissolution of Hg

by providing strong binding sites (Ravichandran, 2004). Total Hg concentrations have been positively correlated with DOC in lake waters (Driscoll et al., 1995), streams during high flow events (Dittman et al., 2010), throughfall and stemflow (Kolka et al., 2001), and rainwater collected in North Carolina (Kieber et al., 2008). This study examines relationships between DOC and Hg in rainwater collected at AI.

Figure III.12 is a graph of the DOC concentration (mg L^{-1}) versus the Hg concentration (ng L^{-1}) and reveals a general pattern of increasing Hg with increasing DOC. The DOC and Hg concentration data distributions were tested for normality using the Shapiro Wilk W Test (JMP) and both datasets exhibit a normal distribution (DOC, $W = 0.94$ $p < W = 0.4475$; $W = 0.973$ $p < W = 0.93$). Pairwise correlation indicates a statistically significant ($p < 0.1$) positive correlation between the DOC and Hg concentrations in rainwater at AI ($r = 0.54$, $p = 0.06$). However, this pattern is not maintained for the two rain events with the greatest DOC concentrations ($> 2 \text{ mg L}^{-1}$). The back trajectories and examination of the major ion composition for these events indicate continental polluted air mass source regions for these two events. The highest DOC concentration, 2.15 mg L^{-1} , occurred on 29 June 2009 and the 72 hour air mass back trajectory indicates a slow eastern moving air mass approached from western Massachusetts and made a counter-clockwise turn to the north and west passing over southern Maine, New Hampshire and Vermont before turning east and passing over AI. This rainwater sample contained a relatively high amount (3rd from highest) of NO_3^- and nss-SO_4^{2+} concentrations in comparison with the other samples and had a low sea salt signal (22%). The second event with a DOC concentration $> 2.00 \text{ mg L}^{-1}$ occurred on 18 July 2009 and the back trajectory indicates the air mass traveled across the Midwestern United States and north along the coast of the eastern US before approaching AI. This rainwater sample had the highest NO_3^- and nss-SO_4^{2+} concentrations during this sampling campaign. This event had a mid-range percentage (41%) of ions that could be

attributed to sea salt. It should be noted that DOC concentrations greater than 2.00 mg L⁻¹ are within the range of volume weighted mean DOC concentrations (0.29 – 2.52 mg L⁻¹) reported previous studies from non-urban locations throughout the globe (Willey et al., 2000 and sources therein).

Kieber et al., (2008) report a statistically significant positive correlation between DOC and Hg concentrations ($r=0.29$, $p=0.008$, $n=83$) in rainwater collected from Wilmington, North Carolina (8.5 km from Atlantic Ocean) over a 2 year period. The lower correlation co-efficient between Hg and DOC observed by Kieber et al., 2008 may result from seasonal differences in their multi-year data set. The VWM Hg concentrations in their study do not vary greatly between the winter and summer seasons. However, a multi-year study of DOC concentrations in rainwater collected at the same location (Wilmington, NC) but over a different time period reports statistically significant seasonal differences in VWM DOC concentration based on storm type (i.e. continental, marine, hurricane) (Wiley et al., 2000). Lombard et al. (2011) report seasonal differences in Hg concentrations in precipitation collected from TF. Seasonal differences in both DOC or Hg concentrations and different atmospheric sources of DOC and Hg may contribute to the variability in the correlations.

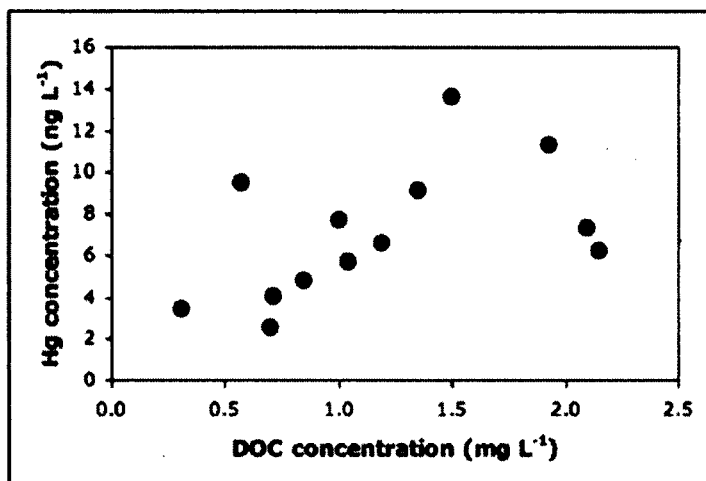


Figure III.12. Hg and DOC concentrations in rain at Al.

Conclusions

One purpose of this study was to compare Hg concentrations in precipitation and Hg wet deposition between a marine and coastal inland site. The VWM Hg concentrations and total Hg wet deposition from this summer 2009 sampling campaign indicate small differences (<5%) between AI and TF2. On an event basis larger differences exist but are not statistically significant. Large differences in sampling efficiency exist between AI and TF2 and cannot be ruled out as effecting the comparison between the locations. Although the samplers used in this study are used approved for use by the MDN the development of better automated precipitation samplers is necessary so that meaningful comparisons between locations on an event basis can be made and discrepancies in sampling efficiency can be eliminated as a cause of the differences in Hg concentrations between locations.

The rainwater samples collected from AI during the summer 2009 were examined further by making comparisons with major ion concentrations from co-located samples. Linear relationships exist between Hg and NO_3^- concentrations and NH_4^+ and Hg concentrations. The relationship between Hg and NO_3^- has been observed by others (VanArsdale et al., 2005) and is generally attributed to similar combustion sources to the atmosphere. The results from this work at AI substantiate previous findings. The relationship at AI between Hg and NH_4^+ concentrations in rainwater is interesting and similar findings have not been reported. Few studies report measuring the two constituents in rainwater and while Caffrey et al. (2010) do measure both Hg and NH_4^+ in rainwater from Florida they do not investigate a potential relationship between the two. The findings at AI suggest that future studies should examine this relationship as it may provide further information on the atmospheric cycling and wet deposition of Hg.

The relationship between Hg and with sea salt in rainwater was examined by comparing the percentage of major ions attributed to sea salt and Hg concentrations at

AI. Our findings indicate that precipitation events dominated by a sea salt signature have low Hg concentrations in rainwater. In this study, precipitation events with a mid range percentage of sea salt have the highest Hg concentrations. These results indicate that sea salt aerosols may enhance the scavenging of gas phase Hg found in polluted continental air masses. This indicates that coastal environments where mixing of continental and marine air masses occurs may experience elevated Hg wet deposition. The possible chemical reactions that result in enhanced Hg concentrations from the mixing of these air masses should be examined in more detail.

Additionally this study examined the relationship between DOC and Hg concentrations in rainwater from AI. Several researchers have documented the association of Hg with DOC in terrestrial aquatic systems (Dittman et al., 2009; Driscoll et al., 1995) however this relationship in rainwater remains relatively unexamined. Kieber et al. (2008) report a correlation between the two in precipitation samples collected over a 2 year period in coastal North Carolina. In this study, a correlation between Hg and DOC concentrations was observed in rainwater collected on AI. Explanations for this correlation in rainwater should be examined in more depth and may provide insights into chemical factors contributing to the entrainment of atmospheric gas and particle phase mercury into precipitation. Future long-term studies of Hg in precipitation should include measurements of DOC to determine if there is a robust connection between the two in precipitation.

References

- Ambrose, J.L., Mayne, H.R., Stutz, J., Russo, R.S., Zhou, Y., Varner, R.K., Nielsen, L.C., White, M., Wingenter, O.W., Haase, K., Talbot, R., Sive, B.C., Nighttime oxidation of VOCs at Appledore Island, ME during ICARTT 2004, 2007. *J. Geophys. Res.*, 112, D21302, doi:10.1029/2007JD008756.
- Caffrey, J.M., Landing, W.M., Nolek, S.D., Gosnell, K.J., Bagui, S.S., Bagui, S.C., 2010. Atmospheric deposition of mercury and major ions to the Pensacola (Florida) watershed: spatial, seasonal and inter-annual variability, *Atmos. Chem. Phys.*, 10.

- Chen, M., Talbot, R., Mao, H., Sive, B., Chen., J., Griffin, R., 2007. Air mass classification in coastal New England and its relationship to meteorological conditions, *J. Geophys. Res.*, 112, D10S05, doi:10.1029/2006JD007687.
- Dittman, J. A., Shanley, J.B., Driscoll, C.T., Aiken, G.R., Chalmers, A.T., Towse, J.E., 2009. Ultraviolet absorbance as a proxy for total dissolved mercury, *Environmental Pollution* 157, 1953–1956.
- Dittman, J. A., J. B. Shanley, C. T. Driscoll, G. R. Aiken, A. T. Chalmers, J. E. Towse, and P. Selvendiran, 2010. Mercury dynamics in relation to dissolved organic carbon concentration and quality during high flow events in three northeastern U.S. streams, *Water Resour. Res.*, 46, W07522, doi:10.1029/2009WR008351.
- Driscoll, C.T., Blette, V., Yan, C., Schofield, C.L., Munson, R., Holsapple, J., 1995. The role of dissolved organic carbon in the chemistry and bioavailability of mercury in remote Adirondack lakes, *Water, Air, and Soil Pollution*, 80, 499-508.
- Draxler, R.R. and Rolph, G.D., 2012. HYSPLIT (Hybrid Single-Particle Lagrangian Integrated Trajectory) Model access via NOAA ARL READY Website (<http://ready.arl.noaa.gov/HYSPLIT.php>). NOAA Air Resources Laboratory, Silver Spring, MD.
- Feddersen, D.M.; Talbot, R.W.; Mao, H., in pre. Size Distribution of Atmospheric Particulate Mercury in Marine and Continental Atmospheres. *Atmos. Chem. Phys.*
- Finlayson-Pitts, B.J., Pitts, Jr., J.N., 2000, *Chemistry of the upper and lower atmosphere*, Academic Press, NY.
- Guo, Y., Feng, X., Li, Z., Tianrong, H, Yan, H., Meng, B., Zhang, J., Qiu, G., 2008. Distribution and wet deposition fluxes of total and methyl mercury in Wujiang River Basin, Guizhou, China, *Atmos. Environ.*, 42:30, 7096-7103.
- Hammerschmidt, C.R., Lamborg, C.H., Fitzgerald, W.F., 2007. Aqueous phase methylation as a potential source of methylmercury in wet deposition, *Atmospheric Environment*, 41, 1663-1668.
- Hedgecock, I.M., Pirrone, N., 2001. Mercury and photochemistry in the marine boundary layer-modelling studies suggest the in situ production of reactive gas phase mercury, *Atmospheric Environment*, 35, 3055-3062.
- Holmes, C.D., Jacob, D.J., Corbitt, E.S., Mao, J., Yang, X., Talbot, R., Slemr, F., 2010. Global atmospheric model for mercury including oxidation by bromine atoms, *Atmos. Chem. Phys.*, 10, 12037-12057.
- Keene, W.C., Pszenny, A.P., Galloway, J.N., Hawley, M.E., 1986. Sea-Salt corrections and interpretation of constituent ratios in marine precipitation, *J. Geophys. Res.*, 91, D6, 6647-6658.
- Kelly, V.R., Weathers, K.C., Lovett, G.M., Likens, G.E., 2012. A comparison of two collectors for monitoring precipitation chemistry, *Water Air Soil Pollution*, 223:951-

- 954, DOI 10.1007/s11270-011-0912-8.
- Kieber, R.J., Parler, N.E., Skrabal, S.A., Willey, J.D., 2008. Speciation and photochemistry of mercury in rainwater, *Journal of Atmospheric Chemistry*, 60:153 – 168, doi 10.1007/s10874-008-9114-1.
- Lin, C.J., Pehkonen, S.O., 1999. The chemistry of atmospheric mercury: a review, *Atmospheric Environment*, 33, 2067-2079.
- Malcolm, E.G., Keeler, G.J., Landis, M.S., 2003. The effects of the coastal environment on the atmospheric mercury cycle, *Journal of Geophysical Research*, 108:D12, 4357, doi:10.1029/2002JD003084.
- Mao, H., Talbot, R., 2004. O₃ and CO in New England: Temporal variations and relationships, *J. Geophys. Res.*, 109, D21304, doi:10.1029/2004JD004913.
- Mao, H., Talbot, R.W., Sigler, J.M., Sive, B.C., Hegarty, J.D., 2008. Seasonal and diurnal variations of Hg⁰ over New England, *Atmos. Chem. Phys.*, 8, 1403-1421, www.atmos-chemphys.net/9/1403/2008/.
- Mao, H., Talbot, R.W., in prep. Speciated mercury at a marine, coastal and inland sites in New England: Part 1. Temporal Variabilities, *Atmos.Chem, Phys. Discuss.*
- Mason, R.P., Fitzgerald, W.F., Vandal, G.M., 1992. The sources and composition of mercury in Pacific Ocean rain, *Journal of Atmospheric Chemistry* 14: 489-500.
- Pirrone, N. et al., 2008. Global Mercury Emissions to the Atmosphere from natural and anthropogenic sources. In *Mercury Fate and Transport in the Global Atmosphere: Measurements, Models, and Policy Implications, Interim Report of the United Nations Environmental Programme Global Mercury Partnership, Mercury Air Transport and Fate Research Partnership Area*, ed. N. Pirrone and R. Mason, p.1-36.
- Pryor, S.C., Spaulding, A.M., Rauwolf, H., 2007. Evolution of the concentration of inorganic ions during the initial stages of precipitation events, *Water Air Soil Pollution*, 180:3-10.
- Ravichandran, M., 2004. Interactions between mercury and dissolved organic matter – a review, *Chemosphere*, 55:3, 319-331.
- Seymour, M.D., Stout, T., 1983. Observations on the chemical composition of rain using short sampling times during a single event, *Atmospheric Environment*, 17:8, 1483-1487.
- Vanarsdale, Weiss, J., Keeler, G., Miller, E., Boulet, G., Brulotte, R., Poissant, L., 2005. Patterns of mercury deposition and concentration in northeastern North America (1996-2002), *Ecotoxicology*, 14, 37-52.
- Wangberg, I., Munthe, J., Berg, T., Ebinghaus, R., Kock, H.H., Temme, C., Bieber, E., Spain, T.G., Stolk, A., 2007. Trends in air concentration and deposition of mercury in the coastal environment of the North Sea Area, *Atmospheric Environment*, 41, 2612-2619.

White, M., Russo, R.S., Zhou, Y., Varner, R.K., Nielsen, L.C., Ambrose, J., Wingenter, O.W., Haase, K., Tlabot, R., Sive, B.C., 2008. Volatile organic compounds in northern New England marine and continental environments during the ICARTT 2004 campaign, *J. Geophys. Res.* 2008, 113, D08S90, doi:10.1029/2007JD009161.

Willey, J.D., Kieber, R.J., Eyman, M.S., Avery, Jr., G.B., 2000. Rainwater dissolved organic carbon: Concentrations and global flux, *Global Biogeochemical Cycles*, 14:1, 139-148.

CHAPTER IV

QUANTIFICATION OF ENVIRONMENTALLY MOBILE Hg^P: METHOD DEVELOPMENT AND APPLICATION TO AN INTENSIVE SAMPLING CAMPAIGN ON APPLIEDORE ISLAND, SUMMER 2009

Introduction

Atmospheric deposition is an important source of mercury (Hg) to terrestrial and aquatic ecosystems. The biogeochemical cycling of Hg is complex due to the variety of chemical forms that exist during ambient environmental conditions including particulate Hg (Hg^P), elemental gaseous Hg (Hg⁰), and reactive gaseous Hg (RGM). RGM and Hg^P concentrations in the atmosphere constitute a relatively small percentage of the total atmospheric Hg. They are more soluble than Hg⁰ and therefore the dominant species deposited through wet and dry deposition (Mason et al., 1997; Schroeder and Munthe, 1998; Selin, 2009).

Several methods have been employed to determine atmospheric concentrations of Hg^P. A common method is to collect bulk aerosol samples on filters, extract the Hg in acid(s) using various techniques, and analyze the Hg abundance within the leachate (Guentzel et al., 1995; Keeler et al., 1995; Mason et al., 1997; Landing et al., 1998; Ebinghaus et al., 1999; Munthe et al., 2001; Arimoto et al., 2004). Variations of these sampling and extraction methods, including the use of different filter materials and acid extraction techniques are summarized in Table IV.1. A consistent method for the filter extraction of Hg^P is lacking and Ebinghaus et al. (1999) state the need for a standard. Several of the studies listed in Table 1 measure Hg^P plus additional trace metals and utilize high temperature techniques to digest all particulate matter, including any environmentally non-mobile fraction of Hg. Additionally, these high temperature

techniques may volatilize a portion of the Hg. An acid extraction method is presented here for Hg^{P} analysis that utilizes low temperature techniques to quantify the environmentally mobile fraction of Hg^{P} under atmospheric conditions. Furthermore, this method uses the same reagents necessary for determining Hg concentrations via cold vapor atomic fluorescence spectrometer (CVAFS) analysis, thus minimizing the use of reagents and production of laboratory waste. This new filter extraction method was used throughout an intensive sampling campaign during summer 2009 at Appledore Island, Maine.

Reference	Filter material	Acid extraction technique	Analyses
Arimoto et al. (2004)	Whatman 41®	Teflon microwave digestion using conc. HNO ₃ , conc. HCl, conc. HF, H ₂ O ₂ , at 180°C for 30 minutes	Hg ^P and Pb
Arimoto et al. (2004)	Whatman 41®	Microwave digestion in conc. HNO ₃ and BrCl heated to 12.4 bar for 30 minutes	Hg ^P
Ebinghaus et al. (1999)	Teflon disc filters, pore size 0.45mm	Acid leaching	Hg ^P
Ebinghaus et al. (1999)	Whatman quartz fiber disc filters, 99.9% retention effectivity for particles >0.1 mm)	Acid leaching and digestion with BrCl	Hg ^P
Guentzel et al. (1995)	0.4 mm polypropylene membranes	PTFE Teflon digestion bombs using 6M 3xQ-HCl/conc. Q-HNO ₃ /conc. HF	Hg ^P and other trace metals
Keeler et al. (1995)	Glass fiber filters	10% solution of a 70% HNO ₃ /30% H ₂ SO ₄ acid mixture (~2N), sonicate for 30 minutes	Hg ^P
Keeler et al. (1995)	Teflon membrane filters (2 mm pore size), glass fiber filters	10% HNO ₃ , microwave digestion for 20 minutes at 160°C, soak for 12 hrs at room temperature	Hg ^P and other trace metals
Munthe et al. (2001)	Cellulose acetate filters, pore size 0.45mm	Microwave digestion in solution of 2ml HNO ₃ and 6ml of H ₂ O ₂ in Teflon vessels	Hg ^P
Munthe et al. (2001)	Glass fiber filters	Microwave digestion in 10% solution of HNO ₃ (Keeler et al., 1995)	Hg ^P
Munthe et al. (2001)	Teflon filters	7:3 HNO ₃ : H ₂ SO ₄ solution at 80°C in Teflon vials	Hg ^P

Table IV.1. A summary of various filter materials and acid extraction methods used previously by other researchers to measure Hg^P.

Methods

Sampling Methods

Samples were collected at the Isle of Shoals Marine Laboratory, an AIRMAP site located on Appledore Island in the Gulf of Maine. Appledore Island (AI) is a small island located approximately 10 km east of the New Hampshire and Maine coasts (42.97°N, 70.62°W). Samples were collected on the roof of a WWII lookout tower at an elevation of 30 m above sea level.

Bulk aerosol filter samples were collected using a custom sampling train consisting of Delrin® filter holders housed in a custom made protective cylindrical casing. During sample collection, ambient air was pulled through the downward facing filters. The target flow rate was 120 L per minute and was controlled via a mass flow controller. No denuders were used.

During the summer 2009 intensive campaign at Appledore Island, filters were changed approximately every three hours and the sample volume measured with a flow totalizer. Samples were manually changed by replacing the filter holder assembly. Sampling personnel followed trace metal clean procedures and all samples were sealed in clean double plastic bags. Field blanks were collected every ten samples by installing a filter for approximately ten minutes with no air passing through the sampler. Samples were frozen until acid extraction. Extractions and Hg analyses were completed within 4 months of the sample collection.

Laboratory Methods

All procedures were carried out in clean lab environments in the geochemistry labs of the Department of Earth Sciences and Institute for the Study of Earth, Oceans, and Space at the University of New Hampshire. Acid solutions were made using trace metal grade acids and 18 MΩ nanopure water.

Bottle and vial cleaning. Fluorinated ethylene propylene (FEP) bottles and vials were used during the filter extractions and dilutions. These were rigorously acid cleaned prior to use.

Filter cleaning. Commercially available Millipore fluoropore filters with a 90 mm diameter and 1mm pore size were used. The filter materials are hydrophobic PTFE bonded to a high density polyethylene support. The low melting point of the support material precluded filter cleaning by combustion. Filters were cleaned in successive 12 hour acid baths of 7.5M nitric acid and 4M hydrochloric acid, rinsed and placed in cleaned filter holders to dry in a laminar flow bench. The custom Delrin® filter holders were cleaned in soapy water and dilute hydrochloric acid. The clean filters were stored in their filter holders and individually packed in cleaned double plastic bags for storage and transport.

Filter extracts. The Hg abundance collected on the bulk filters was quantified by acid extraction. Each filter was soaked in an acid cleaned Teflon vial containing ~40 ml of a 1.5% solution of BrCl and HCl. These were sonicated for 30 minutes and soaked overnight at room temperature for at least 12 hours. The filters and acid solutions were sonicated again for 30 minutes prior to removing the filter and centrifuging the acid extract. The extracts were then diluted to a final volume of ~120ml (0.5% BrCl and HCl) for Hg analysis.

Hg analytical method. Filter extracts were analyzed for total aqueous Hg using a Tekran model 2600, a dual amalgamation CVAFS, following a modified version of EPA method 1631 recommended in the Tekran 2600 user's guide. Prior to analysis hydroxochloroamine hydroxide was added to destroy any free halogens and the samples were reduced with the addition of stannous chloride. Final concentration values were corrected for analytical system blanks. All samples were analyzed in triplicate with the

result reported as the average of the three values. Triplicate values were typically within 5% of each other.

Data Analysis

The volumetric concentration of Hg^P in the ambient air was calculated after the laboratory analysis of the filter extracts for total aqueous Hg. The total mass of Hg in the extract was calculated from the product of the mass concentration and total filter extract volume. The Hg mass was then divided by the volume of air that passed through the filter during sample collection and units were converted from ng of Hg per liter of air to ppqv. The method detection limit is 0.01ppqv based on the EPA method 1631 detection limit of 0.2 ng L⁻¹ in a 120 ml filter extract sample assuming a bulk filter sample collection flow rate of 120 L min⁻¹ over a 180 minute sample period (21600 L). All blank values reported as ppqv assume a filter extract volume of 120ml and an air sample volume of 21600 L.

Results

Bulk aerosol filter samples were collected every three hours on Appledore Island from 20 July 2009 to 4 August 2009. A total of 136 filters, including 13 field blanks and 6 extraction reagent procedure blanks were collected and analyzed. Five of the sample filters went through the filter extraction procedure multiple times to determine extraction efficiency.

Blanks and external standards

A summary of the results from blanks and external standards is included in Table IV.2. The reagent procedure blanks contained the reagents used in the filter extraction method and went through the extraction procedure without filters. The average reagent procedure blank was 0.02 ppqv. Field blanks were collected after every 9 field samples. The average field blank result (n=13) was 0.23 ppqv and a standard deviation of 0.26

ppqv. There is one anomalous field blank value of 1.03 ppqv, excluding this value the highest field blank is 0.38 ppqv and the average value decreases to 0.15 ppqv.

ORMS-4 Elevated Mercury in River Water (National Research Council - Canada) was used as certified reference material. The average measured value of this reference material was 24.2 ng L⁻¹(n=5), which is 0.6 ng L⁻¹ above the upper limit of the accepted value. Two of the five ORMS-4 sample analyses were within the accepted range for the reference material.

	n	Average (ppqv)	Median (ppqv)	Minimum (ppqv)	Maximum (ppqv)
Reagent procedure blanks	6	0.02	0.01	BDL	0.06
Field blanks	13	0.23	0.10	0.03	1.03
	n	Average (ng L ⁻¹)	Median (ng L ⁻¹)	Minimum (ng L ⁻¹)	Maximum (ng L ⁻¹)
ORMS-4 (Certified Reference Material)	5	24.2	24.5	22.7	25.7

Table IV.2. A summary of results from blanks and certified reference material. Detection limit for blanks is 0.01 ppqv. Detection limit for ORMS-4 is 0.2 ng L⁻¹. The certified concentration of Hg in ORMS-4 is 22.0 ± 1.6 ng L⁻¹.

Summer 2009 Appledore Island field samples

This newly developed filter extraction method was used to quantify Hg^P from aerosol bulk filters collected during 3 hour time intervals over a two week time period on Appledore Island, ME during summer 2009. Filter results are shown in Figure IV.1 and reveal a diurnal pattern in the Hg^P mixing ratio with elevated values during the daylight hours and minimum values at night. The minimum measured mixing ratio is 0.14 ppqv and occurred on a filter sample collected from 3 August 2009, 2:00 UTC (10PM local time) to 5:00 UTC (1AM local time) under breezy and foggy conditions. The maximum mixing ratio measured during this sampling campaign occurred on 28 July 2009 from 14:00 UTC (10 AM local time) to 17:00 UTC (1 PM local time) and is 3.28 ppqv. The average mixing ratio over all samples collected is 1.04 ppqv and median is 0.93 ppqv. Talbot et al. (2011) discuss results from this sampling campaign (and others), make

comparisons to Hg^P measurements using automated methods, and compare Hg^P results to other atmospheric gas phase measurements.

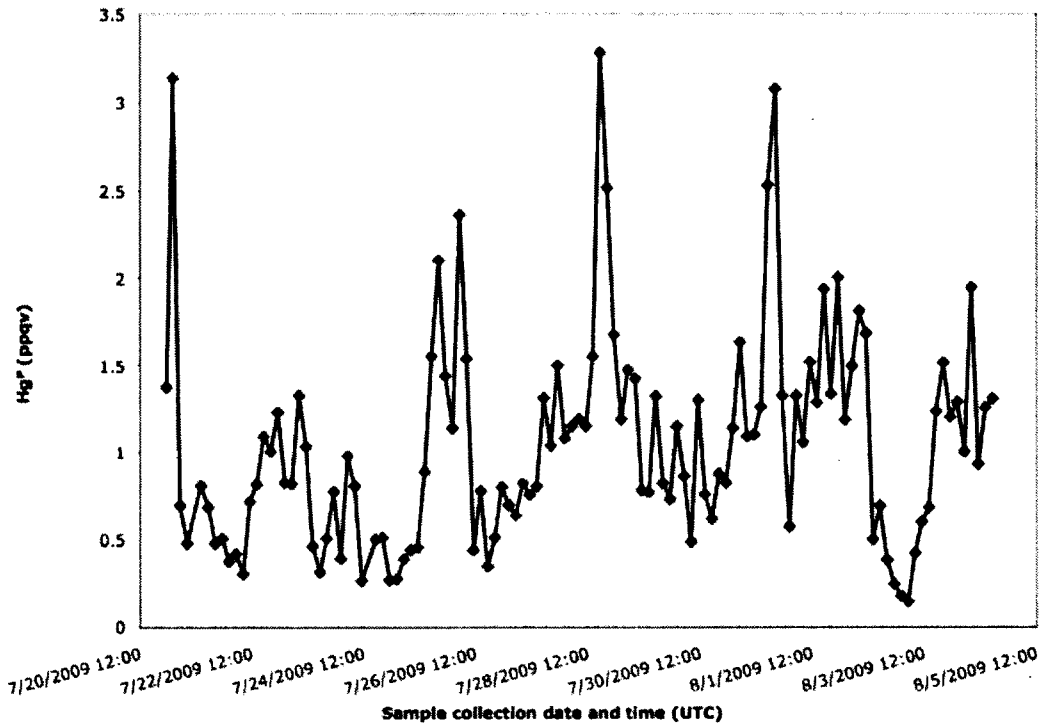


Figure IV.1. Hg^P bulk aerosol filter results from Appledore Island sampling campaign.

Sequential extractions

In an effort to determine the extraction efficiency of this new method, multiple extractions were performed on randomly selected sample filters. Results are shown in Table IV.3 and indicate that extraction efficiencies varied widely between 89 and 53 percent. Minimal amounts of Hg were recovered during the 3rd extraction procedure.

Filter ID	1 st extraction (ppqv)	2 nd extraction (ppqv)	percentage of 1 st extraction	3 rd extraction (ppqv)	percentage of 1 st extraction
11	0.38	0.11	28	NA	
19	0.74	0.09	12	NA	
26	0.74	0.08	11	0.03	4
47	0.41	0.05	13	BDL	0
57	0.76	0.35	47	NA	

Table IV.3. Results from sequential filter extractions.

Discussion and conclusions

The average reagent procedure blank (0.02 ppqv) is minimal compared to the method detection limit (0.01ppqv) indicating that negligible Hg contamination was introduced to the samples during the laboratory extraction procedure. However, the bulk filter field blank results indicate that field contamination or contamination during preparation of the filters is a potential area of concern. The average field blank value (0.23 ppqv) is above the minimum measured field sample value (0.14 ppqv) and 22 percent of the average field sample (1.04 ppqv).

In future work potential sources of field blank contamination should be identified and minimized. A possible source of filter contamination is the acid “cleaning” procedure. During this study, an analysis was not conducted between filters used directly from their packaging and acid cleaned filters. Results from such a comparison may indicate that the lengthy cleaning procedure is unnecessary or alternatively, that additional cleaning precautions are needed. Additional sources of contamination may include the Delrin filter holders, containers used during sample transport, and freezers used for sample storage.

During this study, analytical results from the certified reference material ORMS-4 were generally higher than the range of accepted values. The elevated aqueous concentration of Hg in the ORMS-4 (~22.0 ng L⁻¹) was diluted by one half with 18 MΩ nanopure water prior to measurement with the CVAFS. The dilutions were

measured gravimetrically and the analytical values were calculated using the measured dilution factor. This dilution process may have introduced some error in the results.

The sequential extraction results indicate a variable extraction efficiency ranging from 89% to 53%. Future work should focus on quantifying the extraction efficiency by dosing filters with a standard reference material. Currently there is no certified reference material for Hg in atmospheric aerosol. Potential alternatives are marine sediment reference materials for trace metals available from the National Research Council Canada. Testing of various concentrations of BrCl and HCl for use in the extraction solutions should also be explored for maximizing the filter extraction efficiency.

This new filter extraction technique shows promise for widespread use but further work is necessary to maximize the extraction efficiency, reduce field blank values, and determine its reproducibility. Further development of this method should include a side-by-side comparison of at least two samplers to observe variations in results. More recently some atmospheric Hg studies use commercially available real-time automated systems such as the Tekran 2537A cold vapor atomic fluorescence spectrometer (CVAFS) with the Tekran 1135 species attachment for Hg^P (Engle et al., 2010; Talbot et al., 2011). Talbot et al., 2011 discuss discrepancies between co-located measurements of Hg^P via the bulk filter method explained here and the automated method using the Tekran 1135. Further research in Hg^P methods development and comparisons between methods are necessary to produce meaningful measurements of Hg^P and understand the environmental cycling of this complex element.

References

- Arimoto, R., Schloesslin, C., Davis, D., Hogan, A., Grube, P., Fitzgerald, W., Lamborg, C., 2004. Lead and mercury in aerosol particles collected over the South Pole during ISCAT-2000, *Atmospheric Environment*, 38, 5485-5491.
- Ebinghaus, R., Jennings, S.G., Schroeder, W.H., Berg, T., Donaghy, T., Guentzel, J., Kenny, C., Kock, H.H., Kvietkus, K., Landing, W., Muhleck, T., Munthe, J., Prestbo, E.M., Schneeberger, D., Slemr, F., Sommar, J., Urba, A., Wallschlager, D., Xiao, Z.,

1999. International field intercomparison measurements of atmospheric mercury species at Mace Head, Ireland, *Atmospheric Environment*, 33, 3063-3073.
- Engle, M.A., Tate, M.T., Krabbenhoft, D.P., Schauer, J.J., Kolker, A., Shanley, J.B., Bothner, M.H., 2010. Comparison of atmospheric mercury speciation and deposition at nine sites across central and eastern North America, *J. Geophys. Res.*, 115, D18306, doi:10.1029/2010JD014064.
- Guentzel, J.L., Landing, W.M., Gill, G.A., Pollman, C.D., 1995. Atmospheric deposition of mercury in Florida: The FAMS project (1992-1994), *Water, Air, and Soil Pollution* 80:393-402.
- Keeler, G., Glinsorn, G., Pirrone, N., 1995. Particulate mercury in the atmosphere: Its significance, transport, transformation and sources, *Water, Air, and Soil Pollution*, 80:159-168.
- Landing, W.M., Guentzel, J.L., Gill, G.A., Pollman, C.D., 1998. Methods for measuring mercury in rainfall and aerosols in Florida, *Atmospheric Environment*, 32:5, 909-918.
- Mason, R.P., Lawson, N.M., Sullivan, K.A., 1997. The concentration, speciation and sources of mercury in Chesapeake Bay precipitation, *Atmospheric Environment*, 31:21, 3541-3550.
- Munthe, J., Wangberg, I., Pirrone, N., Iverfeldt, A., Ferrara, R., Ebinghaus, R., Feng, X., Gardfeldt, K., Keeler, G., Lanzillotta, E., Lindberg, S.E., Lu, J., Mamane, Y., Prestbo, E., Schmolke, S., Schroeder, W.H., Sommar, J., Sprovieri, F., Stevens, R.K., Stratton, W., Tuncel, G., Urba, A., 2001. Intercomparison of methods for sampling and analysis of atmospheric mercury species, *Atmospheric Environment*, 35, 3007-3017.
- Talbot, R., Mao, H., Feddersen, D., Smith, M., Kim, S., Sive, B., Haase, K., Ambrose, J., Zhou, Y., Russo, R., 2011. Comparison of particulate mercury measured with manual and automated methods, *Atmosphere*, 2, 1-20; doi:10.3390/atmos2010001.

CHAPTER V

STRONTIUM ISOTOPES IN WATERS FROM THE MT. PAWTUCKAWAY REGION OF THE LAMPREY RIVER WATERSHED

Introduction and background

Accurately determining groundwater flow paths at various spatial scales in fractured bedrock aquifers is a challenging endeavor. The heterogeneity in the occurrence and size of fractures as fracture networks that serve as the primary conduit for water movement through rock are difficult to characterize and predict (Berkowitz, 2002). This presents challenges in the management of fractured bedrock water resources. The state of New Hampshire contains limited amounts of unconsolidated aquifer materials and as a result bedrock aquifers are increasingly tapped to meet the growing water demands of an increasing population (Moore, 2004). Identifying tools and techniques that can characterize bedrock groundwater flow at the watershed scale will be useful in the future management of this essential natural resource.

Naturally occurring radiogenic isotopes are useful environmental tracers. Water – rock interactions can impart geochemical signatures from the rock to the groundwater and consequently the surface water. These tracers exhibit the possibility of serving as a non-invasive method to determine bedrock groundwater flow direction and bedrock groundwater interactions with surface water.

Strontium (Sr) isotopes are an established tool for tracing groundwater flow paths, and groundwater - surface water interactions (Bullen et al., 1996; Hunt et al., 2000; Johnson et al., 2000; Hogan and Blum, 2003; Ojiambo et al., 2003;). In the Sr system both ^{86}Sr and ^{87}Sr are stable isotopes, but ^{87}Sr is the decay product of ^{87}Rb .

The present day ratio $^{87}\text{Sr}/^{86}\text{Sr}$ in a rock depends on the initial ratio present in the reservoir plus the accumulation over time of ^{87}Sr from the decay of ^{87}Rb .

Strontium isotope tracers are especially useful when two bedrock lithologies with distinct present-day ratios occur adjacent to each other. Present-day contrasting ratios may result in lithologies with different Rb/Sr content and/or different ages. The isotopic signature of the rock is imparted to the water through water-rock interactions. Johnson and DePaolo (1997) present a model for evolution of isotope ratios in response to solute transport and water-rock interaction. Despite the slow rate at which reactions occur in low-temperature systems, concentrations of many elements of interest in the groundwater are orders of magnitude smaller than those in the rock, consequently a small reaction flux from the rock has a magnified effect on isotope ratios in the water.

Several studies demonstrate that the geochemical signatures imparted to groundwater from these interactions can successfully map flow at the watershed scale. Johnson et al. (2000) used Sr isotope ratios with major and trace element data to map the spatial occurrence of a fast groundwater flow path zone in a bedrock aquifer of the Snake River Plain. Bedrock lithologies with contrasting geochemical affinities for trace elements and $^{87}\text{Sr}/^{86}\text{Sr}$ isotopic signatures occur adjacent to each other within the watershed. The "fast path" of groundwater was delineated based on mapped trace element concentration and strontium isotope signatures from hundreds of wells that provided high resolution sampling of groundwater compositions. The observed tongue of high Sr isotope values could not be fully explained by simple mixing or reasonable rates of water-rock interaction. Trace element concentrations in groundwater had a similar pattern and reinforced the interpretation of the groundwater flow.

While these geochemical techniques have been developed and used by others to determine groundwater flow in watersheds, they have not commonly been applied to fractured bedrock aquifer systems located in the northeastern United States. The

Lamprey River watershed (Figure V.1) is an ideal study location in New England because strongly contrasting bedrock compositions occur adjacent to each other. Additionally, the Lamprey watershed is one in which land use is primarily forested implying little human alteration and the main stem of the river is easily accessible. Also, this watershed is predicted to undergo substantive population growth in the next decade. The population density over the watershed for the year 2000 was 53 people per square kilometer and is projected to increase by 60 percent by the year 2020 (US Census, 2000). The development of techniques to identify groundwater flow paths may prove useful for future water resource planning.

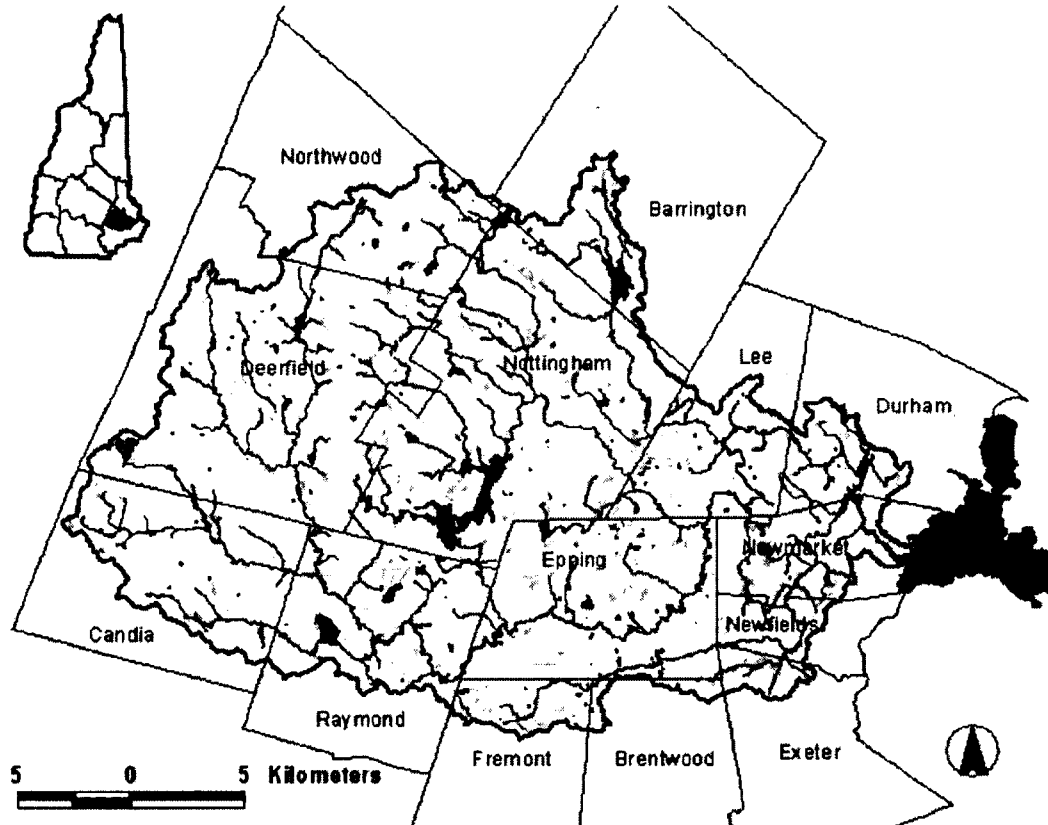


Figure V.1. Location of the Lamprey River Watershed, New Hampshire.

This study focuses on the groundwater and surface water interactions along the boundary between the Mt. Pawtuckaway and Massabesic Gneiss bedrock complexes within the Lamprey River watershed. The Mt. Pawtuckaway Complex, a local

topographic feature, is a part of the White Mountain Plutonic Volcanic Series intruded into the Massabesic Gneiss Complex (Figure V.2). The igneous rocks of the Mt. Pawtuckaway complex are composed primarily of diorites and monzonites with some pyroxenite, gabbros, and syenites. The estimated age of the pluton is 129 ± 5 million years (Eby, 1985). The Massabesic Gneiss Complex is composed of a heterogenous mixture of high grade metamorphic rock. Debate exists about the formation and the amount of igneous rock within the complex (Kelly, 1980; Dorais, 2001; Kerwin, 2007), yet there is greater consensus that the estimated age of these rocks is between 600 to 671 Ma. (Besancon et al., 1977; Kelly, 1980; Aleinkoff and Walter, 1995).

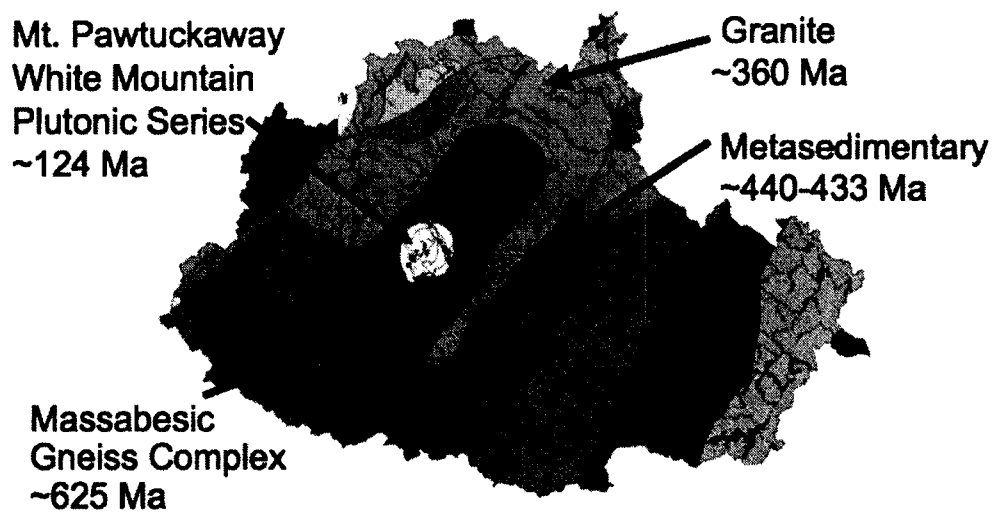


Figure V.2. Bedrock lithology of the Lamprey River watershed. Adapted from Lyons et al., 1997.

Studies have established that weathering of rocks proceeds nonmodally, i.e. certain minerals more readily dissolve due to both thermodynamic stability and kinetic considerations, affecting the resultant $^{87}\text{Sr}/^{86}\text{Sr}$ ratios in groundwater (Bau et al., 2004; Erel et al., 2004). Therefore the mineral mode in groundwater host rock is important to consider because the presence of certain minerals may strongly impact the groundwater

isotope signatures. Biotite, for example, has an extremely high Rb/Sr, resulting in elevated $^{87}\text{Sr}/^{86}\text{Sr}$ in groundwater. Figure V.3 presents a compilation of mineral modes from previous studies on the composition of the Massabesic Gneiss Complex and the diorite and monzonite from the Mount Pawtuckaway Complex. As Figure V.3 shows, the foremost difference between the lithologies is the relative amount of quartz in each, 13% to 50% in the Massabesic Gneiss Complex and an almost entire absence from the Mt. Pawtuckaway rocks. The relative abundance of quartz, however, has little direct influence on the strontium isotope system as both Rb and Sr are incompatible in quartz. Both rock types contain large amounts of plagioclase and alkali feldspars, which would have less radiogenic (plagioclase) and extremely radiogenic (alkali feldspar) strontium signatures. The Mt. Pawtuckaway Complex contains larger amounts of pyroxene and amphiboles while the Massabesic Gneiss Complex, on average, contains higher amounts of biotite. The weathering of these minerals and rock complexes should provide contrasting $^{87}\text{Sr}/^{86}\text{Sr}$ isotopic data based on their difference in age and mineral composition. Extrapolating from whole rock composition data the Massabesic Gneiss Complex is anticipated to have high $^{87}\text{Sr}/^{86}\text{Sr}$ relationships in comparison to the Mt. Pawtuckaway Complex (Table V.1).

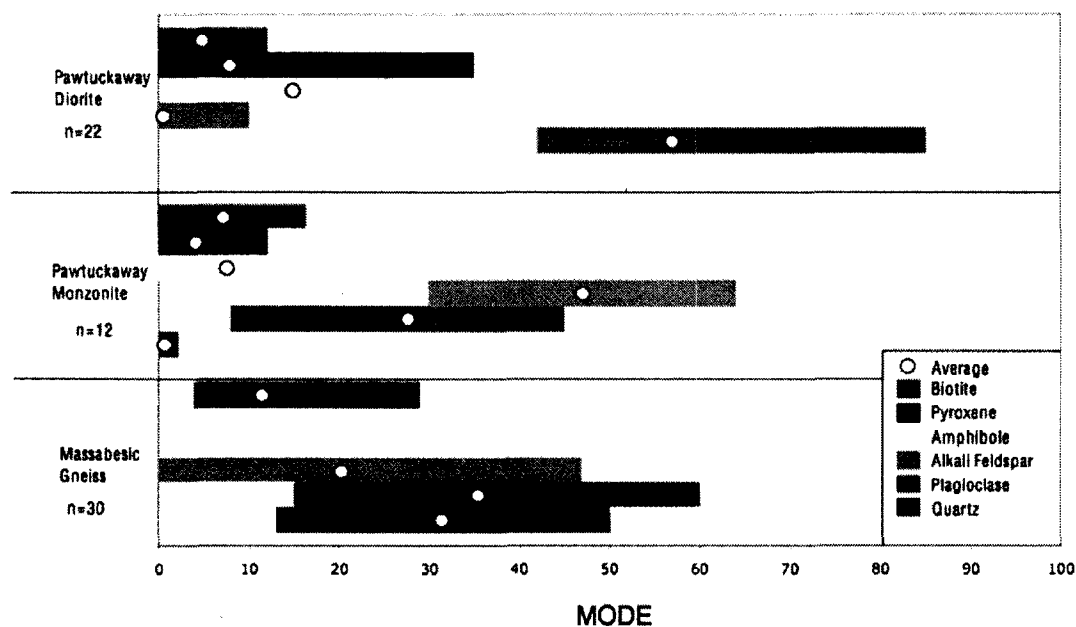


Figure V.3. Mineral modes for the Massabesic Gneiss and Pawtuckaway diorite and monzonite. Data are from (Roy and Freedman, 1944; Shearer, 1976; Kelly, 1980; Eby, 1985; Richards, 1990; Kerwin, 2007).

Sample Type	Bedrock	$^{87}\text{Sr}/^{86}\text{Sr}$
Quartz	Mt. Pawtuckaway White	
Monzonite	Mountain Plutonic	0.7036-0.7056 ¹
Gneiss	Massabesic Gneiss	0.7180-0.7260 ²
Two-mica granite	Concord Granite	0.7110-0.9321 ³

Table V.1. Whole rock $^{87}\text{Sr}/^{86}\text{Sr}$ values in the study area. 2σ on $^{87}\text{Sr}/^{86}\text{Sr}$ are < 0.00040 .

¹http://faculty.uml.edu/Nelson_Eby/Research/monteregian%20hills/MHWM%20Isotopes%20+%20elements.xls

² M. J. Dorais (pers. comm.)

³ Lyons and Livingston (1977)

Methods

Surface water samples were collected in acid cleaned HDPE bottles and transported to the trace metal geochemistry laboratory at the University of New Hampshire. All water samples were passed through 0.45 μm Fluoropore filters and acidified with Optima HNO_3 to a concentration of 0.2%. Samples were evaporated and then reconstituted in 3M HNO_3 and passed through Eichrom Sr spec resin columns to

concentrate the Sr and remove elements that contribute to interferences or otherwise impede high precision measurement (e.g., Rb and Ca). The resulting salts were reconstituted in dilute HNO₃ and loaded with Ta₂O₅ onto rhenium filaments in preparation for analysis via thermal ionization mass spectrometry (TIMS). Barry Hanan at San Diego State University analyzed samples collected in May 2004. Additional samples collected in June 2006 were analyzed at the Boston University TIMS facility. All data are normalized to NIST SRM 987, $^{87}\text{Sr}/^{86}\text{Sr} = 0.710250$. All analytical errors reported for $^{87}\text{Sr}/^{86}\text{Sr}$ values are reported by convention as the standard error on the mean, which corresponds to the internal precision.

Initially, two surface water bodies underlain by the contrasting bedrock types were sampled in May 2004 and analytical results confirmed distinct $^{87}\text{Sr}/^{86}\text{Sr}$ signatures in these waters. Following these results, additional Sr isotope analyses were conducted on surface water samples from the main stem of the Lamprey River, a wetland area draining into the Lamprey River, a well finished in the surficial stratified drift layer, homeowner wells finished in bedrock, and regional precipitation samples (Table V.2).

Samples from the main stem of the Lamprey River, wetland area, and stratified drift well were collected on 12-13 July 2006. Real time measurements from a USGS stream gauge located on the Lamprey River downstream of the study site (USGS ID 01073500) indicate that the average daily discharge during water year 2006 was 570 cubic feet per second (cfs). The average daily discharges on 12 and 13 July 2006 were 157 cfs and 372 cfs, respectively, well below the average daily discharge, indicating baseflow conditions dominated during the period of sample collection. The average daily discharge measurements from the USGS gauge are shown in Figure V.4. Weather records indicate that rain occurred on 11-13 of July 2006. The surface water and stratified drift well sampling occurred on the rising limb of the hydrograph (Figure V.4),

however these samples were collected during generally low flow river conditions and source water is expected to be largely groundwater.

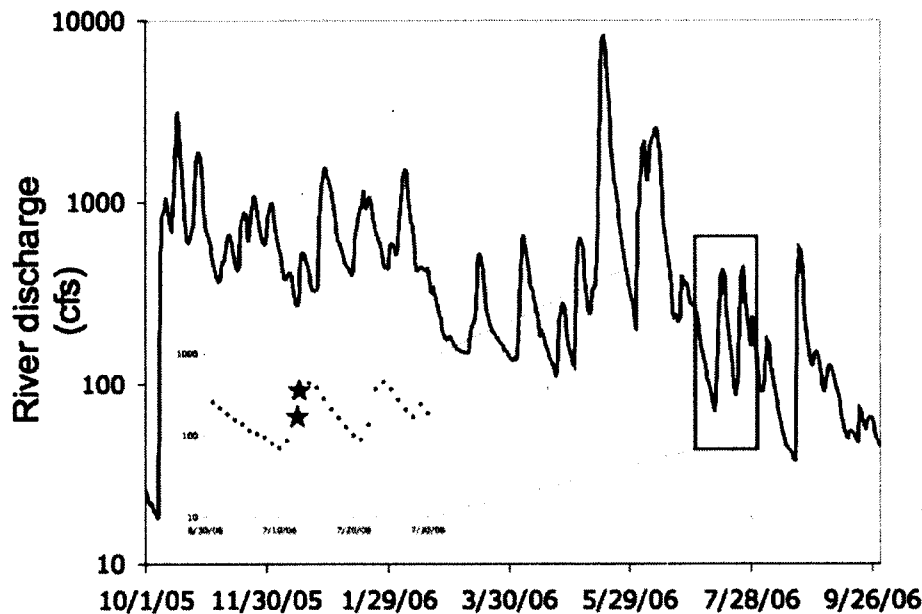


Figure V.4. Lamprey River hydrograph for water year 2006 from USGS gauge site 01073500 located downstream of the study area. The inset is the hydrograph for July 2006 and the two stars represent the sampling days for this study on the Lamprey River.

The stream water samples were collected at intermittent distances along the main stem of the Lamprey River and sampling locations were generally determined by their roadside accessibility. The identification of the bedrock underlying the surface water sites was determined by comparing sampling locations to the bedrock maps of Lyons et al. (2000) and Kerwin (2007). Two bedrock contacts underlie the river in the stretch that was sampled. The two upstream and northernmost sampling locations, Freese's Pond and Jame's City Road, are underlain by granitic bedrock (Concord Granite). The next downstream sampling location, Route 107/43, is in the general area of a bedrock contact between the granitic unit, a metasedimentary unit and the Massabesic Gneiss Complex. The two remaining downstream locations, Cotton Road and Watershed Outlet, are underlain by the Massabesic Gneiss Complex.

The groundwater sample collected from the well finished in the surficial stratified drift layer is a USGS well (ID 430527071140101-NH-DDW 46). A static water level of 37.45 feet below the ground surface was recorded by the USGS on 27 July 2006, two weeks after sampling for Sr isotopes occurred. Since 1984 water level measurements have been recorded on an approximately monthly basis. The average water level from November 1984 to July 2006 was 38.65 feet below the ground surface, indicating water levels near the time of sampling were higher than the average. Water levels in this well declined from April 2006 to October 2006, however, indicating baseflow conditions were likely to dominate during the summer of 2006.

Samples from five homeowner wells were analyzed for $^{87}\text{Sr}/^{86}\text{Sr}$. These samples were collected from 19 August 2005 to 8 September 2005 from homes located on a road north of the Pawtuckaway State Park that runs approximately east to west. Efforts were made to collect samples from water faucets that either by-passed or were located before any home water treatment systems. Detailed and reliable well information is not available for the homeowner wells sampled, however it is assumed they are completed in fractured bedrock.

Two precipitation samples collected at Thompson Farm located in Durham, New Hampshire, approximately 25 kms east of the study area were also analyzed for $^{87}\text{Sr}/^{86}\text{Sr}$. The samples were collected from rain events occurring on 11-12 October 2006 and 20 August 2006 and are included in this study to characterize the isotopic signature from the rainwater inputs to the watershed.

Groundwater flow paths emanating from the Mt. Pawtuckaway area were generated using the Modular Three-Dimensional Finite-Difference Ground-Water Flow Model (MODFLOW) (Harbaugh et al., 2000) a three dimensional finite difference model (Figure V.5, after J.M. Davis, personal communication). This model generation assumed steady state conditions and used a one layer approach with 30 x 30 meter size grid cells.

Input parameters and data sources included topography from the 30m digital elevation model, depth to bedrock from NHDES well data, and GIS coverages for surface water bodies and surficial geology at the 1:24,000 scale and bedrock geology at the 1:250,000 scale. Additionally, the recharge was set at 20 cm per year and bedrock conductivity was set at 0.25 meters/day (J.M. Davis, personal communication).

Results and Discussion

Spatial Variability in $^{87}\text{Sr}/^{86}\text{Sr}$

The initial surface water samples collected in 2004 had distinct Sr isotope ratios. $^{87}\text{Sr}/^{86}\text{Sr}$ was 0.71443 ± 0.00001 taken from Quincy Pond underlain by bedrock of the Massabesic Gneiss Complex and $^{87}\text{Sr}/^{86}\text{Sr}$ was 0.70686 ± 0.00002 from Round Pond underlain by the White Mountain Plutonic Volcanic Series. These results indicated distinct differences in Sr isotope ratios in water bodies within the Lamprey River watershed area.

Subsequently, five surface water samples were collected from the main stem of the Lamprey River. These samples show decreasing $^{87}\text{Sr}/^{86}\text{Sr}$ values as the river flows downstream and passes the area of the Mt. Pawtuckaway Complex (Figure V.5). The most upstream $^{87}\text{Sr}/^{86}\text{Sr}$ is 0.71641 and steadily decreases to 0.71498 (Figure V.5, Table V.2).

<u>Location</u>	<u>Sample date</u>	<u>Geology</u>	<u>$^{87}\text{Sr}/^{86}\text{Sr}$</u>	<u>2σ</u>
Quincy Pond	May 2004	Massabesic Gneiss Complex	0.71443	0.00001
Round Pond	May 2004	Mt. Pawtuckaway Complex	0.70686	0.00002
Freese's Pond (Lamprey River)	12 July 2006	Concord Granite	0.71641	0.00002
James City Road (Lamprey River)	12 July 2006	Concord Granite	0.71640	0.00002
Route 107/43 (Lamprey River)	12 July 2006	Massebesic Gneiss Complex	0.71584	0.00001
Cotton Road (Lamprey River)	12 July 2006	Massebesic Gneiss Complex	0.71502	0.00003
Watershed Outlet (Lamprey River)	13 July 2006	Massebesic Gneiss Complex	0.71498	0.00001
Reservation Road (wetland area)	12 July 2006	Massebesic Gneiss Complex	0.71424	0.00001
Deerfield Well	13 July 2006	Surficial stratified drift	0.71425	0.00002
Homeowner Well 1	8 September 2005	Undifferentiated Rangeley and Perry Mountain Formations	0.71671	0.00002
Homeowner Well 2	19 August 2005	Undifferentiated Rangeley and Perry Mountain Formations	0.70990	0.00001
Homeowner Well 3	29 August 2005	Massabesic Gneiss Complex	0.71257	0.00001
Homeowner Well 4	19 August 2005	Massabesic Gneiss Complex	0.72561	0.00002
Homeowner Well 5	19 August 2005	Massabesic Gneiss Complex	0.71241	0.00001
Precipitation	20 August 2006	Not Applicable	0.70836	0.00002
Precipitation	11-12 October 2006	Not Applicable	0.70862	0.00002

Table V.2. Sample information and $^{87}\text{Sr}/^{86}\text{Sr}$ results for all samples included in this study. The Lamprey River water samples are listed in order from upstream to downstream. The homeowner well numbers are listed from east to west with increasing well number.

A wetland area (Reservation Road site) that drains into the Lamprey River and is located between the Mount Pawtuckaway Complex and the Lamprey River has an intermediate $^{87}\text{Sr}/^{86}\text{Sr}$ value of 0.71424. This sampling site is underlain by the Massabesic Gneiss Complex however the $^{87}\text{Sr}/^{86}\text{Sr}$ value is lower than the Quincy Pond sample collected from surface water in the same bedrock unit. This intermediate value at the Reservation Road site may be a result of mixing between the low $^{87}\text{Sr}/^{86}\text{Sr}$ water from the Mt. Pawtuckaway Complex and the higher ratio from the Massebesic Gneiss

Complex. However, the strontium isotope ratio measured in the Deerfield Well, completed in the surficial stratified drift, has $^{87}\text{Sr}/^{86}\text{Sr}$ of 0.71425, essentially the same as the wetland. The Sr isotope ratio in the water from the wetland area could be strongly influenced by groundwater in the surficial aquifer and not the bedrock groundwater.

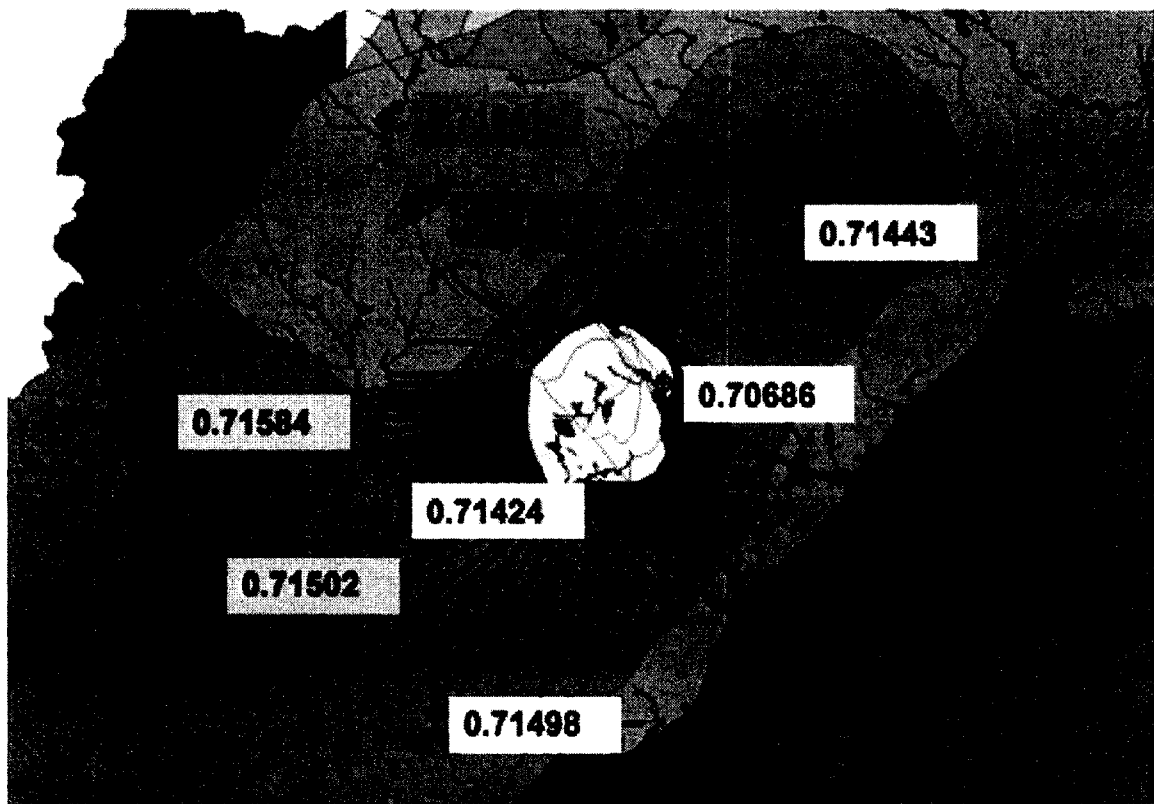


Figure V.5. $^{87}\text{Sr}/^{86}\text{Sr}$ results for surface water samples. Modeled groundwater flow paths (red line) were generated using MODPATH.

The $^{87}\text{Sr}/^{86}\text{Sr}$ ratios from the homeowner wells are highly variable and range from 0.70990 to 0.72561. This variability is good and indicates that the potential exists to use this geochemical signature as a tool in understanding groundwater and surface water interactions in the Lamprey River Watershed. At present the variability has several possible explanations that should be examined in more detail during future work. Homeowners were asked about the presence of any water treatment systems (such as water softeners) prior to sample collection and all homeowners claimed they did not have any treatment systems. Homeowner samples were generally collected from

outside faucets and the indoor water systems were not inspected. It is possible that some homes had treatment systems, which could alter the Sr isotope ratios. Due to the lack of reliable well information it is also possible that all of these wells are not finished in bedrock, some may be in the surficial stratified drift layer. A comparison between the underlying bedrock from the well sampling locations and the Sr isotope signatures does not fully explain the variability. For example the two homeowner wells (presumed) finished in the Massabesic Gneiss Complex have $^{87}\text{Sr}/^{86}\text{Sr}$ ratios of 0.72561 and 0.71241. As Figure V.6 shows, the 0.72561 value is within the range of whole rock values reported for this rock type, however the 0.71241 value is below both the whole rock and surface water values for the Massabesic Gneiss Complex. The low value in the Massabesic Gneiss Complex may indicate mixing with the surficial aquifer system, mixing groundwater from the Mt. Pawtuckaway Complex, or mixing with precipitation. The remaining three homeowner wells are mapped in the Rangeley and Perry Mountain Formations and Sr isotope ratios for surface water or whole rock samples are not available from these rock formations. Although these three well exist in the same bedrock there is a wide range in the Sr isotope ratios (0.70990 – 0.71671). Possible explanations for the low $^{87}\text{Sr}/^{86}\text{Sr}$ value of 0.70990 are a strong influence from run-off (the precipitation values are low), inputs from the Mt. Pawtuckaway Series bedrock groundwater or the surficial aquifer.

Another possible explanation for the observed variability in the Sr isotope ratios is the mineralogical heterogeneity of the host bedrock and the presence of certain minerals that may dominate the Sr isotope signal in groundwater. Bau et al. (2004) conducted an extensive investigation into the mineralogical sources of observed groundwater chemistry in the Cape Cod Aquifer and their findings indicated that the accessory minerals glauconite and plagioclase dominated the observed groundwater Sr isotope ratios. The highly radiogenic $^{87}\text{Sr}/^{86}\text{Sr}$ value in homeowner well 4, for example,

might be dominated by the dissolution of biotite found in the Massabesic Gneiss Complex. The presence of Sr isotope ratio differences in the groundwater and surface waters of this study area and precipitation values indicates that indicates that terrestrial geochemical processes do alter the $^{87}\text{Sr}/^{86}\text{Sr}$ values in the Lamprey River. However, further work is necessary to elucidate the causes of variability in the $^{87}\text{Sr}/^{86}\text{Sr}$ ratios.

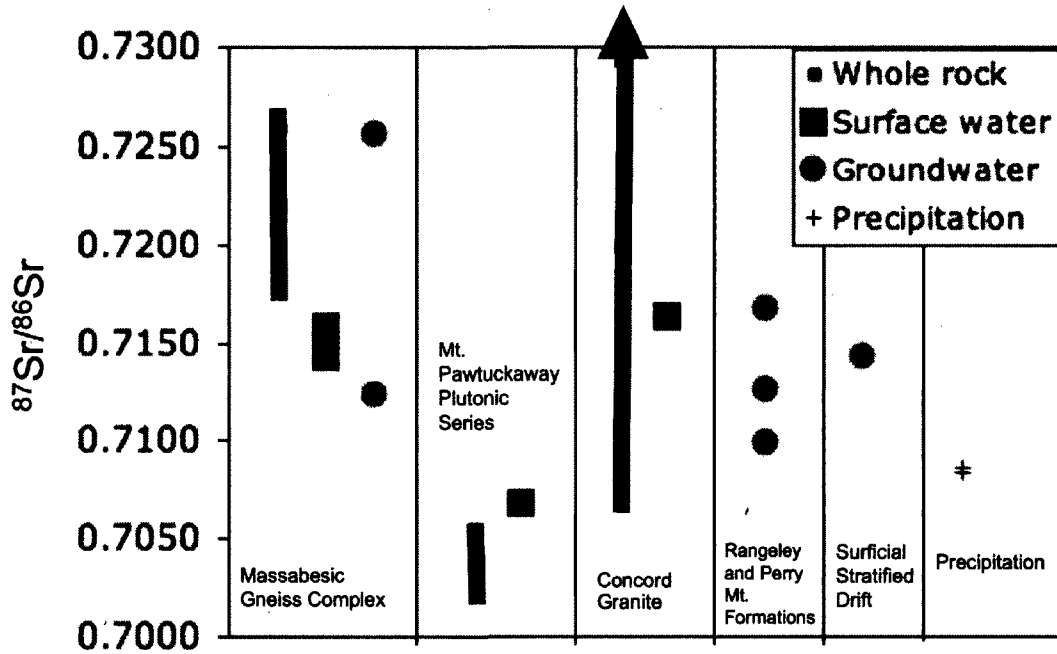


Figure V.6 $^{87}\text{Sr}/^{86}\text{Sr}$ ratios for whole rock, surface water and groundwater samples from the various bedrock units underlying the study area. The $^{87}\text{Sr}/^{86}\text{Sr}$ value for Concord Granite extends to 0.9321. The $^{87}\text{Sr}/^{86}\text{Sr}$ ratios for precipitation samples collected in the watershed are also shown for comparison.

Connections with Stable Isotope Studies in the Lamprey River Watershed

Frades (2008) examines groundwater and surface water inputs into the Lamprey River utilizing stable isotope chemistry and hydrologic measurements in the same watershed area as this study. The stable isotope data are interpreted to identify three groundwater inputs to the Lamprey River that consist of very shallow, shallow, and deep groundwater systems. Frades (2008) concludes that the very shallow groundwater reservoir, consisting of surface water and wetland water, is the primary source of baseflow to the Lamprey River. The downstream decrease in $^{87}\text{Sr}/^{86}\text{Sr}$ ratios and the

similar values between the wetland area and watershed outlet sampling site may be a result of inputs from this very shallow reservoir. Zuidema (2011) uses stable isotopes and a binary mixing model to determine that approximately 20-30% of baseflow at the headwaters of the Lamprey River is from this very shallow or riparian groundwater source. The remaining model end member is discharge from a beaver dammed wet meadow and bedrock groundwater is not considered. Frades (2008) also does not examine the deep groundwater system but concedes that interbasinal deep groundwater flow may account for the missing flux in his water budget calculation. The observed decrease in $^{87}\text{Sr}/^{86}\text{Sr}$ ratios along the main stem of the Lamprey river could also be explained by bedrock groundwater flow from the Mt. Pawtuckaway area. The bedrock groundwater flow lines emanating from the Mt. Pawtuckaway area along with the surface water $^{87}\text{Sr}/^{86}\text{Sr}$ results are shown in Figure V.5. The visual combination suggests that the decreasing $^{87}\text{Sr}/^{86}\text{Sr}$ values along the Lamprey River are due to bedrock groundwater inputs from the Mt. Pawtuckaway area where low $^{87}\text{Sr}/^{86}\text{Sr}$ occurs.

Conclusions

The surface waters of the Lamprey River Watershed in the vicinity of Mt. Pawtuckaway exhibit differences in $^{87}\text{Sr}/^{86}\text{Sr}$ values that correspond to differences in the host bedrock. Nonetheless, large gradients exist in $^{87}\text{Sr}/^{86}\text{Sr}$ across relatively small spatial scales in the homeowner wells indicating that the groundwater ratios are highly variable. Possible explanations for this should be quantitatively examined in depth. This study provides preliminary data requiring further investigation before any robust conclusions can be made about the sources of the different Sr isotope ratios and how they relate to groundwater-surface water interactions within the watershed. Based on the results of this study, Sr isotopes should continue to be investigated as a useful tool in determining hydrogeologic characteristics of the Lamprey River Watershed near Mt. Pawtuckaway.

Coupling trace element ratios with Sr isotope ratios has reinforced interpretations based on Sr isotope ratios alone (Johnson et al., 2000; Bau et al., 2004). Including trace element analysis in future work would be beneficial and may identify a lower-cost technique for pursuing groundwater mapping. Additionally, conducting laboratory dissolution studies of bedrock and overburden would constrain the geochemical signals from each groundwater host. The trace element and Sr isotope patterns from these laboratory scale studies should then be compared to surface water results. This comparison may then allow for the use of mixing models to determine the relative inputs of water from each host reservoir to the Lamprey River.

References

- Aleinikoff, J.N., and Walter J.M., 1995. U-Pb ages of monazite and sphene from rocks of the Massabesic Gneiss Complex and the Berwick Formation, New Hampshire and Massachusetts: Geological Society of America Abstracts with Programs, Northeastern Section, p. 26.
- Bau, M., Alexander, B., Chesley, J.T., Dulski, P., Brantley, S.L., 2004. Mineral dissolution in the Cape Cod aquifer, Massachusetts, USA: I. Reaction stoichiometry and impact of accessory feldspar and glauconite on strontium isotopes, solute concentrations, and REY distributions. *Geochimica et Cosmochimica*. 68: 1199-1216.
- Berkowitz, B., 2002. Characterizing flow and transport in fractured geological media: a review, *Advances in Water Resources* 25, 861-884.
- Besancon, J.R., Gaudette, H.E., Naylor, R.S., 1977. Age of the Massabesic Gneiss, Southeastern New Hampshire: Geological Society of America Abstracts with Programs, v.9, p.242.
- Bullen, T.D., Krabbenhoft, D.P., Kendall C., 1996. Kinetic and mineralogic controls on the evolution of groundwater chemistry and $^{87}\text{Sr}/^{86}\text{Sr}$ in a sandy silicate aquifer, northern Wisconsin, USA. *Geochimica et Cosmochimica*. 60, 1807-1821.
- Dorais, M.J., Wintsch, R.P., Becker, H., 2001. The Massabesic Gneiss Complex, New Hampshire: A study of a portion of the Avalon Terrane. *American Journal of Science*, vol. 301, 657-682.
- Eby, G.N., 1985. Sr and Pb isotopes, U and Th chemistry of the alkaline Monteregian and White Mountain igneous provinces, eastern North America. *Geochimica et Cosmochimica Acta*, Vol. 49 p. 1143-1153.

- Erel, Y., Blum, J.D., Roueff, E., Ganor, J., 2004. Lead and strontium isotopes as monitors of experimental granitoid mineral dissolution, *Geochimica et Cosmochimica Acta*, 68:22, 4649-4663.
- Frades, M., 2008. Hydrologic analysis of the Headwaters Lamprey River Watershed using water isotopes, M.S. Thesis. University of New Hampshire.
- Harbaugh, A.W., Banta, E.R., Hill, M.C., McDonald, M.G., 2000. MODFLOW-2000, The U.S. Geological Survey Modular Ground-water Model – User Guide to Modularization Concepts and the Ground-Water Flow Process. USGS Open File Report 00-92. Reston, VA.
- Hogan, J.F., Blum, J.D., 2003. Tracing hydrologic flow paths in a small forested watershed using variations in $^{87}\text{Sr}/^{86}\text{Sr}$, $[\text{Ca}]/[\text{Sr}]$, $[\text{Ba}]/[\text{Sr}]$ and d^{18}O . *Water Resources Research*. 39: doi:10.1029/2002WR001856.
- Hunt, R.J., Steuer, J.J., 2000. Simulation of the Recharge Area for Federick Springs, Dane County, Wisconsin: U.S. Geological Survey Water Resources Investigations Report 00-4172, 33 p.
- Johnson, T.M., DePaolo, D.J., 1997. Rapid exchange effects on isotope ratios in groundwater systems 1. Development of a transport-dissolution-exchange model, *Water Resources Research*, vol. 33, no.1, p. 187-195.
- Johnson, T.M., Roback, R.C., McLing, T.L., Bullen, T.D., DePaolo, D.J., Doughty, C., Hunt, R.J., Smith, R.W., Cecil, L.D., Murrell, M.T., 2000. Groundwater “fast paths” in the Snake River Plain aquifer: Radiogenic isotope ratios as natural groundwater tracers. *Geology*. 28: 871-874.
- Kelly, W.J., 1980. An isotopic study of the Massabesic Gneiss: Southeast New Hampshire. M.S. Thesis, University of New Hampshire.
- Kerwin, C.M., 2007. Mapping, petrological and geochemical explorations of the Massabesic Gneiss Complex in New Hampshire. Ph.D. Dissertation, University of New Hampshire.
- Lyons, J.B., Bothner, W.A., Moench, R.H., and Thompson, J.B., 1997. Bedrock Geology Map of New Hampshire, color, 2 sheets, 42' x 54'; each, United States Geological Survey.
- Lyons, J., B., Livingston, D.E., 1977. Rb-Sr age of the New Hampshire Plutonic Series, *Geological Society of America Bulletin*, v.88, p.1808-1812.
- Moore, R.B., 2004. Quality of water in the fractured-bedrock aquifer of New Hampshire: U.S. Geological Survey Scientific Investigations Report 2004-5093, 30 p.
- Ojiambo, S.B., Lyons, W.B., Welch, K.A., Poreda, R.J., Johannesson, K.H., 2003. Strontium isotopes and rare earth elements as tracers of groundwater-lake water interactions, Lake Naivasha, Kenya. *Applied Geochemistry*, 18, 1789-1805.

Richards, P.M., 1990. Nature of the emplacement of the Mt. Pawtuckaway Complex, Rockingham County, New Hampshire. M.S. Thesis, University of New Hampshire.

Roy, C.J. and Freedman, J., 1944. Petrology of the Pawtuckaway Mountains, New Hampshire. Geol. Soc. Amer. Bull. 55, 905-920.

Shearer, C.K., 1976. Geochemical and geological investigation of the Pawtuckaway Mountain Plutonic Complex, Rockingham County, New Hampshire. M.S. Thesis, University of New Hampshire.

United States Census, 2000.

Zuidema, S., 2011. Identifying groundwater contributions to baseflow in a temperate headwater catchment. M.S. Thesis. University of New Hampshire.

APPENDIX

UNH ID	Sample location	Deploy Date (Local)	Deploy Time	Collect Date (Local)	Collect Time
TF001	Thompson Farm	07/13/2006		07/24/2006	
TF002	Thompson Farm	07/24/2006		07/31/2006	
TF003	Thompson Farm	07/31/2006		08/04/2006	
TF004	Thompson Farm	08/04/2006		08/16/2006	
TF005	Thompson Farm	08/16/2006		08/21/2006	
TF006	Thompson Farm	08/21/2006		08/25/2006	
TF007	Thompson Farm	08/25/2006		08/28/2006	
TF008	Thompson Farm	08/28/2006		09/05/2006	13:00
TF009	Thompson Farm	09/05/2006	13:00	09/11/2006	12:00
TF010	Thompson Farm	09/11/2006	12:00	09/15/2006	12:00
TF011	Thompson Farm	09/15/2006	12:00	09/20/2006	9:00
TF012	Thompson Farm	09/20/2006	9:00	09/25/2006	9:00
TF013	Thompson Farm	09/25/2006	9:00	10/02/2006	9:00
TF014	Thompson Farm	10/02/2006	9:00	10/05/2006	13:00
TF015	Thompson Farm	10/05/2006	13:00	10/12/2006	9:00
TF016	Thompson Farm	10/12/2006	9:00	10/18/2006	9:00
TF017	Thompson Farm	10/18/2006	9:00	10/23/2006	9:00
TF018	Thompson Farm	10/27/2006	18:00	10/30/2006	13:00
TF019	Thompson Farm	10/30/2006	13:00	11/03/2006	9:00
TF020	Thompson Farm	11/03/2006	9:00	11/08/2006	9:00
TF021	Thompson Farm	11/08/2006	9:00	11/09/2006	9:00
TF022	Thompson Farm	11/09/2006	9:00	11/13/2006	9:00
TF023	Thompson Farm	11/13/2006	9:00	11/14/2006	8:00
TF024	Thompson Farm	11/14/2006	8:00	11/17/2006	8:00
TF025	Thompson Farm	11/17/2006	8:00	11/28/2006	9:00
TF026	Thompson Farm	11/28/2006	9:00	12/02/2006	11:30
TF027	Thompson Farm	12/02/2006	11:30	12/13/2006	13:00
TF028	Thompson Farm	12/13/2006	13:00	12/14/2006	14:30
TF029	Thompson Farm	12/14/2006	14:30	12/28/2006	11:30
TF030	Thompson Farm	12/28/2006	11:30	01/02/2007	16:00
TF031	Thompson Farm	01/02/2007	16:00	01/08/2007	16:00
TF032	Thompson Farm	01/08/2007	16:00	01/16/2007	9:00
TF033	Thompson Farm	01/16/2007	9:00	01/22/2007	16:00
TF034	Thompson Farm	01/31/2007	15:00	02/05/2007	15:00
TF035	Thompson Farm	02/05/2007	15:00	02/15/2007	16:00
TF036	Thompson Farm	02/15/2007	16:00	03/03/2007	10:00
TF037	Thompson Farm	03/06/2007		03/12/2007	18:00
TF038	Thompson Farm	03/14/2007		03/18/2007	
TF039	Thompson Farm	03/18/2007		03/24/2007	
TF040	Thompson Farm	03/24/2007		03/28/2007	
TF041	Thompson Farm	04/01/2007		04/03/2007	
TF042	Thompson Farm	04/03/2007		04/07/2007	
TF043	Thompson Farm	04/07/2007		04/14/2007	
TF044	Thompson Farm	04/14/2007		04/20/2007	
TF045	Thompson Farm	04/20/2007		04/28/2007	

UNH ID	Sample location	Deploy Date (Local)	Deploy Time	Collect Date (Local)	Collect Time
TF046	Thompson Farm	04/28/2007		05/15/2007	
TF047	Thompson Farm	05/15/2007		05/21/2007	
TF048	Thompson Farm	05/26/2007		05/29/2007	
TF049	Thompson Farm	05/30/2007		06/06/2007	
TF050	Thompson Farm	06/06/2007		06/15/2007	
TF051	Thompson Farm	06/15/2007		06/22/2007	
TF052	Thompson Farm	06/29/2007		07/05/2007	
TF053	Thompson Farm	07/05/2007		07/10/2007	
TF054	Thompson Farm	07/10/2007		07/13/2007	
TF055	Thompson Farm	07/13/2007		07/16/2007	
TF056	Thompson Farm	07/16/2007		07/20/2007	
TF057	Thompson Farm	07/23/2007		07/30/2007	
TF058	Thompson Farm	07/30/2007		08/07/2007	
TF060	Thompson Farm	08/13/2007	15:00	08/16/2007	18:30
TF061	Thompson Farm	08/16/2007	18:30	08/17/2007	13:00
TF063	Thompson Farm	09/08/2007	18:30	09/12/2007	16:30
TF064	Thompson Farm	09/12/2007	16:30	09/15/2007	16:30
TF065	Thompson Farm	09/21/2007	17:30	09/29/2007	10:30
TF066	Thompson Farm	10/05/2007	15:20	10/09/2007	15:00
TF067	Thompson Farm	10/09/2007	15:00	10/13/2007	17:30
TF068	Thompson Farm	10/17/2007	8:30	10/20/2007	16:15
TF069	Thompson Farm	10/22/2007		10/26/2007	14:30
TF070	Thompson Farm	10/26/2007	14:30	10/29/2007	17:00
TF071	Thompson Farm	11/02/2007	17:00	11/05/2007	15:30
TF072	Thompson Farm	11/05/2007	15:30	11/07/2007	16:30
TF073	Thompson Farm	11/07/2007	16:30	11/13/2007	16:00
TF074	Thompson Farm	11/14/2007	17:30	11/16/2007	17:00
TF075	Thompson Farm	11/16/2007	17:00	11/27/2007	15:30
TF076	Thompson Farm	11/27/2007	15:30	12/07/2007	14:00
TF077	Thompson Farm	12/07/2007	14:00	12/14/2007	16:30
TF078	Thompson Farm	12/14/2007	16:30	12/21/2007	11:00
TF079	Thompson Farm	12/21/2007	11:00	01/08/2008	15:00
TF080	Thompson Farm	01/08/2008	15:00	01/10/2008	15:00
TF081	Thompson Farm	01/10/2008	15:00	01/15/2008	15:00
TF082	Thompson Farm	01/15/2008	15:00	01/24/2008	14:00
TF084	Thompson Farm	01/29/2008	14:30	01/31/2008	14:00
TF085	Thompson Farm	01/31/2008	14:00	02/04/2008	14:30
TF086	Thompson Farm	02/04/2008	14:30	02/09/2008	15:30
TF087	Thompson Farm	02/09/2008	15:30	02/12/2008	15:30
TF088	Thompson Farm	02/12/2008	15:30	02/15/2008	13:00
TF089	Thompson Farm	02/15/2008	13:00	02/19/2008	16:30
TF090	Thompson Farm	02/19/2008	16:30	02/25/2008	15:30
TF091	Thompson Farm	02/25/2008	15:30	02/28/2008	15:30
TF092	Thompson Farm	02/28/2008	15:30	03/02/2008	13:45
TF093	Thompson Farm	03/02/2008	13:45	03/06/2008	

UNH ID	Sample location	Deploy Date (Local)	Deploy Time	Collect Date (Local)	Collect Time
TF094	Thompson Farm	03/07/2008		03/11/2008	14:00
TF095	Thompson Farm	03/11/2008	14:00	03/13/2008	13:30
TF096	Thompson Farm	03/13/2008	13:30	03/18/2008	14:00
TF097	Thompson Farm	03/18/2008	14:00	03/23/2008	14:00
TF098	Thompson Farm	03/23/2008	14:00	03/27/2008	14:30
TF099	Thompson Farm	03/27/2008	14:30	03/30/2008	15:00
TF100	Thompson Farm	03/30/2008	15:00	04/03/2008	14:30
TF101	Thompson Farm	04/03/2008	14:30	04/07/2008	14:00
TF102	Thompson Farm	04/08/2008	14:30	04/14/2008	16:00
TF103	Thompson Farm	04/25/2008	15:30	04/30/2008	13:30
TF104	Thompson Farm	04/30/2008	13:30	05/05/2008	14:30
TF105	Thompson Farm	05/05/2008	14:30	05/08/2008	15:30
TF106	Thompson Farm	05/13/2008	10:30	05/19/2008	14:30
TF107	Thompson Farm	05/19/2008	14:30	05/22/2008	11:30
TF108	Thompson Farm	05/22/2008	11:30	05/30/2008	16:30
TF109	Thompson Farm	05/30/2008	16:30	06/02/2008	13:30
TF110	Thompson Farm	06/02/2008	13:30	06/09/2008	11:00
TF111	Thompson Farm	06/09/2008	11:00	06/11/2008	13:30
TF112	Thompson Farm	06/11/2008	13:30	06/17/2008	13:30
TF113	Thompson Farm	06/17/2008	13:30	06/18/2008	13:30
TF114	Thompson Farm	06/18/2008	13:30	06/24/2008	11:00
TF115	Thompson Farm	06/24/2008	11:00	06/25/2008	11:00
TF116	Thompson Farm	06/25/2008	11:00	06/29/2008	16:30
TF117	Thompson Farm	06/29/2008	16:30	06/30/2008	13:30
TF118	Thompson Farm	06/30/2008	13:30	07/06/2008	14:30
TF119	Thompson Farm	07/06/2008	14:30	07/10/2008	10:30
TF120	Thompson Farm	07/18/2008		07/22/2008	16:45
TF121	Thompson Farm	07/22/2008	16:45	07/25/2008	8:00
TF122	Thompson Farm	07/25/2008	8:00	07/28/2008	15:00
TF123	Thompson Farm	07/28/2008	15:00	08/01/2008	11:30
TF124	Thompson Farm	08/01/2008	11:30	08/04/2008	8:45
TF125	Thompson Farm	08/04/2008	8:45	08/07/2008	11:30
TF126	Thompson Farm	08/07/2008	11:30	08/08/2008	11:30
TF127	Thompson Farm	08/08/2008	11:30	08/09/2008	14:15
TF128	Thompson Farm	08/09/2008	14:15	08/13/2008	13:15
TF129	Thompson Farm	08/13/2008	13:15	08/21/2008	11:30
TF130	Thompson Farm	09/06/2008	15:00	09/08/2008	18:00
TF131	Thompson Farm	09/08/2008	18:00	09/15/2008	16:00
TF132	Thompson Farm	09/15/2008	16:00	09/23/2008	13:00
TF133	Thompson Farm	09/23/2008	13:00	09/27/2008	12:30
TF134	Thompson Farm	09/27/2008	12:30	09/30/2008	13:00
TF135	Thompson Farm	09/30/2008	13:00	10/03/2008	14:00
TF136	Thompson Farm	10/03/2008	14:00	10/15/2008	15:30
TF137	Thompson Farm	10/15/2008	15:30	10/18/2008	13:00
TF138	Thompson Farm	10/18/2008	13:00	10/23/2008	14:00

UNH ID	Sample location	Deploy Date (Local)	Deploy Time	Collect Date (Local)	Collect Time
TF139	Thompson Farm	10/23/2008	14:00	10/27/2008	14:00
TF140	Thompson Farm	10/27/2008	14:00	10/30/2008	13:00
TF141	Thompson Farm	10/30/2008	13:00	11/11/2008	13:30
TF142	Thompson Farm	11/11/2008	13:30	11/18/2008	14:30
TF143	Thompson Farm	11/18/2008	14:30	11/26/2008	16:30
TF144	Thompson Farm	11/26/2008	16:30	12/02/2008	13:00
TF145	Thompson Farm	12/09/2008	15:30	12/14/2008	16:30
TF146	Thompson Farm	12/14/2008	16:30	12/17/2008	16:30
TF147	Thompson Farm	12/17/2008	16:30	01/05/2009	15:00
TF148	Thompson Farm	01/05/2009	15:00	01/10/2009	15:00
TF149	Thompson Farm	01/10/2009	15:00	01/27/2009	16:30
TF150	Thompson Farm	01/27/2009	16:30	01/29/2009	13:30
TF151	Thompson Farm	01/29/2009	13:30	02/05/2009	15:30
TF152	Thompson Farm	02/05/2009	15:30	02/14/2009	9:30
TF153	Thompson Farm	02/14/2009	9:30	02/27/2009	13:00
TF154	Thompson Farm	02/27/2009	13:00	03/05/2009	18:00
TF155	Thompson Farm	03/05/2009	18:00	03/08/2009	17:00
TF156	Thompson Farm	03/08/2009	17:00	03/10/2009	16:00
TF157	Thompson Farm	03/10/2009	16:00	03/13/2009	18:30
TF158	Thompson Farm	03/13/2009	18:30	03/28/2009	15:30
TF159	Thompson Farm	03/28/2009	15:30	03/31/2009	13:00
TF160	Thompson Farm	03/31/2009	13:00	04/02/2009	18:00
TF161	Thompson Farm	04/02/2009	18:00	04/05/2009	16:30
TF162	Thompson Farm	04/05/2009	16:30	04/08/2009	14:30
TF163	Thompson Farm	04/08/2009	14:30	04/15/2009	14:00
TF164	Thompson Farm	04/15/2009	14:00	04/20/2009	18:00
TF165	Thompson Farm	04/20/2009	18:00	04/28/2009	12:30
TF166	Thompson Farm	04/28/2009	12:30	05/04/2009	18:00
TF167	Thompson Farm	05/04/2009	18:00	05/07/2009	9:00
TF168	Thompson Farm	05/07/2009	9:00	05/14/2009	9:30
TF169	Thompson Farm	05/14/2009	9:30	05/22/2009	15:00
TF170	Thompson Farm	05/22/2009	15:00	06/01/2009	16:30
TF171	Thompson Farm	06/01/2009	16:30	06/08/2009	17:00
TF172	Thompson Farm	06/08/2009	17:00	06/11/2009	10:00
TF173	Thompson Farm	06/11/2009	10:00	06/16/2009	16:00
TF174	Thompson Farm	06/16/2009	16:00	06/23/2009	14:00
TF175	Thompson Farm	06/23/2009	14:00	06/30/2009	10:00
TF176	Thompson Farm	06/30/2009	10:00	07/09/2009	11:30
TF177	Thompson Farm	07/09/2009	11:30	07/14/2009	11:30
TF178	Thompson Farm	07/14/2009	11:30	07/20/2009	17:30
TF179	Thompson Farm	07/20/2009	17:30	07/23/2009	14:30
TF180	Thompson Farm	07/23/2009	14:30	07/27/2009	14:30
TF181	Thompson Farm	07/27/2009	14:30	07/28/2009	17:40
TF182	Thompson Farm	07/28/2009	17:40	07/30/2009	12:45
TF183	Thompson Farm	07/30/2009	12:45	08/03/2009	17:15

UNH ID	Sample location	Deploy Date	Deploy Time (Local)	Collect Date (Local)	Collect Time
TF184	Thompson Farm	08/03/2009	17:15	08/12/2009	12:00
TF185	Thompson Farm	08/12/2009	12:00	08/24/2009	10:00
TF186	Thompson Farm	08/24/2009	10:00	09/02/2009	14:00
TF0201	Thompson Farm2	06/17/2009	11:00	06/23/2009	13:45
TF0202	Thompson Farm2	06/23/2009	13:45	06/30/2009	10:00
TF0203	Thompson Farm2	06/30/2009	10:00	07/09/2009	11:30
TF0204	Thompson Farm2	07/09/2009	11:30	07/14/2009	11:30
TF0205	Thompson Farm2	07/14/2009	11:30	07/20/2009	17:30
TF0206	Thompson Farm2	07/20/2009	17:30	07/23/2009	14:30
TF0207	Thompson Farm2	07/23/2009	14:30	07/27/2009	15:00
TF0208	Thompson Farm2	07/27/2009	15:00	07/28/2009	17:45
TF0209	Thompson Farm2	07/28/2009	17:45	07/30/2009	12:30
TF0210	Thompson Farm2	07/30/2009	12:30	08/03/2009	17:15
TF0211	Thompson Farm2	08/24/2009	10:00	09/02/2009	14:00
AI001	Appledore Island	06/12/2009	13:30	06/15/2009	11:45
AI002	Appledore Island	06/15/2009	11:45	06/19/2009	10:30
AI003	Appledore Island	06/19/2009	10:45	06/20/2009	17:30
AI004	Appledore Island	06/20/2009	17:45	06/29/2009	10:45
AI005	Appledore Island	06/29/2009	11:30	06/30/2009	19:00
AI006	Appledore Island	06/30/2009	19:00	07/02/2009	16:40
AI007	Appledore Island	07/02/2009	16:55	07/08/2009	19:15
AI008	Appledore Island	07/08/2009	19:15	07/13/2009	11:30
AI009	Appledore Island	07/13/2009	11:30	07/18/2009	10:00
AI010	Appledore Island	07/18/2009	10:00	07/22/2009	20:00
AI011	Appledore Island	07/22/2009	20:00	07/25/2009	14:15
AI012	Appledore Island	07/25/2009	14:15	08/02/2009	15:30
AI013	Appledore Island	08/24/2009	13:55	08/30/2009	17:50

UNH ID	Number of precip events	Event1
TF001	2	07/21/06 15:00-07/21/06 19:00
TF002	1	07/28/06 18:00-07/28/06 21:00
TF003	1	08/03/06 20:00-08/04/06 13:00
TF004	2	08/07/06 09:00-08/07/06 10:00
TF005	1	08/20/06 04:00-08/20/06 14:00
TF006	1	08/25/06 07:00-08/25/06 8:00
TF007	1	08/27/06 15:00-08/28/06 6:00
TF008	2	08/29/06 11:00-08/29/06 14:00
TF009		09/06/06 03:00
TF010	1	09/14/06 17:00-09/14/06 22:00
TF011	1	09/19/06 21:00-09/20/06 03:00
TF012	2	09/23/06 8:00-09/23/06 13:00
TF013	2	09/29/06 06:00-09/29/06 15:00
TF014	1	10/05/06 1:00-10/05/06 3:00
TF015	1	10/11/06 19:00-10/12/06 07:00
TF016	1	10/17/06 18:00-10/18/06 07:00
TF017	3	10/18/06 10:00
TF018	1	10/28/06 05:00-10/28/06 20:00
TF019	2	11/01/06 03:00
TF020	1	11/07/06 23:00-11/08/06 09:00
TF021	1	11/08/06 10:00-11/09/06 3:00
TF022	1	11/12/06 14:00-11/12/06 17:00
TF023	1	11/13/06 10:00-11/14/06 08:00
TF024	2	11/14/06 09:00-11/14/06 12:00
TF025	1	11/23/06 12:00-11/23/06 24:00
TF026	2	11/28/06 17:00- 11/28/06 19:00
TF027		12/04/06 09:00
TF028		12/13/06 16:00-17:00
TF029	2	12/22/06 21:00-12/23/06 02:00
TF030	2	12/30/06 12:00-12/30/06 16:00
TF031	2	01/05/07 22:00- 01/06/07 17:00
TF032	1	01/14/07 13:00-01/15/07 22:00
TF033	1	01/18/07 23:00-1/19/07 02:00
TF034	1	02/02/07 20:00-2/3/07 02:00
TF035		02/14/07 03:00-02/14/07 23:00
TF036	2	02/23/07 03:00 AM
TF037	1	03/10/07 23:00-03/11/07 06:00
TF038	2	03/14/07 23:00-03/15/07 17:00
TF039		03/22/07 04:00
TF040	2	03/24/07 20:00-03/25/07 02:00
TF041	1	04/01/07 22:00-04/3/07 11:00
TF042	1	04/04/07 08:00-04/05/07 06:00
TF043	1	04/12/07 12:00-04/12/07 23:00
TF044	1	04/15/07 11:00- 04/16/07 07:00
TF045	1	04/27/07 06:00-04/27/07 13:00

UNH ID	Number of precip events	Event1
TF046	3	04/28/07 23:00- 04/30/07 15:00
TF047	2	05/16/07 2:00-05/16/07 22:00
TF048	1	05/28/07 01:00-05/28/07 03:00
TF049	5	05/31/07 22:00- 06/01/07 6:00
TF050		06/9/2007 14:00
TF051		06/21/07 19:00
TF052	1	07/04/07 21:00- 07/05/07 05:00
TF053	3	07/06/07 02:00-07/06/07 03:00
TF054	1	07/12/2007 01:00
TF055	1	07/15/07 15:00-07/15/07 20:00
TF056	2	07/18/07 06:00-07/18/07 22:00
TF057	2	07/23/07 15:00-07/24/07 02:00
TF058	1	08/06/07 15:00-08/06/07 16:00
TF060	1	08/13/07 18:00
TF061	1	08/16/07 22:00-08/16/07 23:00
TF063	2	09/09/07 05:00-09/09/07 23:00
TF064	1	09/15/07 05:00-09/15/07 12:00
TF065	2	09/27/07 00:00
TF066	2	10/06/07 20:00-10/07/07 01:00
TF067	2	10/09/07 22:00-10/10/07 06:00
TF068	1	10/19/07 17:00-10/20/07 04:00
TF069		10/23/07 23:00-10/25/07 05:00
TF070	1	10/27/07 02:00-10/27/07 19:00
TF071	1	11/03/07 13:00-11/03/07 22:00
TF072	1	11/06/07 06:00-11/06/07 15:00
TF073		11/13/07 05:00-11/13/07 08:00
TF074	1	11/15/07 11:00-11/16/07 10:00
TF075	3	11/20/07 11:00-11/20/07 18:00
TF076	1	12/03/07 02:00-12/03/07 18:00
TF077	4	12/7/07 18:00
TF078	2	12/16/07 05:00-12/16/07 21:00
TF079	6	12/23/07 21:00-12/24/07 02:00
TF080		01/09/08 12:00- 01/09/08 15:00
TF081	2	01/11/08 07:00- 01/11/08 17:00
TF082	1	01/18/08 02:00-01/18/08 11:00
TF084		01/30/08 03:00-01/30/08 15:00
TF085	1	02/01/08 15:00-02/02/08 02:00
TF086	3	02/05/08 03:00-02/05/08 14:00
TF087	1	02/09/08 18:00-02/10/08 14:00
TF088	1	02/12/08 23:00-02/13/08 20:00
TF089	1	02/17/08 23:00-02/18/08 21:00
TF090	1	02/22/08 09:00-02/22/08 23:00
TF091	2	02/26/08 17:00-02/27/08 01:00
TF092	1	02/29/08 00:00-03/01/08 15:00
TF093	1	03/04/08 17:00-03/05/08 10:00

UNH ID	Number of precip events	Event1
TF094	1	03/07/08 22:00-03/08/08 21:00
TF095	1	03/12/08 08:00-03/12/08 14:00
TF096	2	03/14/08 23:00-03/15/08 12:00
TF097	1	03/19/08 10:00-03/20/08 05:00
TF098		03/26/08 02:00
TF099	1	03/28/08 03:00-03/28/08 13:00
TF100	2	03/31/08 12:00-03/31/08 23:00
TF101	1	04/04/08 07:00-04/05/08 09:00
TF102	1	04/11/08 17:00-04/12/08 08:00
TF103	2	04/27/08 10:00-04/27/08 11:00
TF104	2	05/03/08 09:00-05/03/08 15:00
TF105		05/08/08 06:00-05/08/08 07:00
TF106	1	05/16/08 21:00-05/17/08 09:00
TF107		05/21/08 20:00- 05/22/08 00:00
TF108		05/23/2008 19:00
TF109		05/31/2008 15:00
TF110	2	06/04/08 09:00- 06/04/08 23:00
TF111	1	06/11/08 01:00-06/11/08 02:00
TF112	2	06/15/08 02:00-06/15/08 10:00
TF113	1	06/17/08 18:00-06/17/08 21:00
TF114	3	06/20/08 16:00-06/20/08 18:00
TF115	1	06/24/08 17:00
TF116	1	06/29/08 00:00-06/29/08 08:00
TF117	1	06/29/08 18:00-06/30/08 04:00
TF118	2	07/02/08 16:00
TF119	1	07/09/08 19:00
TF120	3	07/18/08 19:00-07/19/08 03:00
TF121	1	07/23/08 16:00-07/24/08 23:00
TF122	2	07/27/08 03:00-07/27/08 05:00
TF123	1	07/31/08 18:00-07/31/08 20:00
TF124	3	08/01/08 19:00
TF125	1	08/06/08 09:00-08/06/08 15:00
TF126	1	08/07/08 19:00-08/08/08 07:00
TF127	1	08/08/08 19:00-08/09/08 13:00
TF128	1	08/11/08 14:00-08/12/08 11:00
TF129	2	08/16/08 16:00
TF130	1	09/06/08 07:00-09/07/08 04:00
TF131	3	09/09/08 12:00-09/09/08 14:00
TF132	1	09/22/08 00:00-09/22/08 01:00
TF133	1	09/26/08 08:00-09/27/08 13:00
TF134	1	09/27/08 13:00-09/29/08 10:00
TF135	2	09/30/08 23:00-10/01/08 03:00
TF136	2	10/5/08 21:00
TF137	1	10/16/08 13:0-10/16/08 17:00
TF138	1	10/21/08 20:00-10/22/08 05:00

UNH ID	Number of precip events	Event1
TF139	1	10/26/08 00:00-10/26/08 08:00
TF140	1	10/28/08 08:00-10/29/08 00:00
TF141	3	11/06/08 15:00-11/07/08 00:00
TF142	1	11/13/08 17:00-11/16/08 09:00
TF143	1	11/24/08 23:00-11/25/08 19:00
TF144	2	11/28/08 11:00-11/28/08 14:00
TF145	1	12/10/08 03:00-12/12/08 14:00
TF146		12/16/08 01:00
TF147	7	12/19/08 15:00-12/20/08 18:00
TF148	1	01/07/09 04:00 AM-01/08/09 14:00
TF149	3	01/11/09 01:00-01/11/09 12:00
TF150	1	01/28/09 07:00-01/28/09 23:00
TF151		02/03/09 17:00-02/04/09 10:00
TF152	1	02/12/09 04:00-02/12/09 07:00
TF153	2	02/18/09 19:00-02/20/09 04:00
TF154	2	02/27/09 21:00-02/28/09 01:00
TF155	1	03/07/09 23:00-03/08/09 07:00
TF156	1	03/09/09 07:00-03/09/09 18:00
TF157	1	03/11/09 04:00-03/11/09 14:00
TF158	1	03/26/09 10:00-03/27/09 05:00
TF159	1	03/29/09 06:00-03/30/09 17:00
TF160	1	04/01/09 23:00-04/02/09 05:00
TF161	1	04/03/09 12:00-04/04/09 07:00
TF162	2	04/06/09 16:00-04/06/09 23:00
TF163	1	04/10/09 12:00-04/11/09 16:00
TF164		04/18/09 23:00-04/18/09 23:00
TF165	3	04/21/09 02:00-04/22/09 00:00
TF166		05/02/2009 05:00
TF167	2	05/05/09 12:00-05/06/09 08:00
TF168	1	05/09/09 08:00-05/09/09 23:00
TF169	2	05/14/09 16:00-05/14/09 21:00
TF170	4	05/24/09 15:00
TF171		06/08/09 05:00
TF172	1	06/09/09 10:00-06/10/09 00:00
TF173	2	06/12/09 00:00-06/12/09 10:00
TF174	3	06/18/09 17:00-06/19/09 15:00
TF175	4	06/23/09 14:00-06/24/09 10:00
TF176	4	07/01/09 17:00-07/02/09 10:00
TF177	1	07/11/09 23:00-07/12/09 00:00
TF178	1	07/18/09 02:00-07/18/09 05:00
TF179	1	07/21/09 08:00-07/22/09 03:00
TF180	2	07/26/09 09:00
TF181	1	07/27/09 19:00- 07/27/09 23:00
TF182	1	07/29/09 19:00-07/30/09 07:00
TF183	1	07/31/09 13:00-07/31/09 19:00

UNH ID	Number of precip events	Event1
TF184	1	08/11/09 08:00 -08/11/09 21:00
TF185	2	08/21/09 20:00-08/21/09 21:00
TF186	2	08/28/09 23:00- 08/29/09 18:00
TF0201	3	06/18/09 17:00-06/19/09 15:00
TF0202	4	06/23/09 14:00-06/24/09 10:00
TF0203	4	07/01/09 17:00-07/02/09 10:00
TF0204	1	07/11/09 23:00-07/12/09 00:00
TF0205	1	07/18/09 02:00-07/18/09 05:00
TF0206	1	07/21/09 08:00-07/22/09 03:00
TF0207	2	07/26/09 09:00
TF0208	1	07/27/09 19:00- 07/27/09 23:00
TF0209	1	07/29/09 19:00-07/30/09 07:00
TF0210	1	07/31/09 13:00-07/31/09 19:00
TF0211	2	08/28/09 23:00- 08/29/09 18:00
AI001		
AI002		
AI003		
AI004		
AI005		
AI006		
AI007		
AI008		
AI009		
AI010		
AI011		
AI012		
AI013		

UNH ID	Event2	Event3
TF001	07/22/06 15:00-07/23/06 08:00	
TF002		
TF003		
TF004	08/15/06 03:00-08/15/06 08:00	
TF005		
TF006		
TF007		
TF008	09/03/06 07:00-09/03/06 21:00	
TF009		
TF010		
TF011		
TF012	09/24/06 15:00-09/24/06 16:00	
TF013	10/01/06 13:00-10/01/06 22:00	
TF014		
TF015		
TF016		
TF017	10/20/06 03:00-10/20/06 20:00	10/23/06 00:00-10/23/06 07:00
TF018		
TF019	11/02/06 07:00-11/02/06 11:00	
TF020		
TF021		
TF022		
TF023		
TF024	11/16/06 10:00-11/17/06 08:00	
TF025		
TF026	12/01/06 15:00-12/01/06 22:00	
TF027	12/08/06 05:00-012/08/06 10:00	
TF028		
TF029	12/25/06 23:00-12/26/06 10:00	
TF030	01/01/07 05:00-01/01/07 21:00	
TF031	01/08/07 03:00-01/08/07 15:00	
TF032		
TF033		
TF034		
TF035		
TF036	03/02/07 04:00-03/02/07 19:00	
TF037		
TF038	03/16/07 15:00- 03/17/07 12:00	
TF039		
TF040	03/26/07 16:00-03/27/07 04:00	
TF041		
TF042		
TF043		
TF044		
TF045		

UNH ID	Event2	Event3
TF046	05/11/07 09:00-05/11/07 12:00	05/15/07 08:00-05/15/07 11:00
TF047	05/18/07 04:00- 05/20/07 18:00	05/18/07 04:00-05/20/07 18:00
TF048		
TF049	06/02/07 09:00	06/02/07 23:00
TF050	06/12/07 22:00	06/13/07 13:00
TF051		
TF052		
TF053	07/06/07 16:00-07/08/07 02:00	07/09/07 10:00-07/10/07 00:00
TF054		
TF055		
TF056	07/19/07 15:00-07/20/07 08:00	
TF057	07/28/07 13:00-07/28/07 14:00	
TF058		
TF060		
TF061		
TF063	09/10/07 14:00-09/11/07 18:00	
TF064		
TF065	09/28/07 05:00	
TF066	10/08/07 05:00-10/08/07 09:00	
TF067	10/11/07 15:00-10/12/07 17:00	
TF068		
TF069		
TF070		
TF071		
TF072		
TF073		
TF074		
TF075	11/21/07 22:00-11/22/07 00:00	11/26/07 04:00-11/27/07 02:00
TF076		
TF077	12/09/07 21:00-12/10/07 13:00	12/11/07 19:00-12/11/07 21:00
TF078	12/19/07 18:00-12/20/07 14:00	
TF079	12/27/07 05:00-12/27/07 20:00	12/29/07 04:00-12/29/07 11:00
TF080		
TF081	01/14/08 06:00- 01/14/08 15:00	
TF082		
TF084		
TF085		
TF086	02/06/08 07:00-02/07/08 15:00	02/08/08 10:00-02/08/08 16:00
TF087		
TF088		
TF089		
TF090		
TF091	02/27/08 20:00-02/28/08 07:00	
TF092		
TF093		

UNH ID	Event2	Event3
TF094		
TF095		
TF096	03/16/08 20:00	
TF097		
TF098		
TF099		
TF100	04/01/08 16:00-04/02/08 00:00	
TF101		
TF102		
TF103	04/28/08 12:00-04/29/08 19:00	
TF104	05/04/08 04:00-05/04/08 12:00	
TF105		
TF106		
TF107		
TF108	05/27/08 14:00	
TF109		
TF110	06/06/08 07:00-06/06/08 14:00	
TF111		
TF112	06/16/08 12:00-06/17/08 21:00	
TF113		
TF114	06/22/08 14:00-06/22/08 17:00	06/23/08 08:00-06/23/08 18:00
TF115		
TF116		
TF117		
TF118	07/03/08 19:00-07/04/08 06:00	
TF119		
TF120	07/19/08 18:00-07/19/08 20:00	07/20/08 20:00-07/21/08 17:00
TF121		
TF122	07/27/08 18:00-07/27/08 20:00	
TF123		
TF124	08/02/08 18:00-08/03/08 01:00	08/03/08 14:00-08/03/08 15:00
TF125		
TF126		
TF127		
TF128		
TF129	08/19/08 05:00-08/19/08 11:00	
TF130		
TF131	09/12/08 17:00-09/13/08 00:00	09/14/08 06:00-09/14/08 13:00
TF132		
TF133		
TF134		
TF135	10/01/08 22:00-10/02/08 08:00	
TF136	10/09/08 03:00-10/09/08 07:00	
TF137		
TF138		

UNH ID	Event2	Event3
TF139		
TF140		
TF141	11/08/08 19:00-11/08/08 20:00	11/09/08 09:00
TF142		
TF143		
TF144	11/30/08 15:00-12/01/08 11:00	
TF145		
TF146	12/17/08 02:00-12/17/08 14:00	
TF147	12/21/08 09:00-12/22/08 00:00	12/24/08 07:00-12/25/08 03:00
TF148)	
TF149	01/12/09 09:00-01/12/09 10:00	01/18/09 04:00-01/19/09 05:00
TF150		
TF151		
TF152		
TF153	02/22/09 14:00-02/23/09 03:00	
TF154	03/01/09 17:00-03/02/09 20:00	
TF155		
TF156		
TF157		
TF158		
TF159		
TF160		
TF161		
TF162	04/07/09 13:00	
TF163		
TF164		
TF165	04/22/09 16:00-04/23/09 03:00	04/27/09 04:00
TF166		
TF167	05/07/09 03:00-05/07/09 21:00	
TF168		
TF169	05/17/09 02:00-05/17/09 10:00	
TF170	05/27/09 05:00-05/29/09 14:00	05/30/09 04:00-05/30/09 05:00
TF171		
TF172		
TF173	06/13/09 23:00-06/14/09 18:00	
TF174	06/21/09 08:00-06/22/09 15:00	06/23/09 14:00-06/24/09 00:00
TF175	06/25/09 04:00	06/26/09 06:00
TF176	07/03/09 16:00-07/03/09 18:00	07/04/09 15:00-07/04/09 16:00
TF177		
TF178		
TF179		
TF180	07/27/09 03:00-07/27/09 06:00	
TF181		
TF182		
TF183		

UNH ID	Event2	Event3
TF184		
TF185	08/22/09 13:00-08/22/09 16:00	
TF186	08/30/09 22:00	
TF0201	06/21/09 08:00-06/22/09 15:00	06/23/09 14:00-06/24/09 00:00
TF0202	06/25/09 04:00	06/26/09 06:00
TF0203	07/03/09 16:00-07/03/09 18:00	07/04/09 15:00-07/04/09 16:00
TF0204		
TF0205		
TF0206		
TF0207	07/27/09 03:00-07/27/09 06:00	
TF0208		
TF0209		
TF0210		
TF0211	08/30/09 22:00	
AI001		
AI002		
AI003		
AI004		
AI005		
AI006		
AI007		
AI008		
AI009		
AI010		
AI011		
AI012		
AI013		

UNH ID Event4

Event5

TF001
TF002
TF003
TF004
TF005
TF006
TF007
TF008
TF009
TF010
TF011
TF012
TF013
TF014
TF015
TF016
TF017
TF018
TF019
TF020
TF021
TF022
TF023
TF024
TF025
TF026
TF027
TF028
TF029
TF030
TF031
TF032
TF033
TF034
TF035
TF036
TF037
TF038
TF039
TF040
TF041
TF042
TF043
TF044
TF045

UNH ID Event4**Event5**

TF046

TF047

TF048

TF049 06/03/07 18:00-06/05/07 00:00 06/05/07 14:00-06/05/07 23:00

TF050

TF051

TF052

TF053

TF054

TF055

TF056

TF057

TF058

TF060

TF061

TF063

TF064

TF065

TF066

TF067

TF068

TF069

TF070

TF071

TF072

TF073

TF074

TF075

TF076

TF077 12/13/07 14:00-12/14/07 04:00

TF078

TF079 12/30/07 23:00-12/31/07 11:00 01/01/08 13:00-01/02/08 11:00

TF080

TF081

TF082

TF084

TF085

TF086

TF087

TF088

TF089

TF090

TF091

TF092

TF093

UNH ID Event4

Event5

TF094
TF095
TF096
TF097
TF098
TF099
TF100
TF101
TF102
TF103
TF104
TF105
TF106
TF107
TF108
TF109
TF110
TF111
TF112
TF113
TF114
TF115
TF116
TF117
TF118
TF119
TF120
TF121
TF122
TF123
TF124
TF125
TF126
TF127
TF128
TF129
TF130
TF131
TF132
TF133
TF134
TF135
TF136
TF137
TF138

UNH ID Event4**Event5**

TF139

TF140

TF141

TF142

TF143

TF144

TF145

TF146

TF147 12/27/08 10:00-12/27/08 11:00-12/30/08 03:00-12/30/08 04:00

TF148

TF149

TF150

TF151

TF152

TF153

TF154

TF155

TF156

TF157

TF158

TF159

TF160

TF161

TF162

TF163

TF164

TF165

TF166

TF167

TF168

TF169

TF170 05/ 31/09 15:00-05/31/09 17:00

TF171

TF172

TF173

TF174

TF175 06/28/09 05:00-06/30/09 00:00

TF176 07/07/09 08:00-07/08/09 18:00

TF177

TF178

TF179

TF180

TF181

TF182

TF183

UNH ID Event4**Event5**

TF184

TF185

TF186

TF0201

TF0202 06/28/09 05:00-06/30/09 00:00

TF0203 07/07/09 08:00-07/08/09 18:00

TF0204

TF0205

TF0206

TF0207

TF0208

TF0209

TF0210

TF0211

AI001

AI002

AI003

AI004

AI005

AI006

AI007

AI008

AI009

AI010

AI011

AI012

AI013

UNH ID	mm of precip	Hg (ng/L)	Notes
TF001	34.3	5.56	
TF002	22.9	4.48	
TF003	11.1	2.67	
TF004	32.7	6.95	
TF005	55.12	1.39	
TF006	3.05	8.86	
TF007	13	4.53	
TF008	19.3	3.55	
TF009			Not included
TF010	9.5	12.51	
TF011	23.6	11.14	
TF012	14.9	9.10	
TF013	16.6	19.74	
TF014	3.1	18.58	
TF015	80.1	7.49	
TF016	12.7	23.06	
TF017	30.3	4.61	
TF018	60.9	2.28	
TF019	7.8	8.59	
TF020	7.5	10.56	
TF021	52.6	2.28	
TF022	11.1	7.67	
TF023	43.2	4.91	
TF024	37.9	6.08	
TF025	8.3	11.45	
TF026	33.2	8.10	
TF027			Not included
TF028			Not included
TF029	52.6	0.96	
TF030	22.5	7.20	
TF031	46.5	5.90	
TF032	12.8	18.50	
TF033	2.9	47.50	
TF034	6.8	8.41	
TF035			Not included
TF036	48.9	1.37	
TF037	8.4	1.95	
TF038	44.4	2.73	
TF039			Not included
TF040	10.7	46.85	
TF041	11.3	34.44	
TF042	30.4	0.99	
TF043	21.5	12.22	
TF044	123.2	1.67	
TF045	16	8.92	
		114	

UNH ID	mm of precip	Hg (ng/L)	Notes
TF046	35.1	15.41	
TF047	63.8	6.11	
TF048	7.7	47.89	
TF049	81.6	6.88	
TF050			Not included
TF051			Not included
TF052	10.9	14.24	
TF053	30.3	9.84	
TF054	3.6	65.09	
TF055	12.9	42.47	
TF056	30.5	11.92	
TF057	18.9	25.57	
TF058	13.9	10.35	
TF060	5.8	39.50	
TF061	19.3	12.96	
TF063	53.8	4.24	
TF064	6	15.07	
TF065	16.1	8.94	
TF066	32.4	5.27	
TF067	37.4	6.18	
TF068	27.6	1.65	
TF069			Not included
TF070	15.5	3.69	
TF071	30.1	0.75	
TF072	18.7	3.57	
TF073			Not included
TF074	20.6	2.12	
TF075	19.8	3.30	N-CON sampler used
TF076	21.2	1.25	N-CON sampler used
TF077	17.8	2.11	
TF078	45.4	1.86	
TF079	60.3	1.41	
TF080			Not included
TF081	44.4	8.98	
TF082	16.3	3.67	N-CON sampler used
TF084			Not included
TF085	29	4.30	
TF086	58.5	3.18	
TF087	7.8	7.20	
TF088	69.6	1.66	
TF089	12.2	9.73	
TF090	10.5	10.88	
TF091	32.4	6.42	
TF092	14.2	4.25	
TF093	27.5	6.47	

UNH ID	mm of precip	Hg (ng/L)	Notes
TF094	41.1	3.92	
TF095	6.3	8.74	
TF096	17.6	8.38	
TF097	28.2	3.50	
TF098			Not included
TF099	25.1	3.48	
TF100	7.6	8.64	
TF101	19.7	5.42	
TF102	6.7	18.94	
TF103	64.4	8.58	
TF104	17.9	6.03	
TF105			Not included
TF106	2.7	24.30	
TF107			Not included
TF108			Not included
TF109			Not included
TF110	22.2	12.04	
TF111	3.6	25.81	
TF112	27.4	8.22	
TF113	5.5	15.97	
TF114	33.6	14.96	
TF115	1.8	30.42	
TF116	0.7	21.02	
TF117	6.3	14.52	
TF118	3.3	16.37	
TF119	2.9	37.72	
TF120	73.9	17.57	
TF121	112.5	15.44	
TF122	14.5	12.52	
TF123	26.7	11.95	
TF124	34	8.95	
TF125	25.5	4.21	
TF126	11.6	5.67	
TF127	6.6	15.15	
TF128	19.3	5.97	
TF129	2.3	27.10	
TF130	127.3	8.58	
TF131	22.4	7.18	
TF132	3.9	10.10	
TF133	52.1	2.24	
TF134	40.5	4.04	
TF135	15.7	8.12	
TF136	6.2	19.21	
TF137	7.5	10.92	
TF138	6.3	8.41	
		116	

UNH ID	mm of precip	Hg (ng/L)	Notes
TF139	36.4	2.77	
TF140	10	6.26	
TF141	4.7	15.17	
TF142	29.8	7.28	
TF143	59.1	3.98	
TF144	26.5	4.23	
TF145	83.9	3.05	
TF146			Not included
TF147	76.8	4.41	
TF148	26.2	4.58	
TF149	34.6	3.65	
TF150	30.3	4.60	
TF151			Not included
TF152	7.5	9.81	
TF153	64.1	2.72	
TF154	28.9	3.61	
TF155	4.4	34.83	
TF156	14.8	3.37	
TF157	11	18.86	
TF158	9.3	5.42	
TF159	21.2	15.56	
TF160	4.1	4.95	
TF161	23.3	7.02	
TF162	29.7	3.57	
TF163	4.5	17.76	
TF164			Not included
TF165	37.2	5.91	
TF166			Not included
TF167	43.6	4.59	
TF168	10.5	13.04	
TF169	10.3	13.10	
TF170	40.4	11.18	
TF171			Not included
TF172	4.2	13.79	
TF173	35.4	7.86	
TF174	48.6	4.83	
TF175	29.6	6.84	
TF176	57.8	9.77	
TF177	2.2	20.62	
TF178	16	9.70	
TF179	10.4	11.16	
TF180	63.6	3.45	
TF181	2.9	16.33	
TF182	3	14.03	
TF183	47.6	3.98	

UNH ID	mm of precip	Hg (ng/L)	Notes
TF184	17.1	6.00	
TF185	28.7	19.21	
TF186	50.4	3.34	
TF0201	51.1	4.57	
TF0202	29.6	6.16	
TF0203	57.8	11.24	
TF0204	2.2		Not included
TF0205	16	8.62	
TF0206	10.4	8.47	
TF0207	59.3	2.69	
TF0208	2.9	13.81	
TF0209	3	9.62	
TF0210	47.6	3.74	
TF0211	50.4	2.81	
AI001	6.9	9.09	
AI002	34.5	3.42	
AI003	11.2	4.80	
AI004	21.3	11.28	
AI005	11.2	6.17	
AI006	38.4	7.67	
AI007	19.6	9.51	
AI008	5.8	6.59	
AI009	8.4	7.34	
AI010	20.3	13.61	
AI011	87.4	4.02	
AI012	27.2	5.68	
AI013	78.0	2.53	